



Faculty of Science and Technology

## MASTER'S THESIS

Study program/Specialization: <b>Offshore Technology/Marine and Subsea</b>	Spring semester, 2016 <b>Open</b>
Writer: <b>Muhammad Nouman Khalid</b>	
Faculty supervisor: <b>Prof. Bjørn Helge Hjertager</b>	
Co-Supervisor: <b>Knut Erik Giljarhus</b>	
Title of thesis: <b>Design Optimization of Tendons of Snorre A Tension Leg Platform (TLP) for Extreme Wave Event</b>	
Credits (ECTS): 30	
Key words: Tension Leg Platform (TLP), extreme event wave, Stokes fifth wave, tendons, superposed wave, tension, lift force, drag force, platform, Waves2Foam, OpenFOAM, free surface, surface elevation.	Pages: 94 Enclosure: Appendix + 1 CD <b>Stavanger, 29-06-2016</b>

(This page is intentionally left blank)

NOTE: ‘Society of Petroleum Engineers style-guide’ document layout is followed in this thesis and APA referencing style is adopted for citation purpose.

(This page is intentionally left blank)

## **ABSTRACT**

Tendons or tension legs is a vital components of a Tension Leg Platform (TLP). The platform integrity solely relies upon the tension legs. During design phase of a TLP, all components are designed for extreme event wave loads. The defining characteristics of extreme event wave can be predicted using statistical models and wave spectra but the calculation of extreme event impact forces is a tricky process. The sea at a given time and location is composed of many waves of different height and time period propagating in all the directions. The extreme event wave, in actual, generates by the superposition of many wave components of different time periods and heights. The heights of all those waves happens to be positive at that point of sea and all these heights add up to form a wave of very large amplitude. After superposition, all the individual components of that extreme event wave scatter in all directions to make the regular sea. It is very hard and time consuming to generate extreme event by modeling of irregular sea as the occurrence of extreme event is a random process. Conventionally, Stokes fifth order waves, with time period and wave height of extreme event, are used to calculate the impact loads of extreme event.

The purpose of the current study is to optimize the design of tendons of a Tension Leg Platform. Study has revealed that the extreme event loads calculated by Stokes fifth waves have many conservations which results in overdesign of the tendons of TLP. Moreover, the process is also not the realization of actual wave event. The better approach is to select a wave spectrum that closely approximates the sea in which TLP is installed and then generate an extreme event wave through the superposition of individual wave components laying within the selected spectrum. Snorre A TLP, installed in North Sea, is chosen for the current study and extreme wave event load analyses using Stokes fifth order wave and superposed wave are performed. In the last sections, the results of both the analyses are compared and discussed. It is found that the extreme event loads calculated by Stokes fifth order wave have conservations and Snorre A platform is over designed for extreme events. Further, future recommendations are given for elimination of these conservations.

(This page is intentionally left blank)

## ***ACKNOWLEDGEMENTS***

I would like to pay my deepest gratitude to *Prof. Bjørn Helge Hjertager* and *Knut Erik Giljarhus* for his consistent support and motivation throughout the completion of this thesis.

Secondly, I am grateful to the *Anand Bahuguni* of Lloyd's Register, London, for providing me useful material which contributed greatly towards the successful completion of this work. I would also like to thank my friend and my colleague *Muhammad Ahmad Tauqueer* for assisting me at some critical situations during the course of this thesis.

(This page is intentionally left blank)

## **TABLE OF CONTENTS**

1	INTRODUCTION .....	1
1.1	History of offshore petroleum .....	1
1.2	Modern Offshore petroleum .....	2
1.3	Types of offshore platforms .....	2
1.3.1	Functional and operational parameters.....	2
1.3.2	Marine architect and hydrodynamic parameters .....	2
1.3.3	Economic parameters .....	3
1.3.4	Fixed Platforms .....	3
1.4	Floating platforms .....	4
1.5	Tension Leg Platform (TLP) .....	5
1.6	Tension legs (tendons).....	9
2	DESIGN PROCESS OF TLP TENDONS .....	10
2.1	Operational phase design.....	10
2.2	Limit state control .....	11
2.3	Environmental loads input for design.....	12
3	RESEARCH OBJECTIVES AND MILESTONES .....	13
4	POTENTIAL FUNCTION AND WAVE THEORIES .....	15
4.1	Regular waves .....	16
4.1.1	Linear wave theory .....	17
4.1.2	Nonlinear wave theories .....	18
4.2	Irregular waves .....	20
4.2.1	Pierson-Moskowitz Spectrum .....	20
4.2.2	JONSWAP Spectrum .....	21
5	WAVES2FOAM – A WAVE GENERATION LIBRARY OF OPENFOAM .....	22
5.1	Fluid flow mechanics followed by OpenFOAM .....	22
5.2	Volume of fluid method for multiphase flow .....	23
5.3	Wave generation procedure .....	24
5.3.1	Relaxation zone physics .....	25
6	TEST CASES .....	26
6.1	2D test case.....	26
6.1.1	Computational Domain .....	26
6.1.2	Pre-processing .....	27
6.1.3	Solving.....	29
6.1.4	Post processing .....	31
6.2	3D test case.....	32

6.2.1	Post-processing.....	34
7	SNORRE A TLP – DIMENSIONS AND INPUT PARAMETERS .....	35
8	EXTREME WAVE EVENT GENERATION USING STOKES FIFTH WAVE .....	37
8.1	Platform model.....	37
8.2	Computational domain .....	38
8.3	Mesh-Setup.....	40
8.4	Pre-processing .....	43
8.5	Mesh convergence study .....	45
8.6	Post-processing.....	46
8.6.1	Methodology for tension calculation.....	48
8.6.2	Results .....	51
9	NEW WAVE THEORY.....	54
9.1	Test cases.....	55
9.1.1	2D test case.....	55
10	EXTREME WAVE EVENT GENERATION USING SUPERPOSITION OF WAVES .....	58
10.1	Matching standard 1 .....	58
10.1.1	Simulation of wave fulfilling matching standard 1 with platform .....	61
10.2	Matching standard 2 .....	62
10.2.1	Simulation of wave fulfilling matching standard 2 with platform .....	64
11	COMPARISON OF RESULTS .....	66
12	CONCLUSION .....	69
13	FUTURE RECOMMENDATIONS .....	70
14	REFERENCES .....	71
15	APPENDIX .....	i

## **LIST OF FIGURES**

Figure 1-1 drilling and production piers at Summerland, California, 1897 (Wells, 2016) .....	1
Figure 1-2 Types of Fixed Platforms a: Complaint Structures, b: Gravity Based, C: Jacket Structures, d: Guyed Towers (World Ocean Review, 2016) .....	4
Figure 1-3 Types of Floating Platforms a: FPSO, b: Semi-Submersible, c: TLP, d: Spar (World Ocean Review, 2016) .....	5
Figure 1-4 A Typical Tension Leg Platform (Offshore technology.com, 2016).....	6
Figure 1-5 conventional Tension Leg Platform (C-TLP) (Paixao, 2016) .....	7
Figure 1-6 Extended Tension Leg Platform (IHRDC, 2016) .....	7
Figure 1-7 A Moses Tension Leg Platform (Offshore technology.com, 2016).....	8
Figure 1-8 A SeaStar Tension Leg Platform (TurboSquid, 2016) .....	8
Figure 4-1 2 Dimensional Airy Wave (Obhraai, 2015).....	17
Figure 4-2 Different Stokes wave orders.....	20
Figure 5-1 Overview of OpenFOAM Structure (CFD Direct, 2016) .....	23
Figure 5-2 Schematic of Waves2Foam Case Setup.....	25
Figure 5-3 Illustration of Relaxation Zones (Wu, Chen, Bahuguni, Lu, & Kumar, 2015).....	25
Figure 6-1 Computational Domain (2D Test Case).....	27
Figure 6-2 Computational Domain Boundaries' Types (2D Test Case) .....	28
Figure 6-3 Steps of Wave Generation in OpenFOAM .....	30
Figure 6-4 Wave Propagation between Time Steps 21-25 seconds (2D Test Case) .....	31
Figure 6-5 Surface Elevation of waves at Time Instant 25 seconds.....	32
Figure 6-6 Computational Domain (3D Test Case).....	32
Figure 6-7 Computational Domain Boundaries Types (3D Test Case) .....	33
Figure 6-8 3D View of Free Water Surface (3D Test Case) .....	34
Figure 6-9 Surface Elevation at Time Instant 87.5 Seconds (3D Test Case) .....	34
Figure 7-1 Artistic View of Snorre A TLP (Johannessen, Haver, Bunnik, & Buchner, 2006) .....	36
Figure 8-1 Snorre A Model Used in Simulations .....	37
Figure 8-2 Computational Domain (Stokes Fifth wave without Platform) .....	38
Figure 8-3 Free Surface 3D view at Time Instant of 60 seconds (Stokes Fifth wave without Platform) .....	39
Figure 8-4 Surface Elevation at 16 meters after the End of Wave Generation Zone for the whole Computation Time (Stokes Fifth wave without Platform) .....	39
Figure 8-5 Computational Domain (Stokes Fifth wave) .....	40
Figure 8-6 Block Topology of Pontoon Layer .....	41
Figure 8-7 2D Mesh of a Section of Pontoon Layer.....	41
Figure 8-8 Pontoon Layer Mesh Closer to Platform .....	42
Figure 8-9 overview of 3D Mesh of Computational Domain (Generated from ParaView) .....	42
Figure 8-10 Assumed Block of Platform for calculation of Metacentric Height .....	44
Figure 8-11 Frontal Area of Platform Exposed to Wave.....	45
Figure 8-12 Comparison of Drag Coefficients for Three Cases.....	46
Figure 8-13 Mesh Convergence Plot.....	46
Figure 8-14 free surface 3D contour for Case 3 (generated from ParaView) .....	47
Figure 8-15 Surface Elevation 10 meters Behind the Platform.....	47
Figure 8-16 Drag Force Plot for Stokes Fifth Wave Case.....	48
Figure 8-17 Lift Force Plot for Stokes Fifth Wave Case.....	50
Figure 8-18 Approximated System for TLP Heave Motion.....	50
Figure 8-19 Approximated System for TLP Roll Motion .....	51
Figure 8-20 Heave Motion of Platform .....	52
Figure 8-21 Roll Motion of Platform .....	52

Figure 8-22 Vertical Displacements of Front and Back Sides .....	52
Figure 8-23 Tension in Front and Back Tendons (Stokes Fifth Wave Case).....	53
Figure 9-1 Computational Domain (2D Test Case).....	55
Figure 9-2 Visualization of Free Surface (from Time Instant 0.15-1.4) .....	57
Figure 9-3 Surface Elevation Plots, a) at Time Instant 0.158 seconds. b) at Distance 3.27 Meters from Inlet.....	57
Figure 10-1 Computational Domain for foc3DNewwave .....	59
Figure 10-2 2D Section of Mesh without Platform .....	59
Figure 10-3 Surface Elevation Ranging from 19-26 seconds.....	60
Figure 10-4 Comparison of Surface Elevation of Stokes Fifth and Superposed Wave.....	60
Figure 10-5 Computational Domain (Matching Standard 1 Case).....	61
Figure 10-6 3D Visualization of Free Surface (Superposed Wave) .....	61
Figure 10-7 2D View of Superposed Wave .....	62
Figure 10-8 Surface Elevation Plot at Focal Point .....	62
Figure 10-9 Tension in Tendons at Front and Back side of Platform (Matching Standard 1 Case).....	62
Figure 10-10 Methodology of Wave Simulation, Fulfilling Matching Standard 2 .....	63
Figure 10-11 Comparison between Matching Standard 2 Wave and Stokes Fifth Wave .....	64
Figure 10-12 Computational Domain (Matching Standard 2 Case).....	65
Figure 10-13 Tension in Tendons at Front and Back side of Platform (Matching Standard 2 Case)....	65
Figure 11-1 Comparison of Tensions in Front Tethers between Matching Standard 1 Case, Stokes Fifth Wave Case and Matching Standard 2 Case .....	66
Figure 11-2 Comparison of Tensions in Back Tethers between Matching Standard 1 Case, Stokes Fifth Wave Case and Matching Standard 2 Case .....	66
Figure 11-3 Comparison of Tensions in Front Tethers between Stokes Fifth Wave Case and Matching Standard 2 Case .....	67
Figure 11-4 Comparison of Tensions in Back Tethers between Stokes Fifth Wave Case and Matching Standard 2 Case .....	67

## **LIST OF TABLES**

Table 2-1 Selection of Environmental Loads for Tether Design.....	12
Table 6-1 Flow Properties for 2D Test Case .....	27
Table 6-2 Mesh Structure for 2D Test Case .....	28
Table 6-3 Boundary Conditions (2D Test Case) .....	29
Table 6-4 Simulation Parameters .....	29
Table 6-5 Properties Calculated by Waves2Foam .....	30
Table 6-6 Flow Properties (3D Test Case) .....	32
Table 6-7 Mesh Structure (3D Test Case).....	33
Table 6-8 Boundary Conditions (3D Test Case) .....	33
Table 6-9 Wave Properties Generated by Waves2Foam.....	34
Table 7-1 Dimensions of Snorre A (Johannessen, Haver, Bunnik, & Buchner, 2006) .....	35
Table 8-1 Missing Dimensions of Snorre A and their Assumed Values .....	37
Table 8-2 Input Parameters (Stokes Fifth wave without Platform).....	39
Table 8-3 Input Parameters (Stokes Fifth wave without Platform).....	43
Table 8-4 Inputs for Calculation of Forces and Force-Coefficients on Platform .....	43
Table 8-5 Wave Properties Generated by Waves2Foam.....	44
Table 8-6 Mesh Parameters for Mesh Convergence Cases .....	45
Table 8-7 RMS Values of Drag Coefficients for Three Cases .....	46
Table 9-1 Input Parameters for 2D Test Case .....	56
Table 10-1 Wave Input Parameters of foc3DNewwave .....	58
Table 10-2 Attributes of Focal Point .....	60
Table 10-3 Computed Actual Location of Focal Point and Focal Time .....	64
Table 11-1 Maximum system Stress for the Three Evaluated Cases .....	68
Table 11-2 RMS values of Front and Back Tether Tension for 3 Evaluated Cases .....	68
Table 11-3 Non-dimensionalizing of Parameters .....	68

(This page is intentionally left blank)

## ***LIST OF SYMBOLS***

<i>d</i>	<i>Water depth</i>
<i>L</i>	<i>Wavelength</i>
<i>g</i>	<i>Gravitational acceleration</i>
$\eta$	<i>Surface elevation</i>
<i>H</i>	<i>wave height</i>
<i>a</i>	<i>crest elevation</i>
$\eta$	<i>water surface elevation from MWL</i>
<i>L</i>	<i>wavelength</i>
<i>u</i>	<i>particle velocity along x-axis</i>
<i>w</i>	<i>particle velocity along z-axis</i>
<i>T</i>	<i>time period i.e. time in seconds between two consecutive crests or troughs</i>
<i>s</i>	<i>Wave steepness</i>
<i>c</i>	<i>Phase velocity of wave</i>
<i>k</i>	<i>Wave number</i>
$\omega$	<i>Angular frequency</i>
<i>n</i>	<i>Order of the Stokes wave</i>
$\Theta(\epsilon^n)$	<i>Truncation error of order <math>\epsilon^n</math></i>
$\epsilon^n$	<i>Order of truncation error</i>
$v_{horiz}$	<i>Horizontal velocity</i>
$a_{horiz}$	<i>Horizontal acceleration</i>
$v_{vert}$	<i>Vertical velocity</i>
$a_{vert}$	<i>Vertical acceleration</i>
$\alpha$	<i>Numerical constant and scalar variable used in VOF method</i>
$\beta$	<i>Numerical constant</i>
$\omega$	<i>Wave-frequency</i>
<i>U</i>	<i>Free stream fluid velocity</i>
$S_{PM}$	<i>Spectral density of Pierson-Moskowitz spectrum</i>
$S_J$	<i>Spectral density of JONSWAP spectrum</i>
$\sigma$	<i>Numerical constant</i>
$\tau$	<i>Shear Stress</i>

$\rho$	<i>Density</i>
$F$	<i>Force</i>
$D$	<i>Differential operator</i>
$\nabla$	<i>Del operator</i>
$q$	<i>Weighing parameter used in relaxation zone</i>
$A_{Ref}$	<i>Under-water frontal area of platform</i>
$M$	<i>Metacenter</i>
$Mt$	<i>Metric ton</i>
$B$	<i>Center of buoyancy</i>
$L_B$	<i>Distance between center of buoyancy and MWL</i>
$BM$	<i>Distance between center of buoyancy and metacenter</i>
$F_D$	<i>Drag force</i>
$F_L$	<i>Lift force</i>
$M_{total}$	<i>Total moment</i>
$M_D$	<i>Moment created by drag force</i>
$M_L$	<i>Moment created by lift force</i>
$F_{Limbalance}$	<i>Imbalance in lift force</i>
$F_{T1}$	<i>Lift force on back side of platform</i>
$F_{T2}$	<i>Lift force on front side of platform</i>
$M$	<i>Mass of platform</i>
$x'$	<i>Vertical velocity of platform</i>
$x$	<i>Vertical displacement of platform</i>
$x''$	<i>Vertical acceleration of platform</i>
$\omega_o$	<i>Natural frequency of platform</i>
$H_s$	<i>Significant wave height</i>
$T_s$	<i>Significant time period</i>
$f_p$	<i>Frequency of superposed wave</i>
$T_p$	<i>Time period of superposed wave</i>

## **ABBREVIATIONS**

<b>TLP</b>	<i>Tension Leg Platform</i>
<b>FPSO</b>	<i>Floating, Production, Storage and Offloading</i>
<b>FSO</b>	<i>Floating Storage and Offloading</i>
<b>C-TLP</b>	<i>Conventional Tension Leg Platform</i>
<b>E-TLP</b>	<i>Extended Tension Leg Platform</i>
<b>Moses TLP</b>	<i>Moses Tension Leg Platform</i>
<b>SeaStar TLP</b>	<i>SeaStar Tension Leg Platform</i>
<b>VIV</b>	<i>Vortex Induced Vibrations</i>
<b>SPMT</b>	<i>Self-Propelled Modular Transport (SPMT)</i>
<b>ULS</b>	<i>Ultimate Limit State</i>
<b>ALS</b>	<i>Accidental Limit State</i>
<b>LAT</b>	<i>Lowest Astronomical Tide</i>
<b>GPL</b>	<i>General Public License</i>
<b>BBC</b>	<i>Bottom Boundary Condition</i>
<b>CFD</b>	<i>Computational Fluid Dynamics</i>
<b>HAT</b>	<i>Highest Astronomical Tide</i>
<b>MWL</b>	<i>Mean Water Level</i>
<b>VOF</b>	<i>Volume of Fluid</i>
<b>CoG</b>	<i>Center of Gravity</i>
<b>2D</b>	<i>2 Dimensional</i>
<b>3D</b>	<i>3 Dimensional</i>

(This page is intentionally left blank)

# **1 INTRODUCTION**

## ***1.1 History of offshore petroleum***

Offshore petroleum industry is almost 120 years old, started off the coast of Summerfield, California in 1896. Henry L. Williams and his associates built wooden piers, 35 feet high and about 300 feet out in the Pacific Ocean (Wells, 2016). They mounted a standard cable-tool rig on them and they started production in 1897. This resulted in 22 more companies joining this boom by developing a row of wooden piers that were up-to 1350 feet away from shoreline, into the ocean. (National Commission on the BP Deepwater Horizon Oil, 2010). The field produced for 25 years and everything was abandoned afterwards leaving behind a blackened beach and debris of piers which stood there until wiped out by a strong tidal wave in 1942 (National Commission on the BP Deepwater Horizon Oil, 2010).

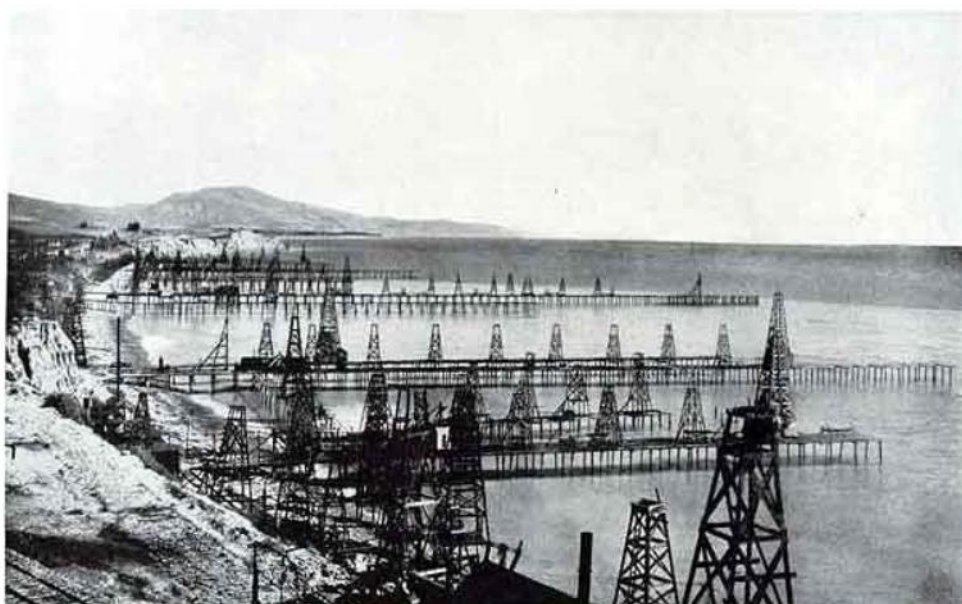


*Figure 1-1 drilling and production piers at Summerland, California, 1897 (Wells, 2016)*

Not much advancements were noted in the offshore industry until 1947 when McGee Industries drilled a production well that was beyond the sight of land. It was located 10.5 miles off the Louisiana coast. The water depth was still very less i.e. 18 feet (National Commission on the BP Deepwater Horizon Oil, 2010). However, that time, due to marked advancements in drilling technologies, sophisticated rotary rigs were used instead of unidirectional pile drivers and a steel structure as a platform was used instead of wooden structure (National Commission on the BP Deepwater Horizon Oil, 2010).

This chain of events gave birth to offshore petroleum industry, an industry that has evolved as much in past few decades as to accommodate 30 percent of today's total petroleum production worldwide (MODEC-Inc, 2016). Today offshore petroleum is a completely different domain of petroleum industry with its own advancements, research activities, problems and solutions.

## ***1.2 Modern Offshore petroleum***

Offshore petroleum nowadays is defined through a remote standalone platform installed in the sea in a water depth ranging from 30 meters to 3,000 meters (MODEC-Inc, 2016). An offshore field is defined today by the type of platform installed. The platform is a vital component of an offshore petroleum field. All the activities whether it is drilling, production, storage or transportation, are controlled through platform. Platform is the first thing to install on the drilling and production site and last thing to remove. A good platform maintains trouble-free production and drilling operations and ensures safety of the working crew.

## ***1.3 Types of offshore platforms***

Throughout the era of offshore industry development, many types of platforms are developed and currently are in use. The choice of type of a platform depends upon the design objectives of the field. To simplify the process of selection of the type of platform suitable for a specific field and its characteristic parameters, design objectives are categorized into three main groups (Task Group on Complaint Offshore Platforms, 1989).

### ***1.3.1 Functional and operational parameters***

- Functional requirements of platform
- Surface area requirements
- Total payload
- Physical requirements e.g. size, displacement, weight, freeboard etc.
- Material requirements
- Fabrication requirements
- Platform transportation options
- Timeframe for design and manufacturing
- Maintenance and operational needs
- Installation requirements
- Environment and safety requirements
- Standards and certifications

### ***1.3.2 Marine architect and hydrodynamic parameters***

- Installation site parameters e.g. water depth, wind data, wave data, current data etc.
- Center of gravity and buoyancy requirements
- Distribution of weight
- Required payload capacity of deck
- Geometry
- Size optimization
- Interaction of members
- Environmental forces
- Fatigue problems
- Risk analysis
- Model testing
- Redundancy and reliability analysis

### ***1.3.3 Economic parameters***

- Budget
- Cost
- Contracts
- Timeframe
- Payoff
- Stakeholders
- Previously available equipment

All these parameters collectively predict the best possible choice of a platform for a specific field.

The offshore industry started with the fixed offshore structures and platforms (as per discussed before). In the recent years of development, the operational activities were restricted to the areas closer to the shore because of safety issues, uncertainties and risks involved and lack of knowledge about the ocean behavior. However, with the passage of time, as the research revealed the mysteries of ocean behavior and uncertainties were eliminated, the companies extended their exploration and production activities toward deeper water depths. Today, the deepest operational platform is the Petrobras America Cascade FPSO in the Walker Ridge 249 field in 2,600 meters of water (Wikipeida, 2016). The increased water depth has changed the environmental and operational parameters of the fields and hence changed the design of platforms as well. Currently, offshore platforms are divided into two general categories.

- Fixed platforms
- Floating platforms

### ***1.3.4 Fixed Platforms***

When the petroleum activities started in offshore environment, the first and easiest choice was fixed platforms. Fixed platform is a structure that is firmly fixed on the seafloor and stays above the water level. In shallow waters, closer to the shore, the fixed platforms are very efficient because of their less mobility. They resist the forces imposed by wind, currents and waves by generating large reaction forces and less motion. They have very small natural period because of high weight to height ratio. In shallow waters, almost all of the operational fixed platforms have natural periods less than five seconds, which lies below the high-energy sea where the dominant wave periods are between five to twenty seconds (Task Group on Complaint Offshore Platforms, 1989). Currently operational fixed platforms and the new designs are available in different configurations but the behavioral characteristics of all configurations are more or less similar. Their operational range extends from 6 meters of water depth up to 412 meters (Balldate (Vannucci & RINA, 2011)). The commonly used configurations of fixed platforms are (Vannucci & RINA, 2011):

- Jacket structure
- Gravity based
- Guyed towers
- Complaint structures

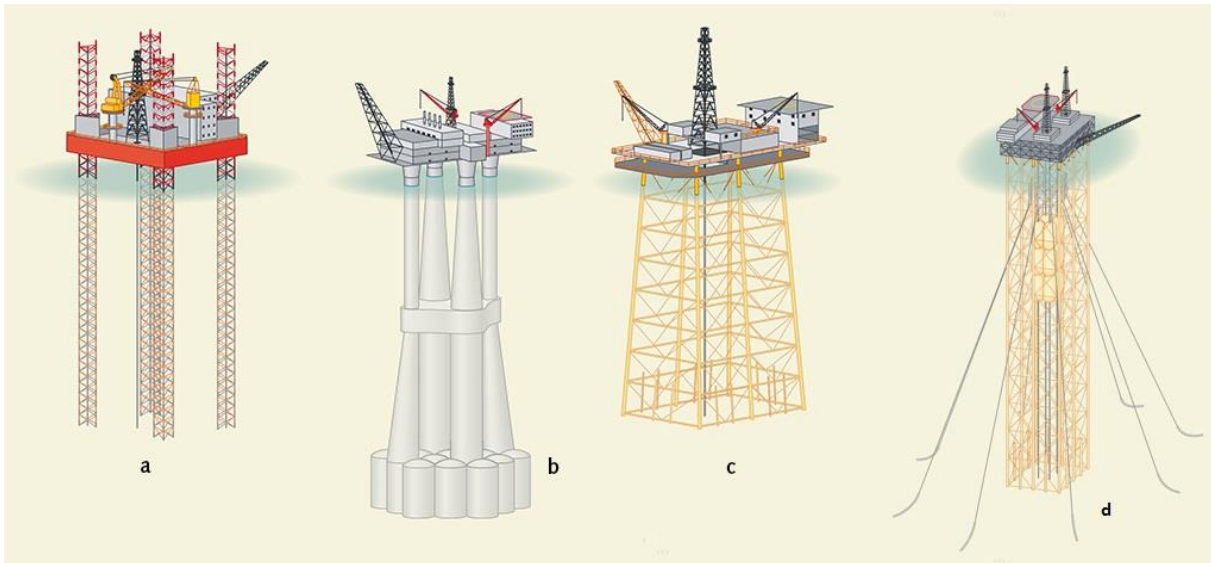


*Figure 1-2 Types of Fixed Platforms a: Complaint Structures, b: Gravity Based, C: Jacket Structures, d: Guyed Towers  
(World Ocean Review, 2016)*

The most common and eldest fixed platform is steel jacket platform on a pile foundation. They are used in very shallow water depths, mostly around 150-180 meters in North Sea, with deepest is Bullwinkle jacket installed in 412 meters of water depth and owned by Shell (Vannucci & RINA, 2011). A complaint tower is similar to the jacket platform in structure but unlike jacket platforms, it is designed to have flexible behavior against waves, currents and wind. They are designed for deeper water depth as compared to the operational areas of jacket platform and have time-periods such that they sustain significant lateral deflections. They are used typically in water depth range of 450-900 meters with the deepest complaint tower is Baldpate installed in water depth of 580 meters (Vannucci & RINA, 2011).

Gravity based structures, on the other hand, are firmed on the seafloor through their weight. They do not need any foundation for support instead, they are just placed on the seafloor and deck is installed on the top. Because of large volume and high weight, concrete is the best material for their construction.

## 1.4 Floating platforms

If a fixed platform is installed in a deeper water depth, the weight to height ratio decreases. It means for larger supporting tower, the weight bearing capability is very low hence response period of such a platform will be greater than five and will come in the high energy sea period range. Moreover, the size of supporting tower will increase both in height and volume hence the cost for manufacturing, transportation and installation will significantly increase. To overcome such problems, the concept of floating platforms was introduced. The floating platforms are more responsive to the external disturbance and they are designed to keep their natural period above the high energy sea period range i.e. above twenty seconds (Task Group on Complaint Offshore Platforms, 1989). They are kept in the place, vertically through their buoyancy and laterally through mooring systems such as chains, ropes, cables and anchors or through tension legs. The modern technique is to use dynamic positioning system that comprises of computer-controlled thrusters and a precise sensing system which senses the movement of the platform and switches the thrusters accordingly. The floating platforms are classified as (Vannucci & RINA, 2011):

- Semi-submersible platforms
- Tension Leg Platforms (TLPs)
- Spar platforms

- Floating, production, Storage and Offloading (FPSO) vessel

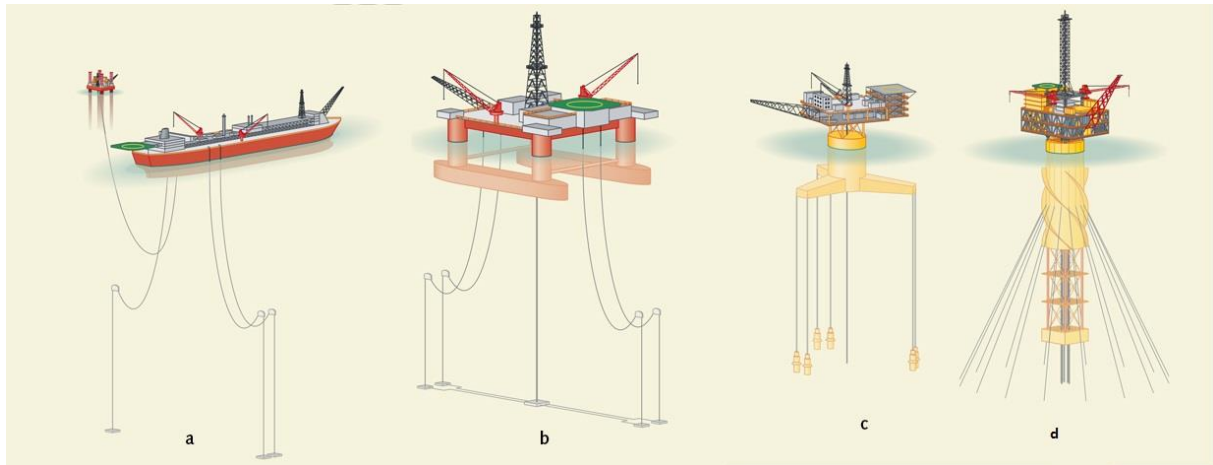


Figure 1-3 Types of Floating Platforms a: FPSO, b: Semi-Submersible, c: TLP, d: Spar (World Ocean Review, 2016)

Fixed platforms are always the best choice for production for offshore fields because of their highly predictable behavior, less criticality, low risks and uncertainties and in some case low costs but for deep waters applications, they are not practical and companies were forced to shift toward the floating platforms. Of all the available types, the FPSO is the most commonly used floating platform but it has narrow range of restrictions of the water depth, size of the field and rate of production. FPSO cannot be implied on large fields and for high production rates. Currently, there are 360 floating offshore platforms in operation of which 170 are Floating, Production, Storage and Offloading (FPSO) platforms, 30 are Tension Leg Platforms (TLPs), 20 are Spars, 40 are Production Semi-Submersibles and 100 are Floating Storage and Offloading (FSO) vessels (MODEC-Inc, 2016). For the current study, Tension Leg Platform (TLP) is of concern.

## 1.5 Tension Leg Platform (TLP)

TLP is not a completely new concept, instead it is a modification and combination of previously available concepts. The basic difference between the TLP and others floating platforms is the fact that the buoyancy of a TLP exceeds beyond its weight, hence to keep the desired freeboard for the platform, and keep it in equilibrium, a mooring system is required to connect the platform to the seafloor. The mooring system is different as compared to other concepts in the sense that taut lines are used in the exact vertical configuration and these lines are pre tensioned in the equilibrium state to keep the desired freeboard of the platform. These vertical mooring lines are called tension legs, tendons or tethers. Tubular pipes, cables and wire ropes are commonly used as tension legs or tendons (Task Group on Complaint Offshore Platforms, 1989).

The research and development work on TLPs initiated in early 1970's by Pauling and Horton (Pauling & Horton, 1970). The first working TLP was deployed by Conoco at the Hutton field, North Sea, United Kingdom (Task Group on Complaint Offshore Platforms, 1989). The real development on TLPs started after this success when the researchers came to know about the need for development in this field. A typical TLP is shown in Figure 1-4 with basic components:

- Hull
- Production facilities
- Platform rig
- Production risers
- Tendons

- Tendons' foundation or pile connections

The basic schematics of platform is very similar to the semi-submersible platform with the only difference in the mooring system being pre-tensioned and tendons are connecting each corner of the hull to the foundation at seafloor. Unlike semi-submersibles, the TLP is not allowed to move in vertical direction due to pre tension but can move sideways (surge, sway and yaw), but this movement is also restricted considerably due to pre-tension (Task Group on Complaint Offshore Platforms, 1989). The deck of TLP is designed such that after carrying all the required operational equipment and accommodation of working crew, the buoyancy still remains larger than the weight to maintain tension in the tendons.

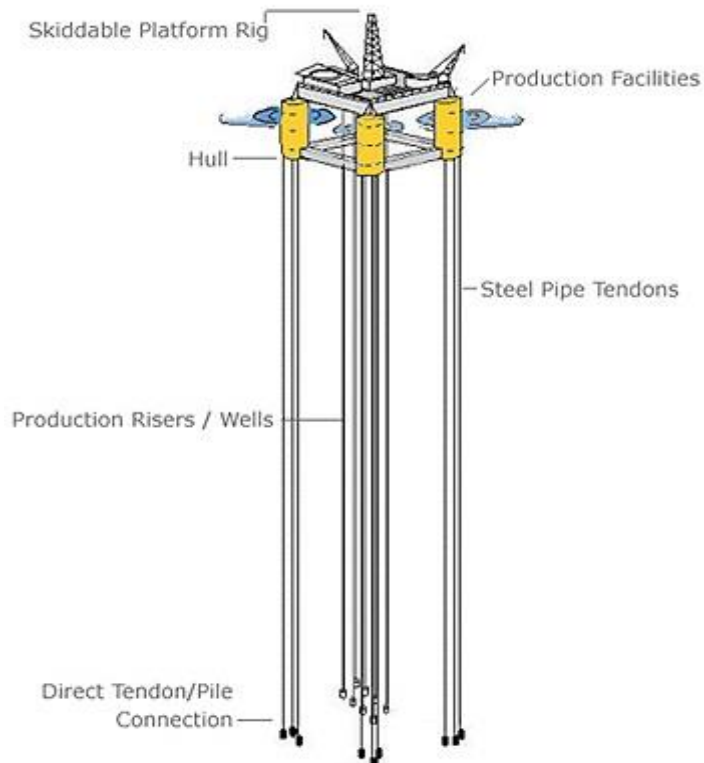


*Figure 1-4 A Typical Tension Leg Platform (Offshore technology.com, 2016)*

There are four general concepts of TLPs (XU, 2009):

**Conventional Tension Leg Platform (C-TLP):** A conventional four leg TLP (shown in Figure 1-5) consists of four columns. Each column is connected with the next through pontoons with a deck at the top. It is the simplest and eldest concept of TLP. The other concepts are more or less modifications or technical improvements of this concept. All the four cylinders are connected to the pile foundations on seafloor through tendons.



*Figure 1-5 conventional Tension Leg Platform (C-TLP) (Paixao, 2016)*

**Extended Tension Leg Platform (E-TLP):** An extended TLP (shown in Figure 1-6), a concept developed by ABB Ltd. (XU, 2009), is exactly the same in construction like a conventional TLP. The only difference is that all tendons are not attached directly to the cylinders, instead a radial pontoon is extended out of each cylinder at the bottom and two tendons are attached to that extrusion. This is helpful for the cases where low column space is required with the same restoration forces. Less column space results in less deck area and hence ease in manufacturing, transportation and installation and also reduced material cost.

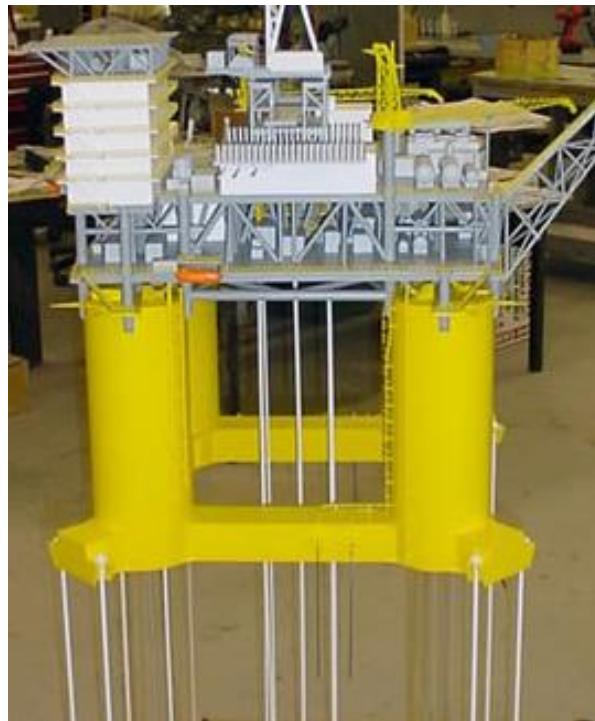


*Figure 1-6 Extended Tension Leg Platform (IHRDC, 2016)*

**Moses Tension Leg Platform (Moses TLP):** The MOSES four leg mini TLP (shown in Figure 1-7) concept was developed by MODEC International LLC (XU, 2009). It consists of four columns with smaller cross-sectional areas but concentrated more towards the center of the platform. At base of each column, there is a large radial hull extrusion as a connecting point for two tendons. This concept is used

for situations where very small deck area is required hence high stability and less material cost is achieved through this concept.



Figure 1-7 A Moses Tension Leg Platform (Offshore technology.com, 2016)

**SeaStar Tension Leg Platform (SeaStar TLP):** A SeaStar TLP (shown in Figure 1-8) is a three-leg mini TLP concept developed by Atlantia Offshore Ltd. (XU, 2009). There is only one large column, at the center of the platform with high cross section area as compared to the individual columns of other TLP concepts. All the Buoyancy is incorporated by the single column. There are 3 radial extensions of the hull at the base of the column that is why it is also called three legged TLP. Each hull supports two tendon porches. The SeaStar TLP has advantage over the other concepts because of its relatively high hull efficiency, simplicity in design, good response and good design optimization characteristics. (Kibbee, Chianis, Davies, & Sarwono, 1994).

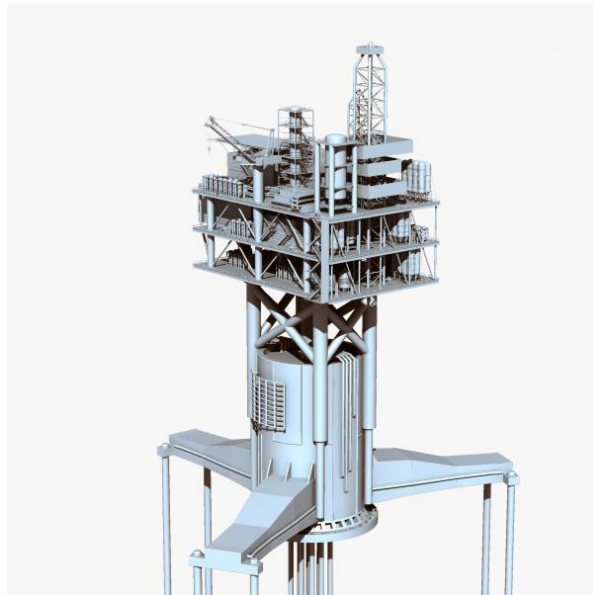


Figure 1-8 A SeaStar Tension Leg Platform (TurboSquid, 2016)

For all the concepts discussed, only the hull design and design of platform components are different, the design of mooring system i.e. tendons or tension legs and pile foundation, is same in sense of physical

concept and functional demands. The current study is not focused on the hull design, instead the tension legs design optimization is the key feature of this report.

## ***1.6 Tension legs (tendons)***

Tension legs, tendons or tethers are the part of mooring system of a TLP. These are permanent mooring lines attaching the hull of platform to the seafloor through pile foundations. The tendons are the unique and the most critical feature of a TLP (Harding & Banon, 1989). Apart from solid pipes and wire ropes, high strength material or composite materials can also be used as tendons.

There are several potential failure modes for a tendon e.g. failure of connection at the pile foundation, failure of connection at the cylinder, fatigue failure, failure due to corrosion, failure due to Vortex Induced Vibrations (VIV), maximum tension, minimum tension, foundation failure, fishing activities failure etc. the two most critical of all possible failure modes are maximum tension i.e. the case when buoyancy rises to critically high value or the platform moves sideways significantly, and minimum tension i.e. when the weight increases sufficiently so that instead of pretension, compression develops in the tendons. No matter which material is used, tendons must have good collapse and buckling properties (Task Group on Complaint Offshore Platforms, 1989).

## **2 DESIGN PROCESS OF TLP TENDONS**

A TLP passes through many phases through its life cycle. The first and most critical phase is the design phase. TLP is designed to withstand all the possible conditions whether they are environmental or accidental, which it may face through all of its life phases. All the characteristic parameters, dimensions, materials, deck area, weight bearing capacity etc. are defined in the design phase. Once the design is approved and manufacturing phase starts, it is almost impossible to change the characteristic design parameters because changing one parameter means redesigning of whole system as all characteristic parameters are interrelated. Design phase is critical because of risk and uncertainties associated with it as well. A fail design means the collapse of whole system which is not only a loss in sense of economics but also in sense of environmental and working crew safety. The following life phases are taken into consideration during design phase:

- **Manufacturing phase:** The components of the system are manufactured according to the design specifications. Manufacturing limitations, stress development during manufacturing, behavior of welds and connections etc. are taken as manufacturing phase design input parameters.
- **Assembly phase:** The components are not manufactured in one part, instead they are manufactured separately for sake of resilience and to simplify process of maintenance. These components are then assembled together onshore or at the offshore production site. The design parameters are defined such that the assembly process is easy and end connections are strong enough to withstand the operational loads.
- **Onshore transportation:** onshore transportation limitations are also taken into consideration during design process.
- **Load-out at offshore:** There are several available options for load-out of platform from onshore to the transport barge including direct lifting, skidding, Self-Propelled Modular Transport (SPMT) and floating on. Every method of load-out has its own pros and cons. One of these methods is selected during design phase and all limitations of selected method are considered during design.
- **Offshore transportation:** The barges available for offshore transportation also have their own limitations for weight, volume, center of gravity of the package etc. These limitations are taken into account during design process.
- **Installation:** Lifting operation during installation phase is a very critical process. In the uncertain sea environment, there are many loads that may influence the lifting process. All of these loads are considered during the design process of platform.
- **Operational phase:** This is the longest phase of a TLP life. A lot of uncertainties are associated with this phase. A platform is keenly designed for this phase as platform is exposed to maximum environmental loads during this phase and this phase is most likely to encounter extreme environmental event as compared to all other phases. Operational phase design and loads will be focused in the current study.
- **Decommissioning phase:** After the end of operational phase, the platform is decommissioned from the operational site for reuse or disposal. Platform is design in a way so that it is possible to decommission the platform and more likely to reuse as well instead of disposal.

### ***2.1 Operational phase design***

Operational phase of a TLP comprises the time when the deck is placed on the platform and activities like drilling, installation of risers, production, storage etc. start on it. The platform displays several

primary responses under the influence of environmental and structural loads during the operational phase of its life. These responses directly affect the tension, orientation and structural integrity of tendons. During the design process, extreme limits of these responses are calculated under the possible extreme loads and a failure criterion is set accordingly. The primary and critical responses of platform that act as input parameters of design process of tendons or tethers are (Task Group on Complaint Offshore Platforms, 1989)

**Offset:** Offset is the drifting of platform sideways from its equilibrium position. This drift-off causes the extra pull on the tendons which increases the tension. There are three types of offset a platform experiences:

a) **Steady offset**

- Mean wind drag on platform (hull and deck above the water surface)
- Current drag on platform (hull below the water surface), tendons and risers
- Wave drift on platform

b) **Low frequency offset**

- Dynamic wind draft
- Subharmonic wave load

c) **Wave-frequency offset**

**Set-down:** It is a phenomenon observed when the platform offsets. Due to the tension of tendons, the platform not only moves sideways, but also moves downwards. This results in decrease in draft of hull and increase in buoyancy force resulting increased tension in tendons.

**Tendon's tension:** The major reasons for tension in tendons, apart from mentioned above, are pretension, foundation dispositioning, tides and overturning moment on hull.

**Tendon's angle:** Tendon's angle is the angle between tendons; when platform is displaced and when platform is in equilibrium. This angle is used in calculation of stresses that develop in the tendon during offset and in case of moments.

**Draft:** The draft is the height of cylinders under the water surface. It is useful because a proper clearance between deck and water surface is required so that in usual operations and during extreme conditions, the waves does not hit the deck or water from wave crest does not seep into the deck equipment. The deck clearance changes during tide, heave motion, set-down and during wave crest hitting the platform.

## 2.2 Limit state control

According to Norwegian rules and regulations mentioned in (NORSOK, 1999) and (PSA, SFT and NSHD, 2001) an offshore structure must be designed against failure at two control levels i.e. Ultimate Limit State (ULS) control and Accidental Limit State (ALS) control (Johannessen, Haver, Bunnik, & Buchner, 2006).

In ULS, the design input parameters are 100 year return load levels for all the possible environmental, operational and functional loads acting on the platform, in case of current study, tendons. It must be ensured in the design that the tendons will not cross the minimum and maximum tension limits specified by ULS control. If tension is exceeding the maximum limit, it will overshoot the load bearing capacity and will damage. Similarly, if it is short of minimum limit then it will collapse due to buckling. Special factors are used for both the characteristic load and load bearing capacity in ULS control to incorporate uncertainties and ensure safety. The ULS control is assumed to be satisfied by the design if the characteristic load multiplied by its corresponding load factor is smaller than the load bearing capacity divided by its corresponding material factor. Different regulations have their own specifications for load factors and material factors. According to (NORSOK, 1999), Safety factor larger than 1 is used for

permanent and functional loads and less than 1 is used for environmental loads. On the other hand, according to (PSA, SFT and NSHD, 2001), safety factor of 1 is used for permanent and functional loads and less than 1 is used for environmental loads.

ALS control is for accidental situations like collisions, fire etc. for this control, the overall system integrity is given keen focus and local damages of some components is not considered in overall analysis (Johannessen, Haver, Bunnik, & Buchner, 2006).

### **2.3 Environmental loads input for design**

In the offshore environment, the basic environmental loads are wind, waves and current, but the design process consider all possible loading conditions that the platform might face. All the rare and extreme load events are considered and platform is designed to withstand all of those loads. The environmental loads considered for design are waves, wind, current, tides and marine growth (Task Group on Complaint Offshore Platforms, 1989).

According to Norwegian rules and regulations, the ULS and ALS design is developed for the tendons loads corresponding to an annual exceedance probability of  $10^{-2}$  and  $10^{-4}$  respectively. For predicting load corresponding to prescribed annual exceedance probability, a long term analysis is required. If we denote slowly varying environmental loads e.g. wind speed, significant wave height, peak period etc. by  $\vec{P}$  and 3-hours extreme tether load by  $X_{3h}$ , the long term distribution will be (Johannessen, Haver, Bunnik, & Buchner, 2006),

$$F_{X_{3h}}(x) = \iint \dots \int F_{X_{3h}|\vec{P}}(x|\vec{p}) f_{\vec{P}}(\vec{p}) d\vec{p} \quad (2.1)$$

Here,

$f_{\vec{P}}(\vec{p})$  is the long term joint distribution of the involved environmental characteristic.  
 $F_{X_{3h}|\vec{P}}(x|\vec{p})$  is a conditional distribution function of 3-hour extreme value given the environmental characteristic.

The most challenging part in the Equation 2-1 is the distribution function of environmental characteristic and conditional distribution of  $X_{3h}$ . Several statistical models and spectra have been proposed so far to approximate the behavior of waves in the ocean. The suitable model for the sea of concern is chosen and conditional distribution function is calculated for that model. For study of extreme events, significant wave height  $H_s$  and spectral peak period  $T_p$  are selected as a primary characteristic and distribution function for waves is developed for these selected conditions using approximated model chosen for the ocean. For the other parameters i.e. currents, wind and tides, fixed values with certain conservations are selected.

To achieve the limit of exceedance probability of  $10^{-2}$  imposed by regulations and standards, a 100 year return period of waves is need to be selected. The selection of the environmental parameters for ULS design is carried out according to the Table 2-1 (Johannessen, Haver, Bunnik, & Buchner, 2006). ULS control is discussed in the current study and wave loads are taken with 100 year retune period.

*Table 2-1 Selection of Environmental Loads for Tether Design*

<b>Loads</b>	<b>Waves</b>	<b>Wind</b>	<b>Current</b>	<b>Tide</b>
<b>ULS Minimum</b>	100 year return period for $H_s$ and $T_p$	100 years	With and without 10 years' current	Lowest Astronomical Tide (LAT)
<b>ULS Maximum</b>	100 year return period for $H_s$ and $T_p$	100 years	With and without 10 years' current	Highest Astronomical Tide (HAT) + 100 years' Storm Surge

### **3 RESEARCH OBJECTIVES AND MILESTONES**

For design of a tension leg platform, first of all a suitable statistical wave model is chosen for the ocean in which platform is supposed to be installed. Afterwards 100 year return period for  $H_s$  and  $T_p$  is calculated through the chosen statistical model. These are the prerequisite for the calculation of design loads. Selection of 100 year return period means, the design is carried out for the extreme event that has probability of exceedance of  $10^{-2}$  in 100 years.

In case of extreme wave event, a high amplitude waves strikes the platforms and applies impact force. Also the water level, in the region around the platform rises. The impact force pushes the platform sideways and the increased water level results in increased buoyancy force which pushes the platform upwards. Under the effect of these displacements, the tension in the tendons increases considerably. Moreover, another criticality in this situation is that after the impact of extreme event wave, the lift forces on side of impact are more than the opposite side due to the difference in water level and impact forces. It creates more tension in tendons on one side of platform than other.

The defining characteristics of extreme event wave can be predicted using statistical models and wave spectra but the calculation of extreme event impact forces is a tricky process. The sea at a given time and location is composed of many waves of different heights and time periods, propagating in all the directions. The extreme event wave, in actual, generates by the superposition of many wave components of different time periods and heights. The heights of all those waves happen to be positive at that point of sea and all these heights add up to form a wave of very large amplitude. After the superposition, all the individual components of that extreme event wave scatter in all directions to make the regular sea. According to the statistical wave models, the extreme event occurs very rarely in the whole life span of a platform as it has a very small probability of exceedance i.e.  $10^{-2}$ . Due to complex structure of platform and dynamic behavior of waves, it is almost impossible to calculate the impact loads of extreme event analytically. Certain approximations are required for analytical calculations but these approximations result in conservations in design and for offshore environment, where everything is very expensive, these conservations increase the cost significantly.

Another method for calculation of extreme event loads is model testing. Model testing is also a very expensive process and it has its own limitations. It is quite hard to develop the extreme event wave in real scenario through statistical wave model as it is a random process and exact time of its occurrence is not known. To make the process simple and to save the time, stokes fifth order waves with the same wave height and time period are generated, and their loads over the platform are taken as design input.

Computational Fluid Dynamics (CFD) simulation is also a solution for calculations up to certain accuracy and to save time and money. These simulations can be counter checked by the experimentations to validate results. Extreme event generation by simulation of statistical wave model is also very time consuming and costly using CFD. Stokes fifth order waves are used in CFD simulations as well, to simplify the process and to save time and money. CFD simulation is easier and less costly as compared to model testing and it has less limitations for environmental conditions generation as compared to model testing because unlike model testing, it doesn't scale down the physical parameters.

It has been observed in the recent decades that the extreme events are more likely to occur than what proposed by statistical wave models (Waseda, Rheem, Sawamura, Yuhara, & Kinoshita, 2005). Further research and experimentations (Sharma & Dean, 1981), (Jensen, Christensen, & Jacobsen, 2014), (Heilskov, 2015), (Wu, Chen, Bahuguni, Lu, & Kumar, 2015) etc., have shown that the approximation of extreme events through stokes fifth order wave or other type of regular waves is not very accurate, instead overestimates the impact loads and proposes overdesign which is quite expensive in offshore

environment. The accurate calculations are obtained by modeling the real extreme events either in model testing or in CFD simulations.

The purpose of the current study is to compare the impact loads of waves calculated by CFD simulation of extreme event wave through stokes fifth wave and generation of extreme event wave through the superposition of individual wave components of a selected statistical wave model at a desired point. The open source CFD software OpenFOAM is used for simulations. Waves2Foam library is used for generation of free surface waves in OpenFOAM. Following milestones are covered during the thesis.

1. Theory of free surface wave generation and methods of wave generation in OpenFOAM using waves2Foam library.
2. 2D and 3D wave generation in an arbitrary computational domain using waves2Foam library to understand the implication of boundary conditions and variables required for the wave generation of desired characteristics.
3. Selection of a TLP operating in North Sea for which dimensions and desired data i.e. statistical wave spectra and 100 year return period for  $H_s$  and  $T_p$  for selected statistical wave spectra, is published online by the operator.
4. Calculation of tension in tendons of selected TLP, by CFD simulation of stokes fifth order waves of selected 100 year return period over the selected TLP.
5. Calculation of tension in tendons of selected TLP, through generation and CFD simulation of extreme event wave according to the selected 100 year return period over the selected TLP.
6. Conclusions and recommendations.

## 4 POTENTIAL FUNCTION AND WAVE THEORIES

Fluid in motion is described by the potential theory. Potential theory is only valid for the ideal fluids. Ideal fluids are the ones that are irrotational and incompressible. In the case of water, the assumption of incompressibility is valid as the density of water shows negligible variation with the change in pressure. This assumption results in a very simple form of continuity equation with all the terms of density eliminated. The continuity equation for incompressible fluid takes the form as shown in Equation 4-1 (Moe)

$$\frac{\partial u}{\partial x} + \frac{\partial v}{\partial y} + \frac{\partial w}{\partial z} = 0 \quad (4-1)$$

Irrotationality in a fluid means that it does not rotate along all of the 3 dimensions of flow. This assumption is valid mostly for the laminar flow having no abrupt behavior and continuous streamlines of fluid. The assumption holds for waves with no swirl and eddies and without any breaking effect. An irrotational fluid flow is described by the following set of equations (Moe).

$$\frac{\partial u}{\partial y} - \frac{\partial v}{\partial x} = 0 \quad (4-2a)$$

$$\frac{\partial v}{\partial z} - \frac{\partial w}{\partial y} = 0 \quad (4-2b)$$

$$\frac{\partial w}{\partial x} - \frac{\partial u}{\partial z} = 0 \quad (4-2c)$$

An analytical relation that satisfies both of the above assumptions is Equation 4-3 (Moe)

$$\frac{\partial^2 \phi}{\partial x^2} + \frac{\partial^2 \phi}{\partial y^2} + \frac{\partial^2 \phi}{\partial z^2} = 0 \quad (4-3)$$

This equation is called Laplace equation. Here  $\phi$  is called velocity potential and Laplace equation is also called potential function.  $\phi$  is related to the velocities  $u$ ,  $v$  and  $w$  along  $x$ ,  $y$  and  $z$ -axis respectively as

$$\frac{\partial \phi}{\partial x} = u \quad (4-4a)$$

$$\frac{\partial \phi}{\partial y} = v \quad (4-4b)$$

$$\frac{\partial \phi}{\partial z} = w \quad (4-4c)$$

The solution for the potential function depends upon the water depth. The assumption of no loss of energy to friction is valid only for the water with infinite depth. For the waters where the depth is very large as compared to the wavelength of wave on the surface, the approximation of infinite depth is reasonably valid. For the water where the wavelength to depth ratio is not very high, other relations for potential are developed. Water depths are divided into 3 categories and different potential functions are developed for each of these categories with different assumptions. The division is according to the following rule (Moe):

- i. Deep water  $(d/L > 1/2)$

$$\varphi = \frac{ag}{\omega} e^{kz} \cos(\omega t - kx) \quad (4-5)$$

ii. Intermediate water       $(1/20 < d/L < 1/2)$

$$\varphi = \frac{ag}{\omega} \frac{\cosh k(z+d)}{\cosh kd} \cos(\omega t - kx) \quad (4-6)$$

iii. Shallow water       $(d/L < 1/20)$

$$\varphi = \frac{ag}{\omega} \frac{\cosh k(z+d)}{\cosh kd} \cos(\omega t - kx) \quad (4-7)$$

Here

$d$	Water depth
$L$	Wavelength
$g$	gravitational acceleration

Although the relation for the potential function is different for each of the categorized water depth, the wave profile or water surface elevation  $\eta$  is defined by the same relation (Equation 4-8) for all the three water depths. The surface profile remains same in all water depths; the only change is in the characteristics of water particles below the surface down to the seafloor.

$$\eta = \text{asin}(\omega t - kx) \quad (4-8)$$

When a particle is disturbed on the surface of water, it tries to retain its equilibrium position and starts to oscillate about its equilibrium position, just like a spring displaced from its equilibrium position. The restoring force in spring is the spring force and in case of water particles, gravity. This phenomenon extends to the whole surface to form the free surface waves (MIT OpenCourseWare, 2016). The most common type of waves generates at the interference between the atmosphere and water due to influence of gravity. Before the wave models, the waves were tried to be explained through wave theories. Each theory had certain assumptions but based on the same grounds of oscillating water particles. These ocean waves are categorized into two main types:

- Regular waves
- Irregular waves

## 4.1 Regular waves

Regular waves are periodic waves that can be expressed by a mathematical function and possesses repetitive characteristics. All linear and non-linear wave models are regular waves. Regular waves are further explained by two different types of theories,

- Linear wave theory
- Non-linear wave theories

### 4.1.1 Linear wave theory

The series of proposed wave theories started by the development of Airy wave theory. Airy wave theory is the simplest of all the wave theories with the assumption of a sinusoidal wave traveling in space and varying with time. A linear wave (Airy wave) along with its all concerning parameters is shown in Figure 4-1. These parameters are either part of or the base for the variables used in the relationship, developed for the Airy waves. It is a 2D representation but the relationship developed is for 3 dimensions.

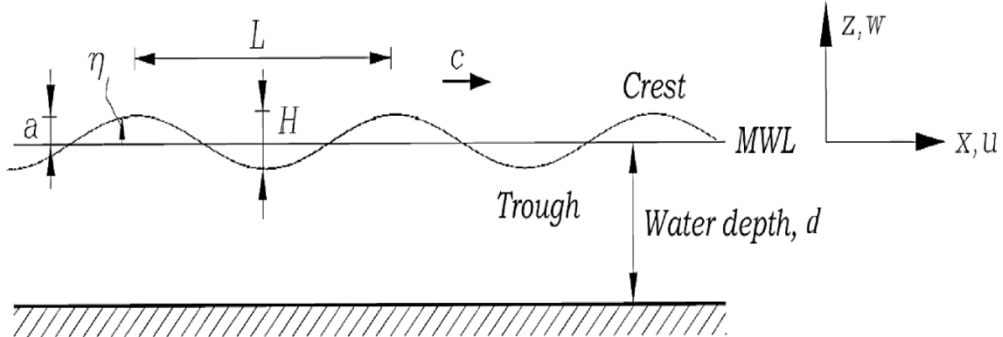


Figure 4-1 2 Dimensional Airy Wave (Obhrai, 2015)

Where in Figure 4-1:

$H$	wave height
$a$	crest elevation
MWL	Mean Water Level
$\eta$	water surface elevation from MWL
$L$	wavelength
$u$	particle velocity along x-axis
$w$	particle velocity along z-axis
$T$	time period i.e. time in seconds between two consecutive crests or troughs

Other parameters derived from the ones mentioned above are:

$$s = \frac{H}{L} \text{ wave steepness}$$

$$c = \frac{L}{T} \text{ phase velocity of wave}$$

$$k = \frac{2\pi}{L} \text{ wave number}$$

$$\omega = \frac{2\pi}{T} \text{ angular frequency}$$

Airy theory is based upon the potential theory for calculation of velocity fields with the assumption of no energy loss against friction. Airy wave theory is the only proposed linear wave theory. It linearizes free surface boundary conditions and the differential equation (Moe).

### 4.1.2 Nonlinear wave theories

Nonlinear waves are modelled by nonlinear equations. Nonlinear wave equations are mathematically complex and difficult to analyze. Stokes higher order waves are nonlinear waves and are discussed further since they are used in the current study.

As mentioned before, all the wave theories are developed on the same grounds of oscillating water particles. The nonlinear theories are developed on the same principle as the linear theory with addition of ‘n’ number of harmonics while defining the free surface. These theories are called Stokes higher order wave theories with general relation (Palomares, 2015):

$$\eta = \sum_{i=1}^n \eta_i = \sum_{i=1}^n a_i \cdot \varepsilon^{n-1} \cos(i(kx - \omega t)) + \Theta(\varepsilon^n) \quad (4-9)$$

Here

$$\begin{array}{ll} n & \text{order of the Stokes wave} \\ \Theta(\varepsilon^n) & \text{truncation error of order } \varepsilon^n \end{array}$$

Each ith component of Stokes wave has frequency double of its consecutive lower order and their amplitude can be calculated by applying Bottom Boundary Condition (BBC) i.e. horizontal velocity at seafloor is zero because of no-slip condition (Obhrai, 2015), kinematic boundary condition i.e. relationship between the velocity of particles at surface and velocity of surface (Obhrai, 2015) and dynamic boundary conditions i.e. pressure along the free surface must be equal to the atmospheric pressure (Obhrai, 2015). For defining the dynamic and kinematic boundary conditions, the assumption of linearity is eliminated up to the order of stokes theory. For example, for 2<sup>nd</sup> order Stokes wave theory, the dynamic boundary condition is expressed (Equation 4-10) in Tylor series of order 2 (Equation 4-10) (Palomares, 2015)

$$\frac{\partial^2 \varphi}{\partial t^2} + g \frac{\partial \varphi}{\partial z} + 2\nabla \varphi \cdot \nabla \frac{\partial \varphi}{\partial t} - \frac{1}{g} \frac{\partial \varphi}{\partial t} \frac{\partial}{\partial z} \left( \frac{\partial^2 \varphi}{\partial t^2} + g \frac{\partial \varphi}{\partial z} \right) = 0 + \Theta(\varphi^3) \quad (4-10)$$

Similarly, the kinematic boundary condition is expressed as (Palomares, 2015)

$$\eta = \frac{1}{g} \left( \frac{\partial \varphi}{\partial t} + \frac{1}{2} \nabla \varphi \cdot \nabla - \frac{1}{g} \frac{\partial \varphi}{\partial t} \frac{\partial^2}{\partial z \partial t} \right) + \Theta(\varphi^3) \quad (4-11)$$

This expression of boundary conditions through 2<sup>nd</sup> order Tylor series is named as Stokes expansion. The solution of Stokes 2<sup>nd</sup> order wave theory appears in the following form

$$\eta = A \cos(kx - \omega t) + \frac{1}{2} k^2 A^2 \cos(2(kx - \omega t)) \quad (4-12)$$

#### 4.1.2.1 5th order Stokes wave

The Stokes wave is a model for regular, steady state and unidirectional waves. Stokes model has assumed that all variation in the horizontal direction can be represented by Fourier series. It must be noted here that the relations involved in the development of Stokes theory are simplified through assumptions hence the final relation is very simple to solve and apprehend. In real scenarios, the free surface waves are quite hard to approximate as linear waves. The free surface behavior is very random and waves are not actually sinusoidal. Other wave theories, as a step forward of Stokes theory, were developed to account for this fact.

A Stokes wave has following key characteristics:

- a non-linear wave
- a periodic surface wave
- applicable for inviscid fluid layer of constant mean depth
- used for intermediate and deep water depths
- applicable for long waves of small amplitude

Stokes waves theories up to fifth order has been developed with stokes fifth wave having a very long expression. The mathematical formulation of surface elevation, wave speed, velocities and acceleration for the 5<sup>th</sup> order Stokes wave are presented in Equation set 4-13 (a-e) as (Wu, Chen, Bahuguni, Lu, & Kumar, 2015),

$$\eta = \frac{1}{k} \sum_{i=1}^n (\eta_n \cdot \cos(n - \theta)) \quad (4-13a)$$

$$c = \sqrt{\frac{gd \tanh(kd)}{kd} (1 + \lambda^2 \cdot C_1(kd) + \lambda^4 \cdot C_2(kd))} \quad (4-13b)$$

$$v_{horiz} = c \sum_{n=1}^5 (n \cdot \phi_n \cdot \cosh(n \cdot k \cdot s) \cos(n \cdot \theta)) \quad (4-13c)$$

$$a_{horiz} = \frac{2\pi}{T} c \sum_{n=1}^5 (n^2 \cdot \phi_n \cdot \cosh(n \cdot k \cdot s) \sin(n \cdot \theta)) \quad (4-13d)$$

$$v_{vert} = c \sum_{n=1}^5 (n \cdot \phi_n \cdot \sinh(n \cdot k \cdot s) \cos(n \cdot \theta)) \quad (4-13e)$$

$$a_{vert} = \frac{-2\pi}{T} c \sum_{n=1}^5 (n^2 \cdot \phi_n \cdot \sinh(n \cdot k \cdot s) \cos(n \cdot \theta)) \quad (4-13e)$$

For proper applicability of Stokes fifth order wave, the limitation is that value of d/L must be greater than 0.15 (Palomares, 2015).

As the wave steepness is increased, the accuracy of Stokes theory improves. However, high order is not always advantageous as increasing the order not only increases the complexity but also imposes limitation to the applicability of theory. Experimental results presented in several publications have shown that the 5<sup>th</sup> order Stokes wave model is suitable for North Sea applications. Stokes wave at different orders are presented in Figure 4-2. It can be seen that the 5<sup>th</sup> order Stokes wave has the highest steepness among all the different Stokes wave and therefore has highest accuracy. The Stokes fifth order wave is of interest for current study.

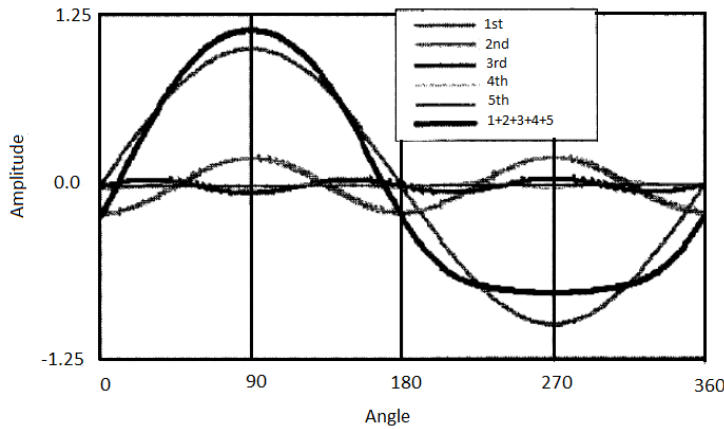


Figure 4-2 Different Stokes wave orders

## 4.2 Irregular waves

Irregular waves are stochastic waves that cannot be expressed by a mathematical function. They are random in nature and are modelled in terms of wave spectrum. Different wave spectra are used to describe different irregular sea states at different parts of the world. The most commonly used spectra are:

- Pierson-Moskowitz Spectrum
- JONSWAP Spectrum
- Tosaugen Spectrum
- ISSC Spectrum

### 4.2.1 Pierson-Moskowitz Spectrum

The Pierson-Moskowitz spectrum is an empirically determined spectrum that defines the distribution of energy with respect to frequency within the ocean. The Pierson-Moskowitz spectrum assumes that if the wind is blowing steadily for a long period of time, then the waves will reach in equilibrium with the wind. Such a sea state is known as fully developed sea. **Invalid source specified.** The relationship for Pierson-Moskowitz spectrum is shown in Equation 4-14.

$$S_{PM}(\omega) = \frac{\alpha g^2}{\omega^5} \exp \left[ -\beta \left( \frac{g}{\omega U} \right)^4 \right] \quad (4-14)$$

Here:

$\alpha$  is a numerical constant = 0.0081

$\beta$  is also a numerical constant = 0.74

$g$  is gravitational acceleration = 9.81 m/s<sup>2</sup>

$\omega$  is wave-frequency

$U$  is wind speed at 19.4 meters above the sea surface

## 4.2.2 JONSWAP Spectrum

Joint North Sea Wave Project (JONSWAP) spectrum is an empirical spectrum developed specifically for North Sea.

The JONSWAP spectrum is similar to the Pierson-Moskowitz spectrum with a limited fetch. JONSWAP spectrum nullifies the assumption of equilibrium between wind and sea surface, adopted by Pierson-Moskowitz spectrum. It was found through experiments that a sea never fully developed and has the potential to continue to develop due to non-linear wave interactions. Therefore, in the JONSWAP spectrum the waves continue to grow as stated by the  $\alpha$  term, and the peak of the spectrum is dependent on  $\gamma$  term. **Invalid source specified..** A typical expression of Jonswap spectrum is expressed as:

$$S_J(\omega) = \frac{\alpha g^2}{\omega^5} \exp\left[-\beta\left(\frac{\omega_p}{\omega}\right)^4\right] \gamma^\alpha \quad (4-15)$$

Here:

$\omega$  is angular frequency

$\omega_p$  is peak angular frequency

$$\alpha = \exp\left[-\frac{(\omega - \omega_p)^2}{2\omega_p^2\sigma^2}\right]$$

$$\sigma = \begin{cases} 0.07 & \text{if } \omega \leq \omega_p \\ 0.09 & \text{if } \omega > \omega_p \end{cases}$$

$\alpha$  is taken as constant with its value ranging from 0.0081 to 0.01. Its value depends upon the wind speed and fetch length of wind.

$$\beta = 5/4$$

For the North Sea, the most widely used wave spectrum is JONSWAP Spectrum and is used in the current study. Other spectrums are not discussed since they are out of scope.

## 5 WAVES2FOAM – A WAVE GENERATION LIBRARY OF OPENFOAM

The library waves2Foam is a toolbox of OpenFOAM used to generate and absorb free surface water waves (Jacobsen, Fuhrman, & Fredsøe, 2012). It is solely developed to generate different types of free surfaces waves and study of their impact on structures. Waves2Foam follows the same analytical expressions developed by researchers to define free surface waves. Waves2Foam itself is not a complete package for generation of waves and calculation of wave forces instead it aids OpenFOAM to execute free surface calculations. For understanding the physics behind Waves2Foam, the basic understanding of operational theory of OpenFOAM is required.

### 5.1 Fluid flow mechanics followed by OpenFOAM

Navier Stokes equations are the fundamental equation for fluid flow. The OpenFOAM computational code is based upon the Navier Stokes equations. To solve a specific number of variables, same amount of equations containing those variables are required. A fluid flow can completely be defined by eight variables i.e. velocities along x, y and z component of domain ( $u$ ,  $v$  and  $w$ ), pressure ( $p$ ), temperature ( $T$ ), viscosity ( $\mu$ ), heat conductivity ( $k$ ) and density ( $\rho$ ). To calculate the values of these variables at all the points of flow domain, the software needs eight equations and solving them at all points of flow domain will give the flow parameters throughout the domain. These eight equations are:

1. Mass balance (continuity equation) (Cengel & Cimbala)

$$\frac{\partial \rho}{\partial t} + \frac{\partial(\rho u)}{\partial x} + \frac{\partial(\rho v)}{\partial y} + \frac{\partial(\rho w)}{\partial z} = 0 \quad (5-1)$$

2. Momentum balance along x, y and z-axis of flow domain (Navier Stokes equations)

In general, Navier Stokes equation is in the form (Cengel & Cimbala):

$$\rho \frac{D \vec{v}}{Dt} = -\vec{\nabla} \cdot p + \vec{\nabla} \cdot \vec{\tau} + \vec{F} \quad (5-2)$$

For a particular direction, the expanded form of Navier Stokes equation is (Cengel & Cimbala):

$$\begin{aligned} \rho \frac{\partial u}{\partial t} + \rho \cdot u \cdot \frac{\partial u}{\partial x} + \rho \cdot v \cdot \frac{\partial u}{\partial y} + \rho \cdot w \cdot \frac{\partial u}{\partial z} &= \rho \frac{Du}{Dt} \\ &= -\frac{\partial p}{\partial x} + \frac{\partial}{\partial t}(\tau_{xx}) + \frac{\partial}{\partial y}(\tau_{yx}) + \frac{\partial}{\partial z}(\tau_{zx}) + F_x \end{aligned} \quad (5-3)$$

3. Energy balance (First law of thermodynamics) (Cengel & Cimbala)
4. Equation of state
5. Empirical relation between viscosity and heat conductivity comprise 2 final equations

These equations are complex differential equations and it is almost impossible to solve them simultaneously through analytical procedures. Numerical methods are applied by OpenFOAM to solve these equations simultaneously to get the values of the eight variables at all points of fluid flow. Only the equations relevant to this study are mentioned here. The other equations are for heat conduction and convention processes. It is also to mention here that these equations solve the fluid flow in laminar state only. To define the turbulent flow, different types of turbulence models are used. Every model has its own defined variables to solve the turbulent flow problem. For every specific variable, the model also has an equation added to the system of equations to maintain the balance between the number of

variables and number of equations. As the current study is a free surface wave problem, only free surface generation in OpenFOAM will be discussed thoroughly.

OpenFOAM is a widely used open source software for CFD. It is owned by the OpenFOAM foundation and is distributed under the General Public License (GPL). It gives the user the freedom to modify and redistribute the modified version of the software within the terms of license (CFD Direct, 2016). It is based on the programming language C++. It is the first and foremost C++ library to create executables called applications. Applications are categorized into two domains i.e. solvers and utilities. The complete simulation using OpenFOAM includes certain steps in a sequences (shown in Figure 5-1). It is supplied with pre-processing and post-processing environments, interface to them are OpenFOAM utilities, ensuring consistent data handling across all environments (Christopher, 2015).

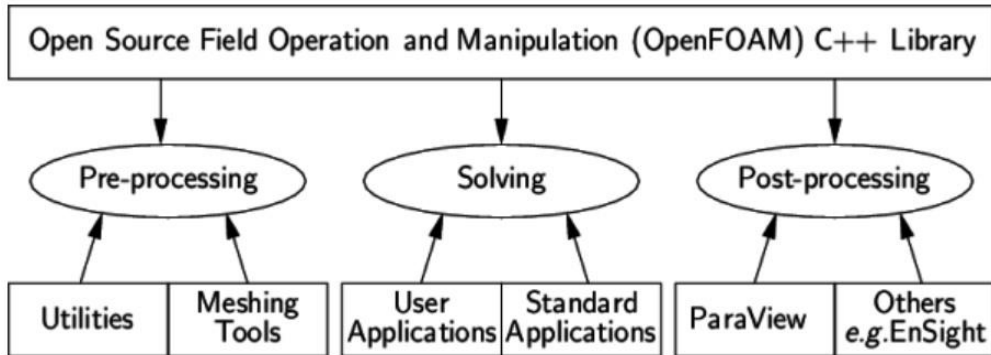


Figure 5-1 Overview of OpenFOAM Structure (CFD Direct, 2016)

The overview of OpenFOAM structure is shown in Figure 5-1. The pre-processing and post-processing are user controlled steps in CFD simulation process. The computational domain setup, meshing and introduction of boundary conditions are the main features of pre-processing. The post-processing includes the visualization and plotting of desired variables and results. The solving step of OpenFOAM structure is the one without the user interference. The user only has to select the solving utility and rest is done by OpenFOAM itself. In CFD, the volume of fluid (VOF) method is used to model the free surface. It models the free surface as fluid-fluid interface.

## 5.2 Volume of fluid method for multiphase flow

VOF is an Eulerian method which is described by a stationary or dynamic mesh. It is an advection scheme, therefore the Navier–Stokes equations describing the fluid flow motion characteristics have to be solved separately. Previously, Boussinesq-type or statistical method is used to model free surface waves. Both of these methods share a common limitation that they cannot resolve the distribution of turbulence in the surf zone. This problem was solved by Reynolds averaged Navier–Stokes equations approach.

VOF method is a technique developed by (Hirt & Nichols, 1981). It uses the approximation at the interface of water and air by introducing a scalar variable  $\alpha$  in the governing equations. The significance of  $\alpha$  is that it represents a portion of a volume of both fluids that are filled in the cells. The value of  $\alpha$  is bounded between 0 and 1. Generally,  $\alpha = 1$  means the cell is filled with water and  $\alpha = 0$  means cell is filled with air. The value of  $\alpha$  in between represents the portion of water, by percentage of volume, in the cell. This method is implemented with the Reynolds-Averaged Navier Stokes (RANS) equation for incompressible flows by adding a scalar transport for  $\alpha$  as shown in set of Equations 5-4.

$$\nabla \cdot \vec{U} = 0 \quad (5-4a)$$

$$\frac{\partial \rho \vec{U}}{\partial t} + \nabla \cdot (\rho \vec{U} \vec{U}) - \nabla (\mu_{eff} \nabla \vec{U}) = -\nabla p^* - \vec{g} \vec{r} \nabla \rho + \nabla \vec{U} \cdot \nabla \mu_{eff} + \sigma \kappa \nabla \alpha \quad (5-4b)$$

$$\frac{\partial \alpha}{\partial t} + \nabla \cdot \alpha \vec{U} + \nabla \cdot \alpha \vec{U}_c (1 - \alpha) = 0 \quad (5-4c)$$

The equations above are the governing equations for air and water flows in the present study. VOF method allows to express any of the fluid properties at any location of domain by means of a single analytical expression. The value of  $\alpha$  is calculated at all points throughout the domain and desired properties are calculated by simply weighing the properties of two phases in relation to their volume ratio  $\alpha$ . For instance, if density is required at a specific point in the flow domain, with  $\alpha$  known, it can be computed through the following relation:

$$\rho = \rho_w * \alpha + \rho_a * (1 - \alpha) \quad (5-5)$$

Here:

$\rho_w$	density of water
$\rho_a$	density of air

To avoid spreading of the free-surface, the transport equation needs to be computed by a numerical method to avoid excessive diffusion, therefore, VOF method depends greatly on the scheme used for the advection of the  $\alpha$  field. While a first order upwind scheme creates spreading at the interface, a downwind scheme with the same order creates a false spreading. The problem in solving VOF method is the inaccuracy of lower order numerical schemes. On the other hand, higher order schemes produce unstable results. In the original VOF publication by (Hirt & Nichols, 1981), a donor-acceptor scheme was introduced. This scheme laid basis for the compressive differencing. Currently, there are three different schemes used to solve VOF.

- Donor-acceptor scheme
- Higher order differencing schemes
- Line techniques

Without the VOF method, the free surface can only be simulated by generating dynamic mesh at the surface which is far more complex and less robust. VOF method also has some drawbacks (Afshar, 2010)

- i. It is not efficient method for wave generation in fluids with high surface tension
- ii. It doesn't compute reliable results for high wave steepness i.e. for  $s = H/L > 0.05$

Both of these drawbacks are not important to consider for current study as fluid involved is sea water and waves are large gravity waves hence surface tension effect is not much evident in the flow. Moreover, wave steepness is less than 0.05 for all simulation cases studied in current study.

### 5.3 Wave generation procedure

As discussed before, waves2Foam itself is not a complete platform for free surface wave generation and impact calculations over structures, instead it is a tool (library) of OpenFOAM to generate waves in the OpenFOAM domain and all the other involved operations are performed by OpenFOAM. Currently the method applies the relaxation zone technique (active sponge layer) and a large range of wave theories are supported and are already integrated in waves2Foam. A part from that, users also has option to create their own wave theory with desired relationships and input parameters.

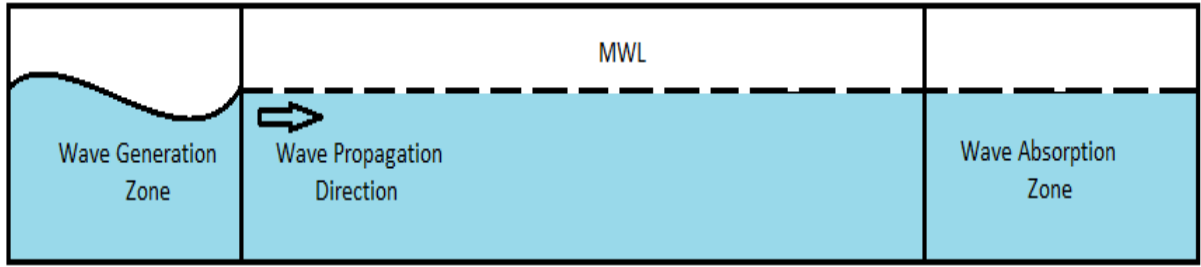


Figure 5-2 Schematic of Waves2Foam Case Setup

Figure 5-2 shows a schematic of waves2Foam case setup. The rectangular relaxation zones are shown at inlet, for wave generation and at outlet, for wave absorption. Relaxation zones keep the flow smooth by restricting the wave reflection and secondary wave components generation adjacent to the vertical boundaries.

### 5.3.1 Relaxation zone physics

VOF method allows the inlet relaxation zone to smoothly transform the analytical solution at its start, to a fully non-linear CFD solution at its end. Similarly, the outlet relaxation zone to no-wave (constant current) condition at the outlet boundary through outlet relaxation zone. A weighing parameter ‘q’, is introduced that increases exponentially from 0, at the inlet, to 1 at the end of inlet relaxation zone (Figure 5-3). Similarly, value of this weighing parameter decreases exponentially from 1 at the start of outlet relaxation zone to 0 at outlet (Figure 5-3). Where in Figure 5-3:

$L_{in}^{relax}$	Inlet relaxation zone
$L_{out}^{relax}$	Outlet relaxation zone

The Equations 5-6 show the smooth transition of horizontal velocity,  $\vec{u}$  and volume scalar variable,  $\alpha$  in equation form.

$$\vec{u} = (1 - q)\vec{u}_{target} + q\vec{u}_{computed} \quad (5-6a)$$

$$\alpha = (1 - q)\alpha_{target} + q\alpha_{computed} \quad (5-6b)$$

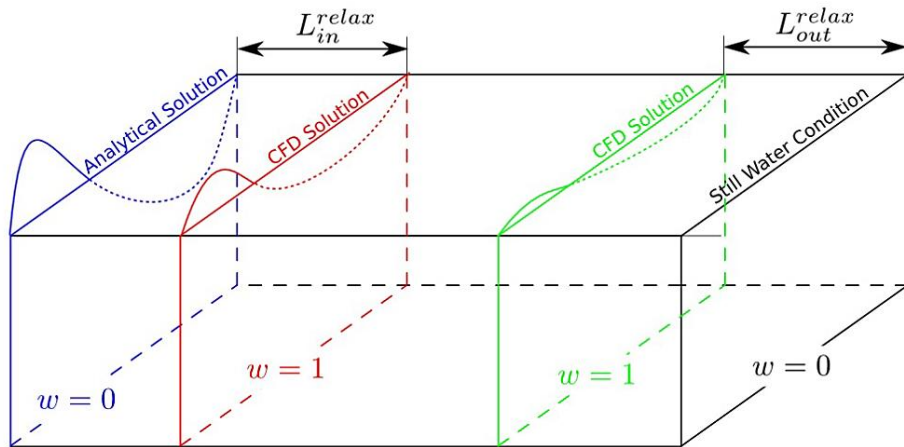


Figure 5-3 Illustration of Relaxation Zones (Wu, Chen, Bahuguni, Lu, & Kumar, 2015)

## **6 TEST CASES**

The simulation procedure in OpenFOAM involves many input parameters and different types of boundary conditions and flow parameters are possible to apply on the flow domain. Changing any of these parameters affect the flow chemistry along the flow domain. One out of many possible combinations gives the accurate flow characteristics. If the combinations of input parameters and boundary conditions is not correct, then either the simulation will give error or the results will not be accurate. To get the right combination and as a start, 2D and then a 3D wave generation case is developed using Waves2Foam library and explained in this section, by following the step by step simulation procedure of OpenFOAM.

### **6.1 2D test case**

The wave generation procedure is like developing a fully developed flow domain in OpenFOAM. The major steps to follow are same with some minor changes with respect to the type of flow or library used for simulation. The whole simulation in OpenFOAM comprises of three major steps (Figure 4-1).

- i. Pre-processing
- ii. Solving
- iii. Post-processing

Before the three major steps, another important task is to define computational domain. Defining the computational domain is the planning phase of the simulation in which the attributes of flow domain are set on the basis of previous literature's conclusions and recommendations.

#### **6.1.1 Computational Domain**

The size of the computational domain is very important factor which influences directly the time required for simulation, the cost of simulation, accuracy and difficulty in handling the mesh and results. The computational domain for wave generation has three regions i.e. wave generation region, CFD simulation region and wave absorption region. The size of every region is defined based on different factors. If sizes of the regions are small, the fluid does not have enough space to develop the flow properly which greatly affects the results. If computational domain is large as compared to as much required by the regions, it results in extra computational cost and complexity in handling mesh and results.

Figure 6-1 shows the computational domain chosen for the 2D test case. In the Figure 6-1, the dimensions are not according to a defined scale. These lengths are chosen according to one of the tutorial cases given in the wave2Foam files.

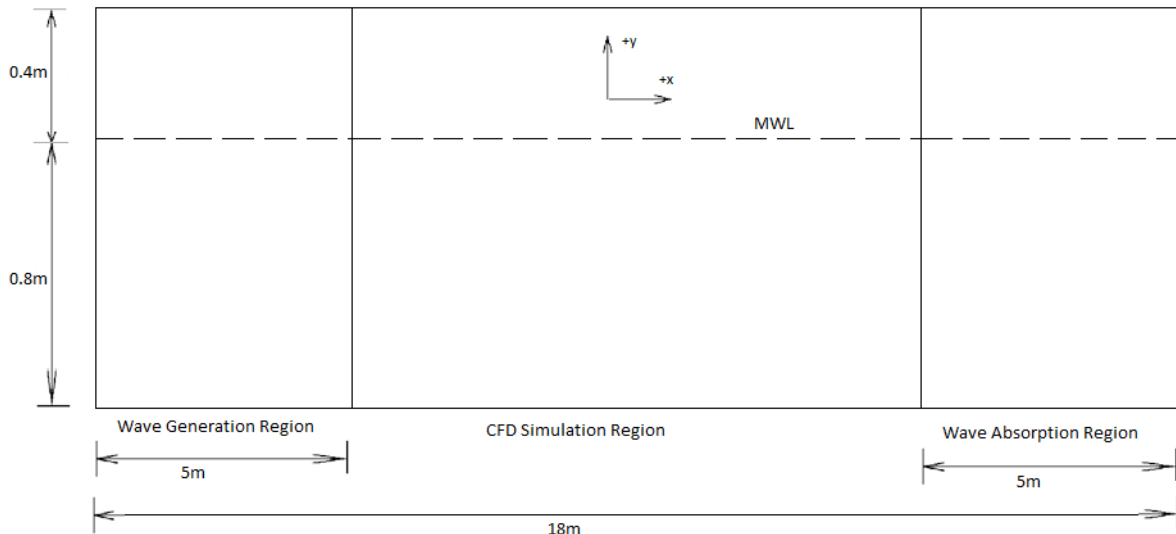


Figure 6-1 Computational Domain (2D Test Case)

The OpenFOAM cannot simulate totally 2D flow instead a 3D domain is required with a very small, one cell thickness as compared to other dimensions (0.1 meters in current case) with empty boundary condition on the side walls. This prevents the fluid flow along the thickness (into the page in the Figure 6-1) hence flow behaves like a 2D flow.

### 6.1.2 Pre-processing

It is the main step of OpenFOAM simulation structure. All the inputs are defined in this step. This step is totally under user control. The results in post-processing appear depending upon the inputs in this step.

Pre-processing has three types of inputs, defined by set of files in three different folders.

- i. Constant folder
- ii. 0 folder
- iii. System folder

#### 6.1.2.1 Constant folder

Constant folder includes the files for computational domain, mesh structure, physical properties of fluid and environment, dimension of regions of flow domain and characteristic properties of waves. For the 2D test case, the major features defined in constant folder are shown in Table 6-1. The dimensions or regions in computational domain are defined as in Figure 6-1. The mesh is defined in the file *blockMeshDict*, contained in the folder *polyMesh*, in the form of number of cells along each axis (Table 6-2). As the geometry of computational domain is simple, it is more convenient and efficient to develop mesh using the *blockMesh* utility. For complex geometries, like in the current study, the flow over a TLP, mesh generation software is used which are more flexible and user friendly in mesh generation process.

Table 6-1 Flow Properties for 2D Test Case

Property	value
Type of Mesh (Dynamic or static)	Static mesh
Gravitational acceleration	9.81 m/s <sup>2</sup> along negative y-axis

<b>Probe definition</b>	Wave gauges are defined along the length of flow domain for measuring free surface elevation.
<b>Type of fluid (water) (Newtonian or Non-Newtonian)</b>	Newtonian
<b>Viscosity of water</b>	1e-06 m <sup>2</sup> /s
<b>Density of water</b>	1000 kg/m <sup>3</sup>
<b>Type of fluid (air)</b>	Newtonian
<b>Viscosity of air</b>	1.48e-05 m <sup>2</sup> /s
<b>Density of air</b>	1 kg/m <sup>3</sup>
<b>Type of flow (Laminar or turbulent)</b>	Laminar
<b>Wave theory</b>	Stokes first order
<b>Water depth</b>	0.8 m
<b>Time period of wave</b>	2.0 s
<b>Phase shift in wave</b>	0
<b>Wave height</b>	0.1 m
<b>Wave direction</b>	Along positive x-axis

Table 6-2 Mesh Structure for 2D Test Case

Coordinate axis	Number of cells
x-axis	357
y-axis	60
z-axis	1

Apart from mesh definition, types of surfaces comprising boundaries of computational domain are also defined in the file *blockMeshDict* (Figure 6-2). Each boundary is assigned a specific type depending upon its possible role in the flow domain.

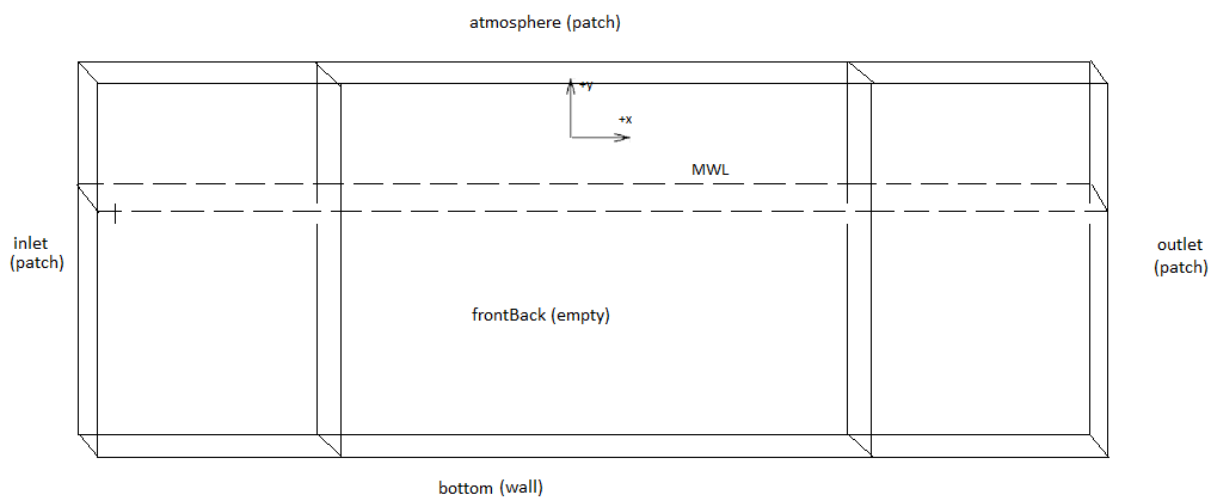


Figure 6-2 Computational Domain Boundaries' Types (2D Test Case)

The wave elevation is not calculated by OpenFOAM itself, instead wave elevation measuring gauges are installed at desired points in the computational domain to have the free surface plots at desired time instants. For 2D simulations, as there is only one section of flow, one line of gauges is installed along the length of computational domain. The gauges are defined in the file *constant/probeDefinitions*. Further to command the gauges to measure the desired properties, a file,

*constant/postProcessingProperties* is added. This file includes the parameters which gauges has to measure i.e. surface elevation in current case. OpenFOAM stores the measurements of surface elevation from each gauge, at every time step. These values are stored in two folders:

- i. ***postProcessedWaves2Foam***: it stores the measurements from each gauge separately, for all time steps, in separate files.
- ii. ***surfaceElevationAnyName***: it stores the measurements of all gauges at all time steps in a single file.

### 6.1.2.2 0 folder

0 folder includes files for setting boundary conditions at the boundary surfaces defined in *polyMesh*. For the 2D test case, boundary conditions defined are shown in Table 6-3. Boundary conditions for velocity, pressure and volume scalar variable,  $\alpha$  are defined on each boundary surface. For velocity and pressure, OpenFOAM requires only one of the two values on the boundary, the other value is computed by applying the flow equations (Christopher, 2015). Giving values of both velocity and pressure, results in over information which may cause problems in further simulation.

Table 6-3 Boundary Conditions (2D Test Case)

Boundary	$\alpha$ (alpha.water)	Pressure (p_rgh)	Velocity (U)
<b>inlet</b>	waveAlpha	zeroGradient	waveVelocity
<b>outlet</b>	zeroGradient	zeroGradient	fixedValue
<b>atmosphere</b>	inletOutlet	totalPressure	pressureInletOutletVelocity
<b>bottom</b>	zeroGradient	zeroGradient	fixedValue
<b>frontBack</b>	empty	empty	empty

### 6.1.2.3 System folder

This folder includes the files to define the solving utility, duration of simulation, the time step between each iteration, time step between each value storage and the tolerances. All the tolerances are pre-defined in tutorial files hence there is no need to change them unless there is a specific need or demand to do so. Only the solving utility, time step, duration of simulation and time step between each value storage are changed. The important values defined in this folder are shown in Table 6-4. The write control is set to *adjustableTimeRun*, which means that the value of time step (*deltaT*) is not fixed, it can be changed, while solving, by OpenFOAM upon need.

Table 6-4 Simulation Parameters

Parameters	Value
<b>startTime</b>	0
<b>endTime</b>	25
<b>deltaT</b>	0.001
<b>writeControl</b>	adjustableRunTime
<b>writeInterval</b>	0.2

### 6.1.3 Solving

There are four steps involved in the wave generation process by OpenFOAM after pre-processing is completed (shown in Figure 6-3). The execution of these steps depends upon the perfection in pre-

processing. If these are some shortcomings in pre-processing, errors may appear in any of the four steps depending upon the fault.

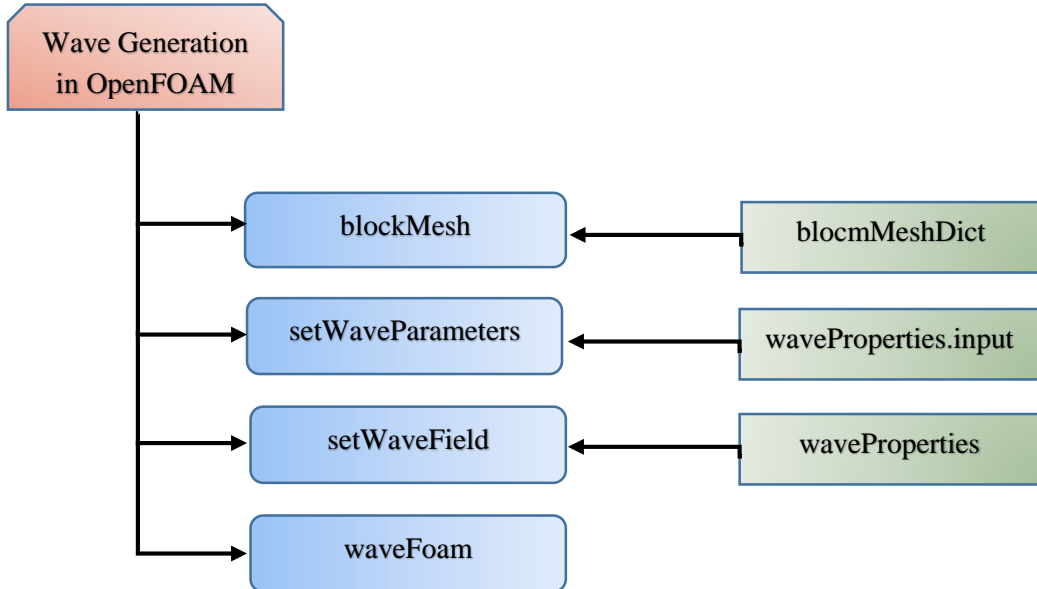


Figure 6-3 Steps of Wave Generation in OpenFOAM

- i. The command *blockMesh* generates the boundaries, faces, points and cells as per defined in the file *blockMeshDict*. If the computational domain is not defined properly, OpenFOAM will not be able to generate mesh attributes and some error will appear on the command line.
- ii. Once the mesh is created, a utility *setWaveProperties* (as shown in Figure 6-3) is used to set the wave parameters. For each wave theory, waves2Foam demands only few parameters an input to generate the wave. The rest of them it calculates itself using the built-in relations of wave theory specified in input. The required wave parameters are defined in the file *constant/waveProperties.input*.

After executing *setWaveProperties* command, a file, *constant/waveProperties* appears. This file contains all the wave properties, both provided in *waveProperties.input* and those calculated by the waves2Foam. The new parameters of wave that appeared for the 2D test case are presented in Table 6-5. It is very important to analyse these parameters as they define whether the *endTime* chosen for simulation is right and also an idea about required length of regions of computational domain.

Table 6-5 Properties Calculated by Waves2Foam

Properties	Value
Angular velocity ( $\omega$ )	3.14159 rad/s
Wave number ( $k$ )	1.70048 m <sup>-1</sup>

$$\text{wavelength } (L) = \frac{2\pi}{k} = \frac{2 * 3.14159}{1.70048} = 3.695 \text{ m}$$

$$c = \frac{L}{T} = \frac{3.695}{2} = 1.8 \text{ m/s}$$

With phase velocity of 1.8m/s, the wave should take about  $18\text{m}/1.8\text{m/s} = 10$  seconds to travel whole length of computational domain, where 18 meters is the length of computational domain. In the CFD simulations, when the first wave enters the still water, it's quite hard for it to make it till the end because of energy loss while moving through the stationary water. From experience, it was observed that about 2 waves lose their energies to make the

- water get in coherence with the inlet relaxation zone, hence  $10\text{ seconds} + 2 \text{ time periods} = 14$  seconds will be required by waves to travel along the computational domain. It means the *endTime* (25 seconds) set for simulation is right.
- iii. The utility *setWaveField* sets the initial condition in the computational domain as per defined in the file *constant/waveProperties*. This utility minimizes the time for simulation by calculating and setting the free surface elevation and fluid velocities at the initial conditions.
  - iv. After the mesh has been generated and all initial conditions are set, *waveFoam* command is executed to start the simulation.

#### **6.1.4 Post processing**

paraView is the open software used for post-processing. Other commercial post-processing software are also available with different options of post-processing. An overview of the wave generated for 2D test case, developed in paraView, is shown in Figure 6-4. The wave elevation of only a portion of the computational domain is shown for better view, as computational domain is very large as compared to its height hence cannot fit properly in the page. The wave elevation for time steps ranging from 21-25 seconds are shown to display the wave propagation phenomenon.

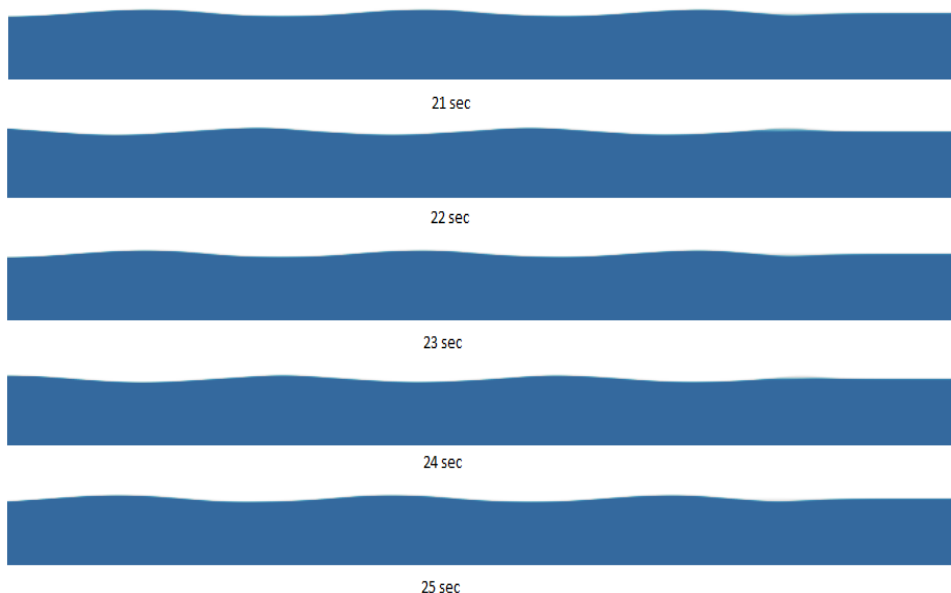


*Figure 6-4 Wave Propagation between Time Steps 21-25 seconds (2D Test Case)*

The surface elevation reading at time instant of 25 seconds is shown in Figure 6-5. The surface elevation of complete computational domain is displayed. At outlet relaxation zone, the wave fully dissipates approximately within half of the distance of the zone. It means the length of relaxation zone chosen for the test case is sufficient for dissipating the waves. In context of wavelength, outlet relaxation zone of approximately 50 percent of wavelength is required to totally dissipate the wave.

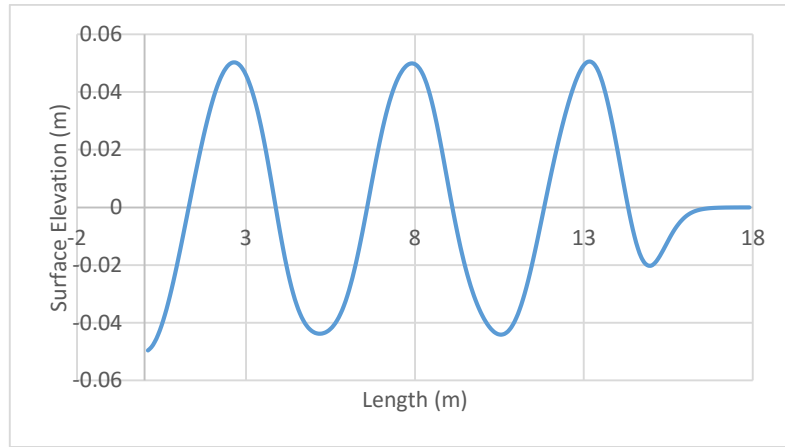


Figure 6-5 Surface Elevation of waves at Time Instant 25 seconds

## 6.2 3D test case

This section includes the inputs and post-processing results of 3D test case. 3D computational domain is shown in Figure 6-6.

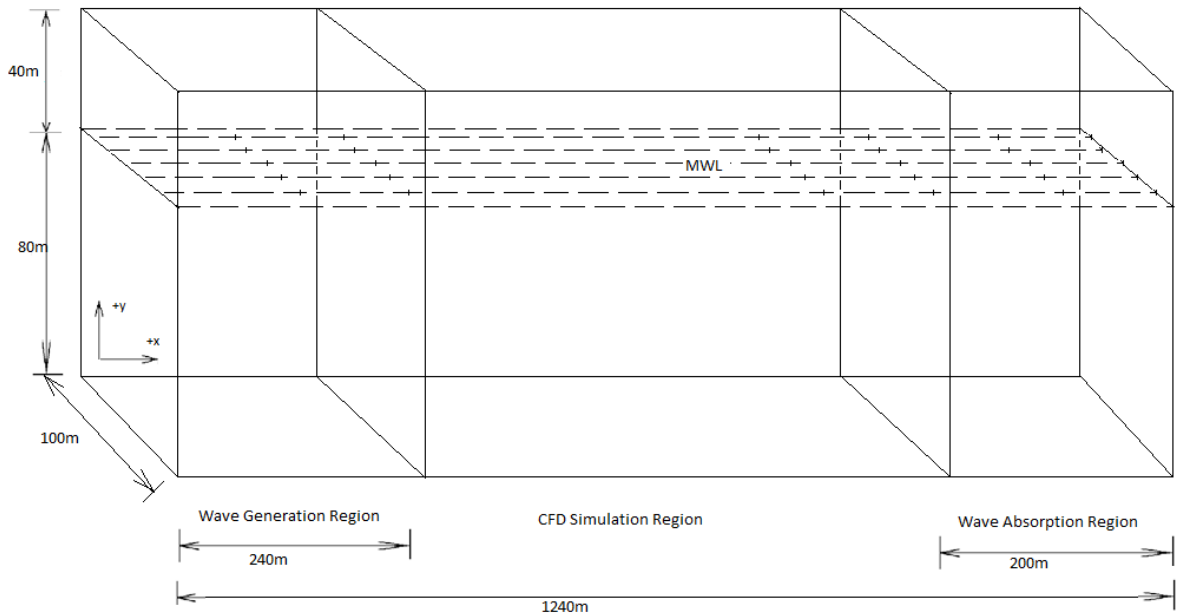


Figure 6-6 Computational Domain (3D Test Case)

The input parameters for 3D test case are displayed in Table 6-6. Mesh attributes are given in Table 6-7.

Table 6-6 Flow Properties (3D Test Case)

Property	value
<b>Viscosity of water</b>	1.12e-06 m <sup>2</sup> /s
<b>Density of water</b>	1000 kg/m <sup>3</sup>
<b>Type of fluid (air)</b>	Newtonian
<b>Viscosity of air</b>	1.79e-05 m <sup>2</sup> /s

<b>Density of air</b>	1.23 kg/m <sup>3</sup>
<b>Type of flow (Laminar or turbulent)</b>	Laminar
<b>Wave theory</b>	Stokes fifth order
<b>Water depth</b>	80 m
<b>Time period of wave</b>	14.5 s
<b>Phase shift in wave</b>	0
<b>Wave height</b>	24.3 m
<b>Wave direction</b>	Along positive x-axis
<b>endTime</b>	100 seconds

Table 6-7 Mesh Structure (3D Test Case)

Coordinate axis	Number of cells
x-axis	620
y-axis	96
z-axis	56

Mesh generated for the 3D test case is very fine with 2m x 1.25m x 1.75m cell size throughout the computational domain. The reason for such a fine mesh is to get an idea about the time requirements for the final simulations.

The boundaries along with their types are shown in Figure 6-7. The boundary conditions applied on the boundaries are presented in Table 6-8.

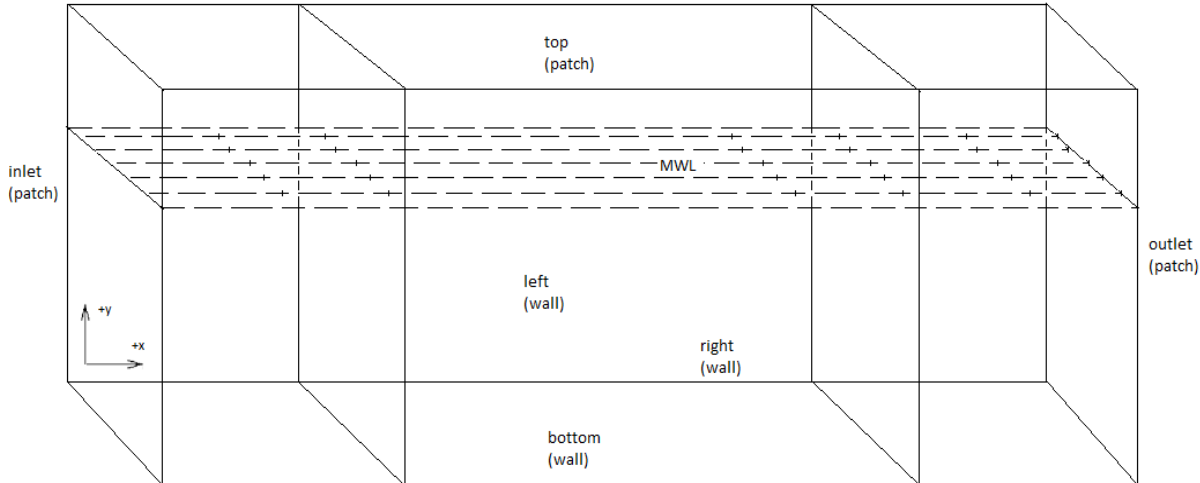


Figure 6-7 Computational Domain Boundaries Types (3D Test Case)

Table 6-8 Boundary Conditions (3D Test Case)

Boundary	$\alpha$ (alpha.water)	Pressure (p)	Velocity (U)
<b>inlet</b>	waveAlpha	zeroGradient	waveVelocity
<b>outlet</b>	zeroGradient	zeroGradient	fixedValue
<b>top</b>	inletOutlet	totalPressure	pressureInletOutletVelocity
<b>bottom</b>	zeroGradient	zeroGradient	fixedValue
<b>left</b>	zeroGradient	zeroGradient	inletOutlet
<b>right</b>	zeroGradient	zeroGradient	inletOutlet

## 6.2.1 Post-processing

The wave properties generated through `setWaveParameters` command are presented in Table 6-9.

Table 6-9 Wave Properties Generated by Waves2Foam

Properties	Value
Angular velocity ( $\omega$ )	0.4333323 rad/s
Wave number (k)	0.0200414 m <sup>-1</sup>

$$\text{wavelength } (L) = \frac{2\pi}{k} = \frac{2 * 3.14159}{0.0200414} = 313 \text{ m}$$

$$c = \frac{L}{T} = \frac{313}{14.5} = 21.59 \text{ m/s}$$

With phase velocity of around 22m/s, the wave will take  $1024/22 = 47$  seconds, approximately to travel the whole computational domain. Hence  $47 + 2 \times 14.5$  (time period) = 76 seconds, the `endTime` of 100 seconds is reasonable.

The simulation was run in parallel on 8 cores and results were generated in around 44 hours. The 3D generated wave can be viewed in Figure 6-8 at time instant 87.5 seconds. Larger `endTime` is required because computational domain is very large and also the first two waves dissipates while propagating because of stationary fluid surface.

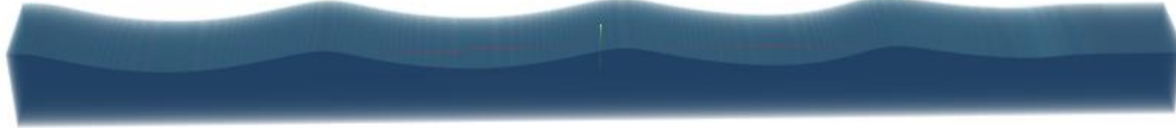


Figure 6-8 3D View of Free Water Surface (3D Test Case)

The surface elevation on the cross section at the middle of computational domain, along z axis (perpendicular to wave propagation), at time instant 87.5 is shown in Figure 6-9.

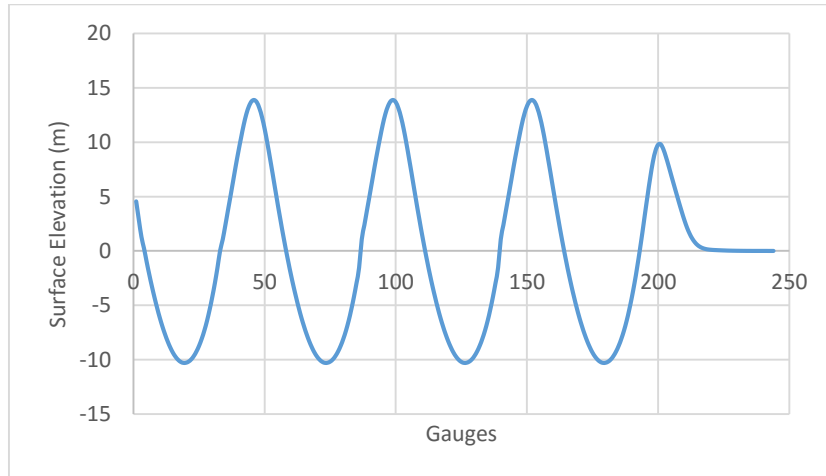


Figure 6-9 Surface Elevation at Time Instant 87.5 Seconds (3D Test Case)

## **7 SNORRE A TLP – DIMENSIONS AND INPUT PARAMETERS**

After surfing through the published data, of all TLPs installed in North Sea, Snorre A was the TLP found with the reasonable amount of data published.

Snorre A is an integrated drilling, production and accommodation TLP primarily made up of steel. It was installed in the Tampen area in the Northern North Sea in 1992. The Snorre A is the third tension leg platform (TLP) installed in North Sea after the Hutton TLP and the Jolliet TLP (Johannessen, Haver, Bunnik, & Buchner, 2006). The dimensions of Snorre A TLP are published in (Johannessen, Haver, Bunnik, & Buchner, 2006). The published date is presented in Table 7-1. The term Mt in the Table means metric ton.

*Table 7-1 Dimensions of Snorre A (Johannessen, Haver, Bunnik, & Buchner, 2006)*

<b>Parameters</b>	<b>Values</b>
<b>Displacement</b>	108491 Mt
<b>Mass</b>	80 754 Mt
<b>Number of tethers</b>	16 (4 at each corner)
<b>Tether Tension</b>	24340 Mt
<b>Riser Tension</b>	3397 Mt
<b>Column c-c spacing</b>	76 m
<b>Column Diameter</b>	25 m
<b>Pontoon Height x Width</b>	11.5 m x 11.5 m
<b>Pontoon Bilge Radius</b>	2.0 m
<b>Underside of Double Bottom of Deck</b>	64.5 m above keel
<b>Water Depth</b>	308 m
<b>Draft</b>	38.3 m
<b>Natural period in Surge &amp; Sway</b>	84 s
<b>Natural Period in Yaw</b>	69 s
<b>Natural Period in Heave</b>	2.3 s
<b>Natural Period in Roll &amp; Pitch</b>	2.4 s

Figure 7-1 shows an aerial view of Snorre A. this is an artistic image to get the better understanding of its appearance both above and below MWL.



Figure 7-1 Artistic View of Snorre A TLP (Johannessen, Haver, Bunnik, & Buchner, 2006)

Some of the dimensions are not published for Snorre A platform for example, dimensions of deck, location of deck relative to the cylinders, proper information about the shape of pontoons etc. These dimensions are reasonably assumed and are explained thoroughly in Section 8.1.

JONSWAP spectrum is considered to be the closest approximation to the irregular North Sea. For an optimized ULS design, the 100 year return period for waves of JONSWAP spectrum should be used (Johannessen, Haver, Bunnik, & Buchner, 2006). In (Johannessen, Haver, Bunnik, & Buchner, 2006), to save the time and computational cost, instead of simulating the irregular sea and generating random extreme event, Stokes fifth waves having the maximum wave height and time period for North Sea with 100 years return period is used. For the ULS design, waves are given the wave height of 29.7 meters and period of 13 seconds. Maximum wave height is an extreme and rare event with probability of occurrence of  $10^{-2}$ . The wave height of 29.7 meters and time period of 13 seconds is selected as characteristics parameters of extreme event for the current study as it is available in published data.

## **8 EXTREME WAVE EVENT GENERATION USING STOKES FIFTH WAVE**

This section is about the impact load calculation on the full scale model of Snorre A TLP through extreme wave event generation using Stokes fifth wave.

### **8.1 Platform model**

The platform model developed for this study is shown in Figure 8-1. As per discussed in previous section, in the published data, some of the dimensions of Snorre A TLP are missing. These dimensions are reasonably assumed.

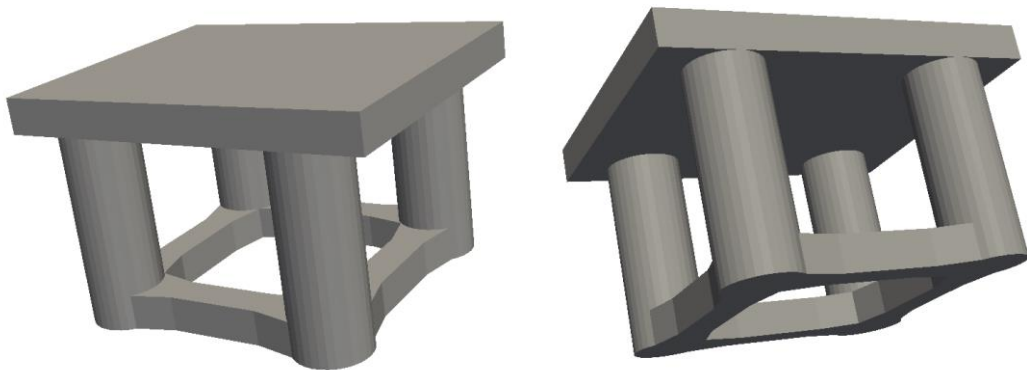


*Figure 8-1 Snorre A Model Used in Simulations*

The assumed dimensions are discussed in Table 8-1 below. The dimensions of deck have negligible effect on the overall loading because the deck is 26.3 meters above the MWL and wave height of extreme event wave is 29.7 meters. As the wave height is measured from crest to trough, almost half of the wave will be below the MWL, hence there are negligible chances for the wave to hit the deck.

The pontoons are not in the form of continuous rectangular bars, instead closer to the cylinders, their width increases progressively. The location of a pontoon from where the width starts to increases is assumed relatively with other dimensions from the pictures available. These assumptions surely will affect the accuracy of the calculated loads on the platform somehow but the current study is basically about the comparison of two approaches to calculate the design loads. As assumptions and input parameters are totally same for both the approaches adopted, the comparison will not be affected much. If results are fruitful then the dimensions can easily be changed upon the availability of missing data.

*Table 8-1 Missing Dimensions of Snorre A and their Assumed Values*

Dimension	Assumed Value	Comments
<b>Thickness of deck</b>	12 meters	Assumed by comparing the dimensions with other components from the published pictures
<b>Length of deck</b>	123.6776 meters	Assumed by comparing the dimensions with other components from the published pictures
<b>Width of deck</b>	101 meters	Equal to the length between the outer edges of cylinders

<b>Location of deck comparative to cylinders</b>	Symmetric	Deck is extruded out of the edges of cylinder equally from both sides
<b>Location of pontoon where width starts increasing</b>	10 meters from the cylinder	Assumed by comparing the dimensions with other components from the published pictures

## 8.2 Computational domain

As discussed before, a fixed platform is the structures in which all the six types of motion of platform is restricted completely. Platform is firmly fixed with the seafloor and the large scale motions are negligible. On the other hand, the floating platform is one in which the structure is free to undergo all of the six types of motions. There is no external system to restrict these motions. Only the mooring lines are installed to avoid the drift away of platform from the operational field. A TLP is a structure in between the two mentioned above, in context of motion freedom. Platform has restrictions towards all the six types of motions but not as firm as fixed platform, hence a TLP can undergo all six types of motions to some extent. Under normal working conditions and in small waves, platform can reasonably be assumed as stationary. Even for the case of small number of large waves, the platform does not show significant motion. As the purpose of current study is to analyses the behavior of platform in the situation of extreme wave event and tension induced by the extreme wave in tendons, hence it is quite reasonable to assume the platform as stationary and fixed in its place. The further motion of platform, after calculation of forces and moments induced by extreme wave event, is analyzed in the later sections.

The result bearing simulations require very fine meshes. Moreover, mesh convergence study is also planned to be performed hence the total time required by simulations will becomes high. To get optimized dimensions of computational domain regions, optimized computational time and to keep a track of the wave height hitting the platform, a simulation is performed without the platform, with the same input parameters, required by platform, and with reasonable dimensions of computational domain regions. The mesh is kept coarser to avoid extra simulation time. The computational domain for this case is shown in Figure 8-2.

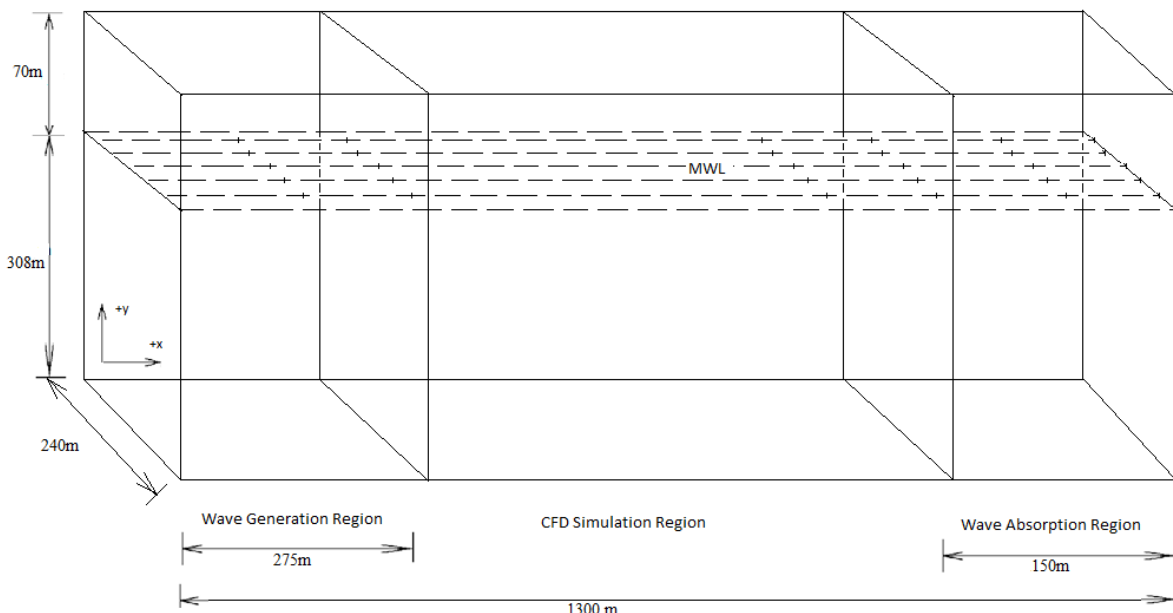


Figure 8-2 Computational Domain (Stokes Fifth wave without Platform)

Table 8-2 Input Parameters (Stokes Fifth wave without Platform)

Property	value
<b>Wave theory</b>	Stokes fifth order
<b>Water depth</b>	308 m
<b>Time period of wave</b>	13 s
<b>Phase shift in wave</b>	0
<b>Wave height</b>	29.7 m
<b>Wave direction</b>	Along positive x-axis
<b>endTime</b>	100 seconds

The wave gauges are installed at the section where left edges of left cylinders would touch if platform is placed according to the decided dimensions (Figure 8-5) and the wave height is measured for throughout computational time. The 3D view of free water surface and surface elevation plot for the section 16.3 meters from the end of wave generation region are displayed in Figure 8-3 and Figure 8-4 respectively.



Figure 8-3 Free Surface 3D view at Time Instant of 60 seconds (Stokes Fifth wave without Platform)

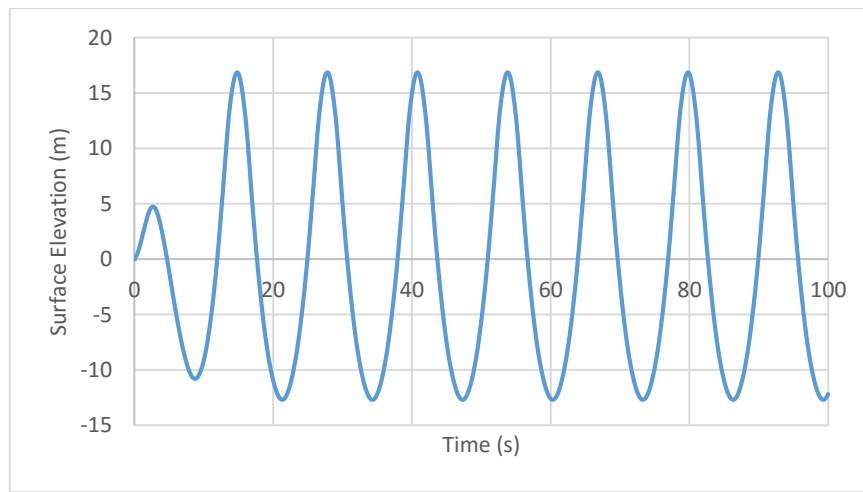


Figure 8-4 Surface Elevation at 16 meters after the End of Wave Generation Zone for the whole Computation Time (Stokes Fifth wave without Platform)

The computational domain chosen for final simulation for the extreme event generation using Stokes fifth wave is chosen according to the Figure 8-5. The wave is coming from the left and hitting the platform on the side where the deck is hanging beyond the edges of cylinders. The decision of which side should be exposed to the wave is taken from the previous published in (Johannessen, Haver, Bunnik,

& Buchner, 2006). The lengths of the regions are chosen according to the previous experience from the test cases. The base of platform is at the distance of 16.3 meters from the end of wave generation region. The height of air column above the MWL is chosen randomly. Different sizes of air column do not have any effect on simulation results. The height must be so that the wave does not reach the boundary.

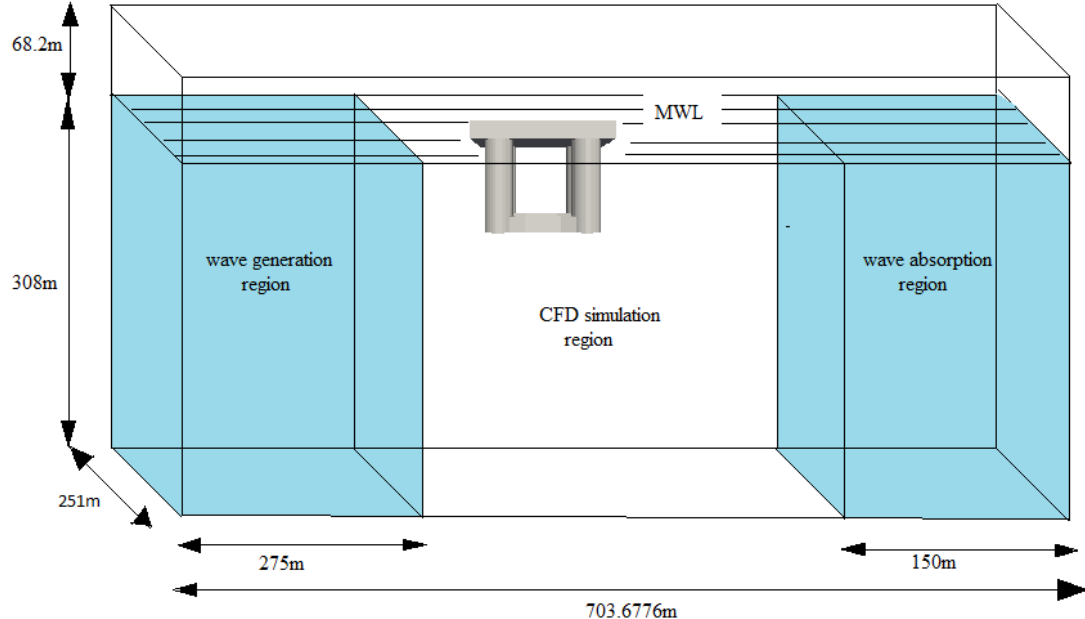


Figure 8-5 Computational Domain (Stokes Fifth wave)

### 8.3 Mesh-Setup

A structured mesh with block topology is being used in the current study. Many blocks (or volumes) are built around the model of platform and mesh in each block was defined in the form of points on the lines of the blocks. With opposite lines having equal number of points, joining these points within the block develops cubic elements within the block. As the geometry of the platform is very complex, the mesh is developed in the form of layers from the bottom of platform until the top. Each layer has its own number of volumes and block topology. To have a better understanding, each layer is designated with a name as follows.

- Water channel layer
- Pontoon layer
- Cylinder layer
- Topside layer
- Atmospheric layer

Mesh generation software GMSH is used to develop the mesh. The most critical layers out of these five are pontoon layer, cylinder layer and topside layer because of presence of platform in them. The block topology for pontoon layer is shown in Figure 8-6. The Figure 8-6 is 2 dimensional showing block topology of region closer to the platform on a section of pontoon layer. 2D mesh of the whole domain is displayed Figure 8-7. This is one of the many sections of 3D mesh of the pontoon layer. These sections are exactly copied and stack on each other to form the pontoon layer mesh. Mesh is kept finer in the blocks closer to the platform. Moreover, in the outer blocks, a positive progression of points on the lines toward the platform is defined. This resulted in decrease in distance between the connective points as the line progresses towards the platform. Hence the mesh is denser closer to the in outer blocks as well. The few imperfections can be spotted in the mesh like thin fine mesh areas starting from each cylinder

until the left and right boundaries. Such imperfections do not affect the computational results instead; they only increase the computational time. On the other hand, the structured mesh is developed to increase the results accuracy and decrease the computational time hence such imperfections, overall have negligible effect on the efficiency of structured mesh.

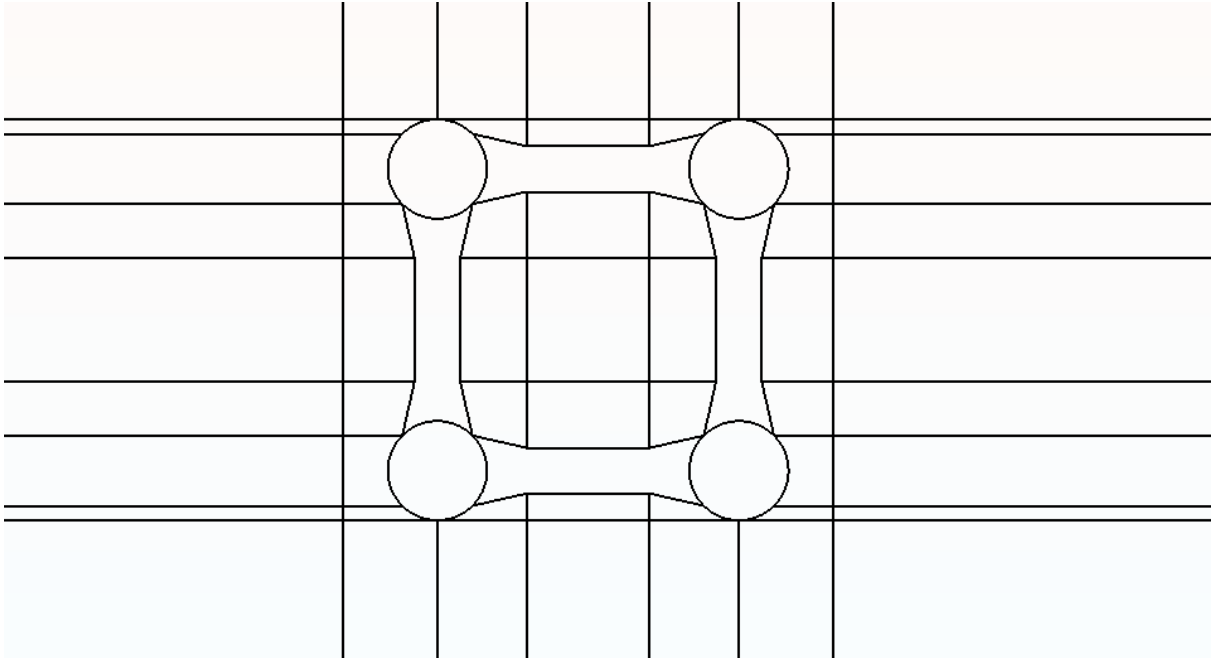


*Figure 8-6 Block Topology of Pontoon Layer*

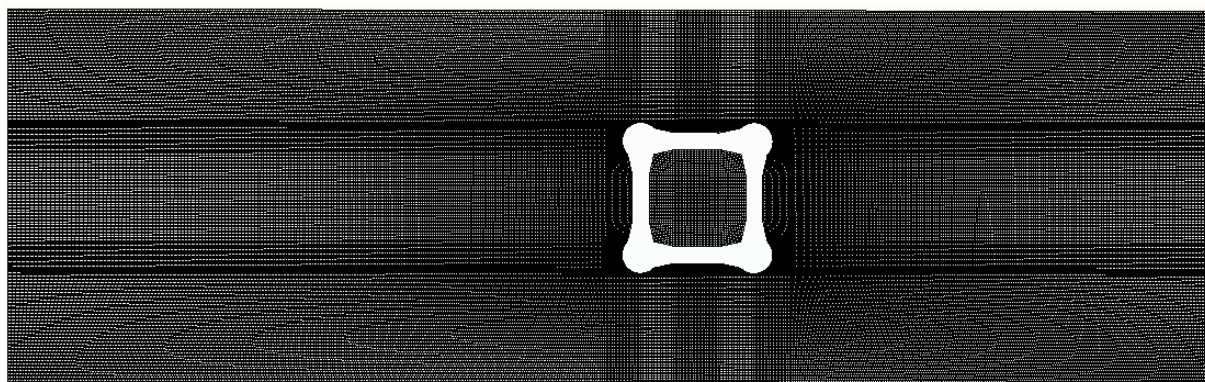


*Figure 8-7 2D Mesh of a Section of Pontoon Layer*

The closer look of the mesh of the same layer displayed in Figure 8-7, around the platform is shown in Figure 8-8. This is the critical region of the domain where the flow will have abrupt behavior hence fine mesh is applied in this region as compared to the other regions away from the platform. The progression feature is also visible in the Figure 8-8.

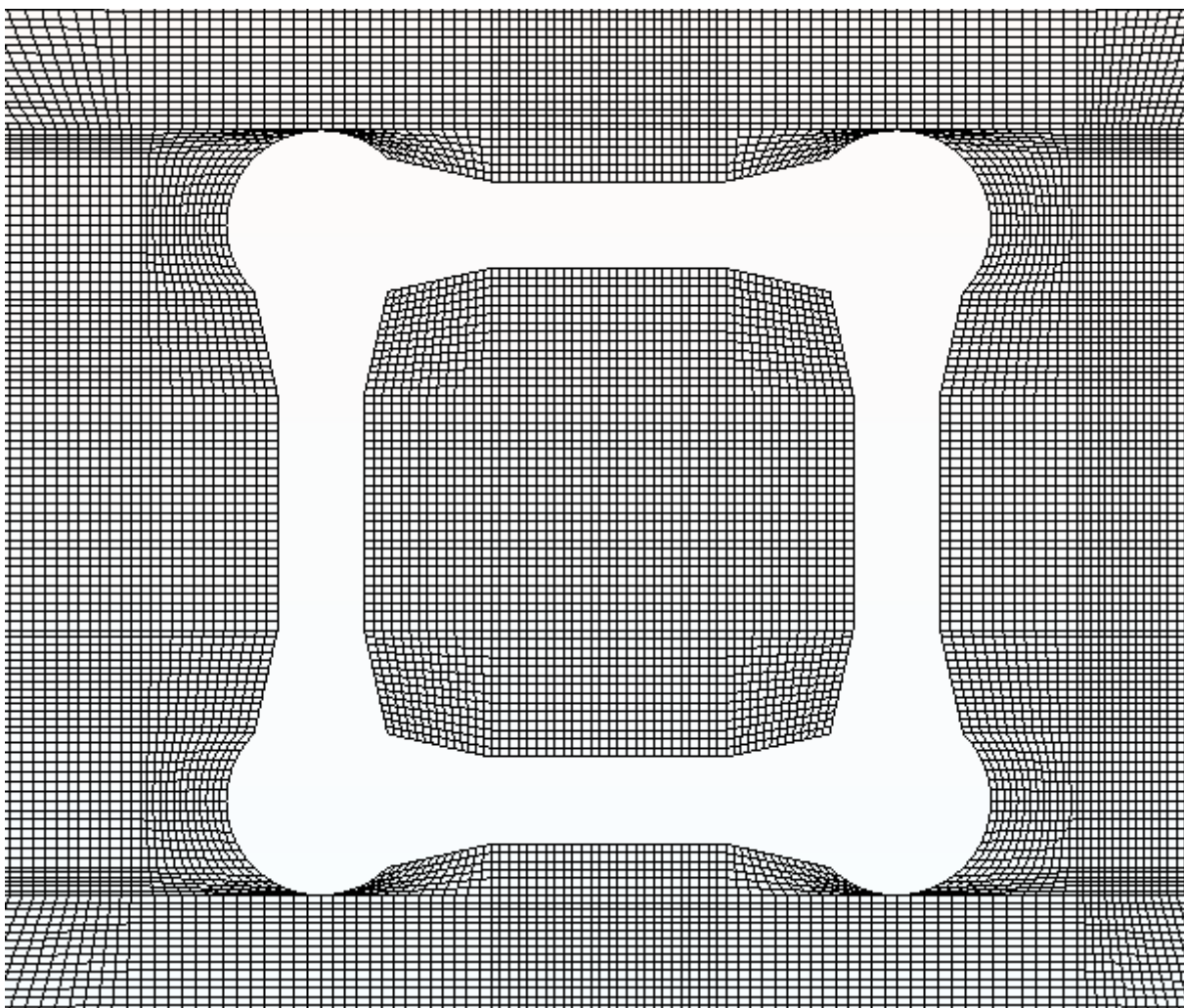


Figure 8-8 Pontoon Layer Mesh Closer to Platform

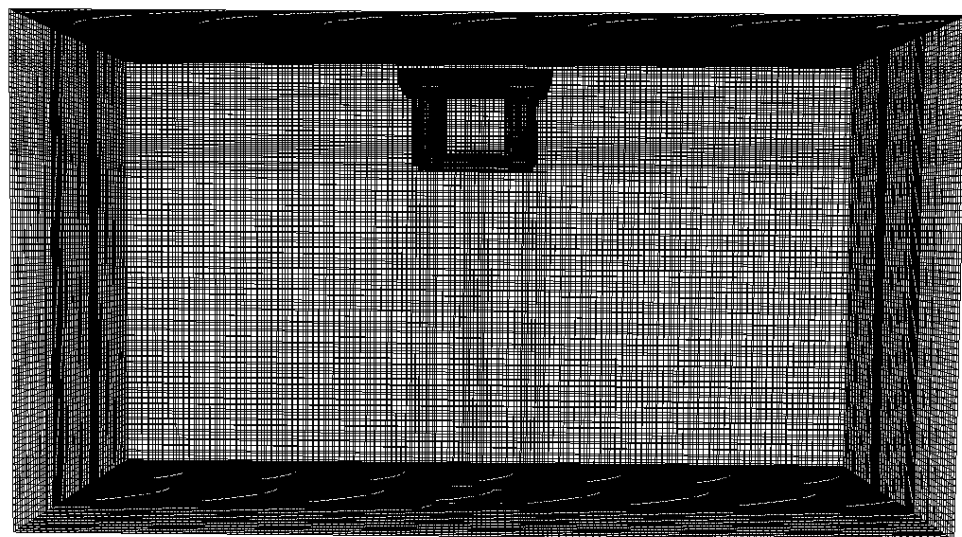


Figure 8-9 overview of 3D Mesh of Computational Domain (Generated from ParaView)

## 8.4 Pre-processing

Fifth order Stokes wave input parameters are presented in Table 8-3. An important feature of this simulation is calculation of lift and drag forces, moments and force-coefficients on the platform. A force library is introduced in the file *controlDict* for calculation of these forces and force-coefficients. Certain inputs are required for the library to calculate these forces. The inputs given to the software for the calculation of forces are shown in Table 8-4.

Table 8-3 Input Parameters (Stokes Fifth wave without Platform)

Property	value
<b>Wave theory</b>	Stokes fifth order
<b>Water depth</b>	308 m
<b>Time period of wave</b>	13 s
<b>Phase shift in wave</b>	0
<b>Wave height</b>	29.7 m
<b>Wave direction</b>	Along positive x-axis
<b>endTime</b>	100 seconds

Table 8-4 Inputs for Calculation of Forces and Force-Coefficients on Platform

Inputs	Values	Comments
<b>cofR</b>	(50.5 27 50.5)	Location of metacenter
<b>magUInf</b>	16.5 m/s	Incoming velocity
<b>lRef</b>	1	Reference length
<b>ARef</b>	2501.5 m <sup>2</sup>	Frontal area

A structure in the ocean experiences six type of motions i.e. surge, sway, heave, roll, pitch and yaw. The first three are translational motions while the rest three are angular motions. When a structure undergoes angular motion, it rotates around a specific point while having all of three angular motions. The point is called metacenter and its location varies from structure to structure. Each structure has its own metacenter depending upon its shape, dimensions and weight.

CofR is the location of metacenter of platform. Its location is not specified in the literature. The metacenter is calculated based upon following assumptions.

As the cylinders and pontoons are the buoyant part of the platform, their density is quite low as compared to the deck, hence the location of center of gravity is assumed to be 5 meters below the base of the deck. For the platform to be initially stable, the location of metacenter is to be above the center of gravity. The distance between the center of gravity and metacenter is assumed to be 6 meters. Moreover, for the x and z axis, because of symmetry, the location of meta center is assumed to be in the geometric center of platform along x and z axis i.e. 50.5 meters from the corner. These assumptions are made based upon the work of (Gie & Boom, 1981). The data from (Gie & Boom, 1981) is used for making reasonable assumptions.

The physical representation of assumed block of platform is shown in Figure 8-10.

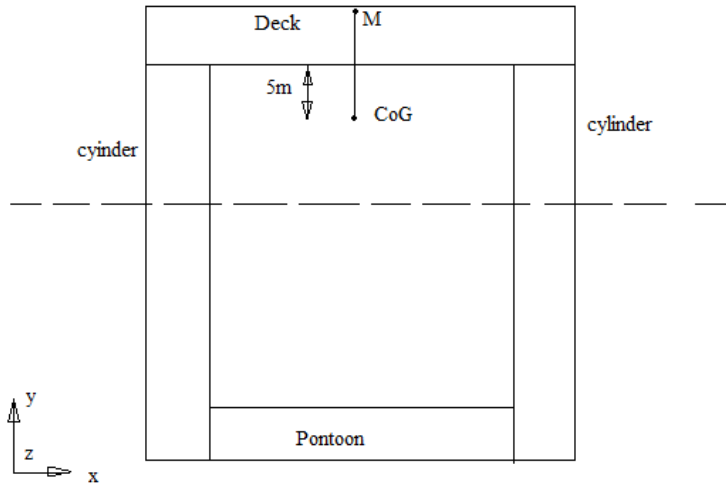


Figure 8-10 Assumed Block of Platform for calculation of Metacentric Height

*magUInf* is obtained through the wave number and angular velocity calculated by the *wave2Foam*. After running the command *setWaveParameters*, following wave parameters are generated (Table 8-5).

Table 8-5 Wave Properties Generated by Waves2Foam

Properties	Value
Angular velocity ( $\omega$ )	0.483322 rad/s
Wave number (k)	0.0217569 m <sup>-1</sup>

$$wavelength (L) = \frac{2\pi}{k} = \frac{2 * 3.14159}{0.0217569} = 289 \text{ m}$$

$$c = \frac{L}{T} = \frac{289}{13} = 22.23 \text{ m/s}$$

the phase velocity is 22 m/s approx. According to the experiments conducted by John Grue (Grue, Clamond, Huseby, & Jensen, 2003), the wave velocity under the crest is about 75 percent of the phase velocity. the phase velocity for the current case is 22 m/s approx. hence the crest velocity i.e. *megUInf* will be  $22 \times 0.75 = 16.5 \text{ m/s}$ .

The *lRef* is the reference length used in the case of continuous geometry perpendicular to the flow. The TLP is not a simple continuous geometry hence *lRef* is put 1 and the value of frontal area i.e. *ARef* is introduced instead. The *A ref* is the frontal area of platform, exposed to wave and below the MWL. The visualization of frontal area is shown in Figure 8-11. It is calculated as follows:

$$ARef = 38.3 * 25 * 2 + 11.5 * 51 = 2501.5 \text{ m}^2$$

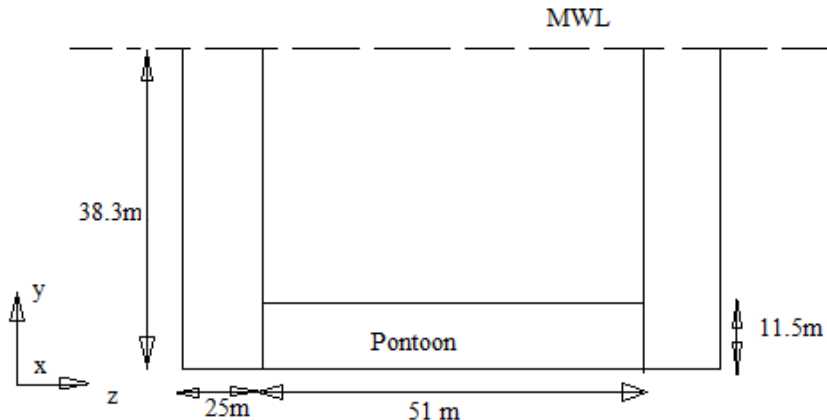


Figure 8-11 Frontal Area of Platform Exposed to Wave

## 8.5 Mesh convergence study

In numerical methods, a finer mesh results in a solution that is more accurate. However, as mesh gets finer, more computational power and time is required, hence the simulation becomes more expensive. Moreover, as we step from coarser to finer mesh, results show big differences, but for further refining the mesh, the difference becomes smaller. To develop a mesh that reasonably balance the accuracy and available computational resources, time and money, mesh convergence study is performed. Following are the basic steps to perform a mesh convergence study (AUTODESK, 2016).

- Perform the simulation using a coarser mesh with reasonable number of elements.
- Repeat the simulation by recreate a finer mesh in the whole domain with denser elements in the critical regions as compared to noncritical regions.
- Repeat the simulation again by recreating even finer mesh.
- Minimum of three simulations with different mesh density is required to plot mesh convergence curve. The number of simulation can be increased to get results that are more precise.
- Plot the convergence curve using the results from simulations.

For the current study, three simulations were performed. The details of mesh parameters are explained in Table 8-6. Mesh density was different in all of the three cases studied. The region around the platform being critical hence, for all the cases, the mesh is kept finer in this region.

Table 8-6 Mesh Parameters for Mesh Convergence Cases

Mesh Parameters	Case no 1	Case no 2	Case no 3
No of elements	1010535	1682980	2594260
Size of elements away from platform	4.7x2.875x3	3.5x2.87x2.5	2.6x2.4x2.15
Size of elements closer to platform	3x2.87x3.2	2.6x2.87x2.5	2x2.4x2.15

For the sake of comparison, only the drag coefficients are compared for the three cases. The plots of drag coefficients for the three cases are shown in the Figure 8-12. It can be observed that the curves are approximately overwriting each other. There are only minor differences on the sharp edges of the curves. This is the only accuracy in results added by finer mesh of case 3.

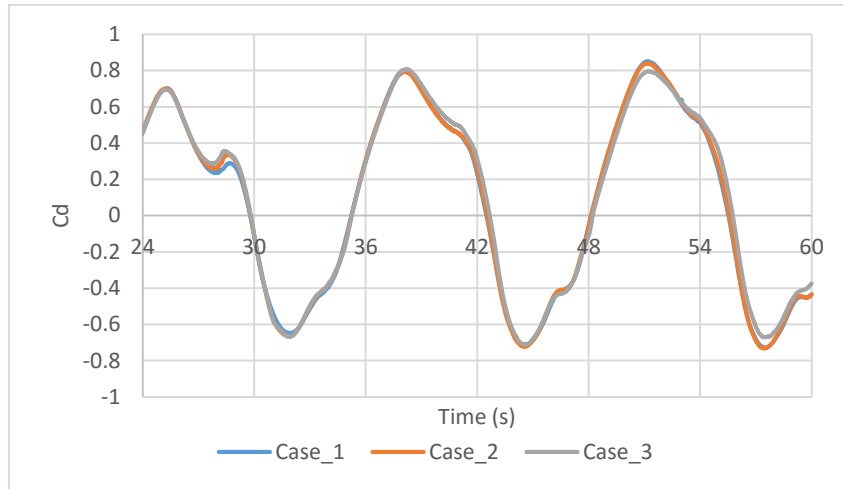


Figure 8-12 Comparison of Drag Coefficients for Three Cases

The RMS values of drag coefficient for each case (Table 8-7) is calculated to plot the mesh convergence curve. The mesh convergence plot is displayed in Figure 8-13. The RMS value of first case is quite different from the 2<sup>nd</sup> and 3<sup>rd</sup> case. The RMS values of 2<sup>nd</sup> and 3<sup>rd</sup> care same until the second decimal digit. It means that the results of first case are not quite accurate but the results of 2<sup>nd</sup> and 3<sup>rd</sup> case are almost equal hence mesh convergence is achieved.

Table 8-7 RMS Values of Drag Coefficients for Three Cases

Case No	RMS values
1	0.44469
2	0.513422
3	0.527784

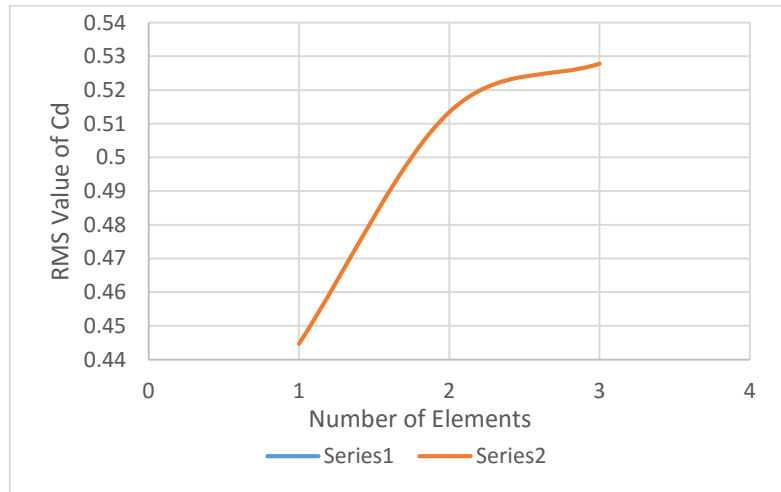


Figure 8-13 Mesh Convergence Plot

## 8.6 Post-processing

In this section, results of simulations of extreme event wave using Stokes fifth wave are presented. Out of three cases, only the results of case 3, being the most accurate of the three, are presented in this section.

The free surface 3D contour, showing the flow across the platform is shown in Figure 8-14. The effect of platform in the form of disturbance of free surface can clearly be visualized around the platform.

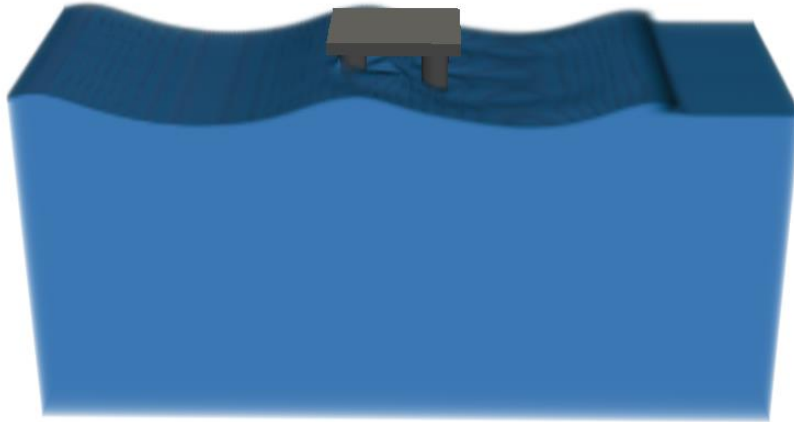


Figure 8-14 free surface 3D contour for Case 3 (generated from ParaView)

The free surface elevation, 10 meters behind the base of platform, is shown in Figure 8-15. The first crest has very small height because of delay in wave generation imposed by the stationary water in the CFD simulation region. The effect of presence of platform starts to appear at the 2<sup>nd</sup> crest where height is larger as compared to normal wave height. When the 3<sup>rd</sup> crest reaches this point, the crest height decreases and trough depression increases because of the disturbance created by platform in the water ahead. The waves come in equilibrium with platform after the 3<sup>rd</sup> crest as it can be seen that the crest and trough of 4<sup>th</sup> wave has the same shape as the crest and trough of 3<sup>rd</sup> wave respectively.

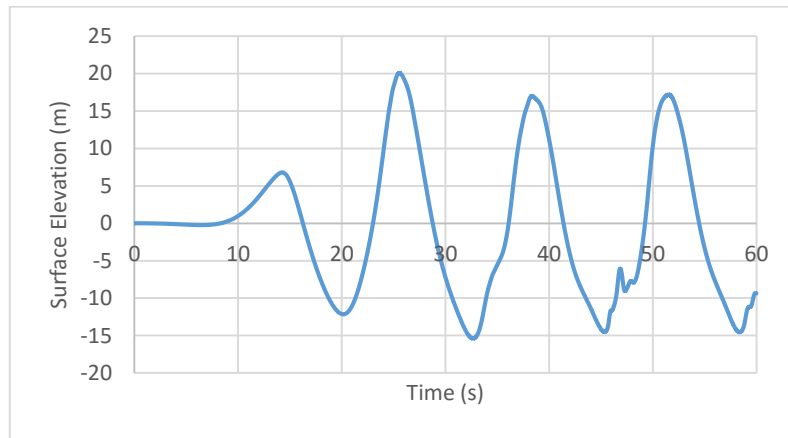


Figure 8-15 Surface Elevation 10 meters Behind the Platform

The characteristics of free surface are different at different time instants and at different locations hence, the forces imposed by waves on platform at all time instants are unequally distributed. This imbalance in drag, lift and buoyancy forces generate moment along the TLP platform. The results are unequal tension in the tethers at all time instants. A simplified approach is adopted in the current study to calculate the tension in different tethers. As mentioned previously that the TPL platform under consideration has 16 tethers. These tethers are divided into two groups based upon their location. Each of the 8 tethers at the leading edge of the TLP have same tension and are designated as tether group 1 and each of the 8 tethers at trailing edge of the TLP have same tension and are placed in tether group 2. The tensions for tether groups 1 and 2 are calculated from the moment forces computed by OpenFOAM. The moment force is used to calculate the unbalance of lift and drag forces at both sides of the platform.

### 8.6.1 Methodology for tension calculation

The drag force plot on the platform is shown in Figure 8-16. It can be noted that the drag force oscillates with the same period as the incident wave. Just like wave, it has crest i.e. where drag is positive (towards positive x-axis), and trough i.e. where drag is negative (towards negative x-axis). Because of this oscillatory drag force, the net force acting along positive x-axis is not much higher, resulting in small drift off. Hence it is assumed in the current study that the drag force will not drift off the platform, during the specific duration of extreme event wave.

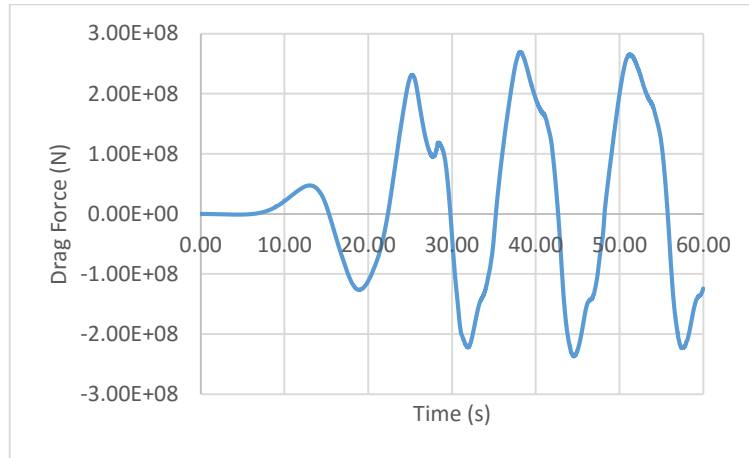


Figure 8-16 Drag Force Plot for Stokes Fifth Wave Case

The drag force acts on the volume of cylinder below the surface of water. The forces on a body, below the surface of water acts on its center of buoyancy (B). Moreover, the metacentric height of platform is 27 meters above the MWL. Hence, while holding the above mentioned assumption, all the drag force will create moment in the platform with moment arm equals to the distance between center of buoyancy and metacentric height.

The center of buoyancy is the volumetric center of the structure under water, as buoyancy force is only dependent upon volume of the structure under water, not on the mass. The volume of platform below MWL, along with the dimensions is shown in Figure 8-11 (2D). As flow is unidirectional, hence there are not significant drag forces acting along z-axis, hence center of buoyancy for xy plane will be sufficient for the current study. It lies at the point where the volume above and below is same. The total displaced mass by platform and tendons is give in Table 7-1. Dividing it with density of water (from Table 6-1) gives the total displaced volume as:

$$\frac{108491Mt}{1000} = 108491 m^3$$

Volume above the center of buoyancy is:

$$\frac{108491}{2} = 54245.5 m^3$$

As above the center of buoyancy, there are only cylinders, hence the location of B with respect to MWL ( $L_B$ ) is:

$$54245.5 = L_B * 3.14 * 12.5^2 * 4$$

$$L_B = 27.64 m$$

As metacenter (M) lies 27 meters above MWL, hence distance between metacenter and center of buoyancy (BM) for the current case is:

$$BM = 27 + 27.64 = 54.64 \text{ m}$$

Now, the moment imposed by the drag ( $M_D$ ) is equal to:

$$M_D = F_D * BM \quad (8-1)$$

Here  $F_D$  is the drag force computed through CFD analysis. The analysis is transient hence the  $M_D$  is obtained at every time step. CFD analysis also computed the overall moment force acting on the platform. It is in-fact, the combination of moment contributed by both lift and drag forces. As we calculated the moment contributed by drag, moment contributed by lift ( $M_L$ ) is obtained by following relation:

$$M_L = M_{\text{total}} - F_D \times BM \quad (8-2)$$

$M_L$  appears because of the imbalance of lift forces between the both sides of platform, namely front, the sides exposed to wave, and back, the side opposite to the front side. Each side has 8 tethers attached to them. The tethers of front side are named as tether 1 and tethers of back side are named as tether 2. The unbalance force is calculated by resolving the moment  $M_L$  along the tether 1 location as:

$$F_{L \text{ unbalance}} = \frac{M_L}{\frac{\text{Width of TLP}}{2}} \quad (8-3)$$

$F_{L \text{ unbalance}}$  is the force that produces roll notion in the TLP. The difference of lift force between tether 1 and 2 is  $F_{L \text{ unbalance}}$ .

$$F_{T1} - F_{T2} = F_{L \text{ unbalance}} \quad (8-4)$$

Similarly, the sum of vertical forces between tether 1 and 2 is the total lift force  $F_{L \text{ total}}$ .

$$F_{T1} + F_{T2} = F_L \quad (8-5)$$

From the Equations 8-4 and 8-5,  $F_{T1}$  and  $F_{T2}$  are calculated by solving them simultaneously. Another phenomenon to mention here is that the lift force computed by CFD analysis has a constant positive value added to the platform along the whole transient analysis, as can be seen in Figure 8-17. This constant lift is the buoyancy force calculated by CFD analysis as lift force. The actual buoyancy force is known from the published data, which is equal to the weight of platform and pre-tension in the tension legs, but the actual buoyancy also incorporates the volume of water displaced by the tethers. As in the current study, platform is taken as a fixed structure during analysis, there is no need to attached tether with the platform hence tethers are not modelled. Hence, the buoyancy force computed by CFD analysis is less than the published buoyancy of Snorre A platform. For the current study, only the computed buoyancy is subtracted from the computed vertical force to get the variable lift force acting on the platform.

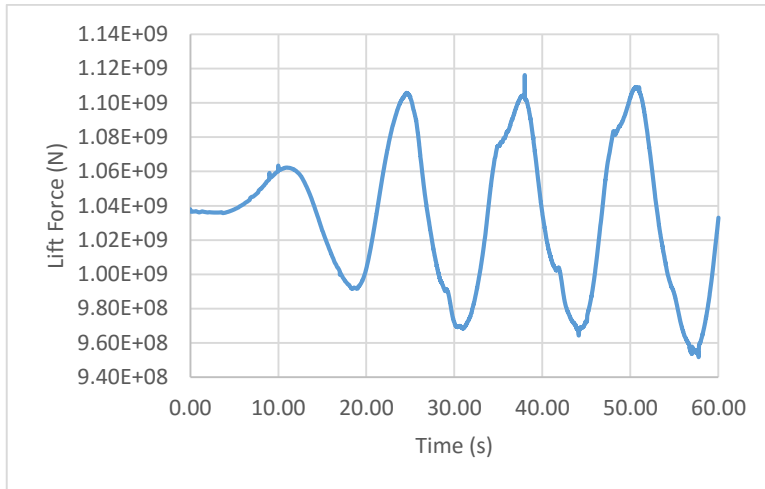


Figure 8-17 Lift Force Plot for Stokes Fifth Wave Case

From the tether 1 and 2 forces calculated previously, we can resolve the lift force into two main components. The balanced force i.e. lift force acting at center of gravity of platform and causing only heave motion, and unbalanced force i.e. the force causing only roll motion. After this resolution, the heave and roll motion of tether 1 and tether 2 are calculated separately.

For heave motion, the motion characteristic of TLP is similar to the motion of mass attached with two springs undergoing forced oscillations, as shown in Figure 8-18. The tethers act as spring with capability of storing energy. as the pre tension is eliminated from the vertical force, hence at MWL, tethers are assumed to be with no tension. The motion of such system is defined by following equation:

$$mx(t)'' + kx(t) = F \quad (8-6)$$

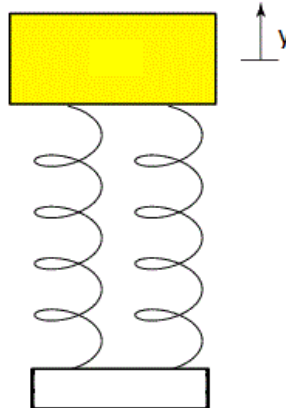


Figure 8-18 Approximated System for TLP Heave Motion

here  $x$  is the displacement of TLP,  $m$  is the mass of TLP,  $t$  is the time,  $x''$  is the acceleration,  $k = \omega_0^2 m$  is stiffness of tethers,  $\omega_0$  is the natural frequency of TLP, calculated using natural time period of heave (2.3 seconds) available in published data (Table 7-1), and  $F$  is the applied force which is balanced lift force. The solution to this differential equation is as follow:

$$x(t) = C_1 \sin t \omega_0 t + C_2 \cos \omega_0 t + \frac{F}{k} \quad (8-7)$$

Here,  $C_1$  and  $C_2$  are constants that are determined by the initial conditions. Equation 8-6 is solved for two initial conditions i.e.  $x(0) = 0$  and  $x'(0)=0$  at first time interval. As  $\delta T$  of CFD analysis is very small, the overall heave motion is calculated by assuming force acting during each time interval is constant and solving equation 8-6 at every time interval using the initial conditions of previous interval. Tension in the tethers is further calculated from this displacement using tether stiffness  $k$  through Hooks law, which states that:

$$\text{Tension} = T = -F = kx \quad (8-8)$$

For the roll motion of system shown in Figure 8-18, when one spring stretches, the other elongates and vice versa, hence roll motion of TLP is calculated by approximating the platform to the system shown in Figure 8-19. For very small roll angle, the arc along with the platform rotates can be approximated as vertical straight line for one side of platform. As roll motion in platform is very small in real situations, the approximation is reasonably valid. The solution of this system is the same equation as used for heave motion (Equation 8-5). Vertical displacement of one side of platform is calculated following the same procedure as for heave motion. Displacement is exactly opposite for the opposite side. It must be noted here that the force used in this calculation is the one obtained by multiplying the moment, calculated by CFD analysis, with moment arm. The roll period of 2.4 seconds (Table 7-1) is used in this calculation.

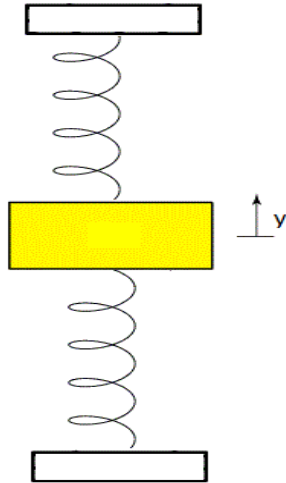


Figure 8-19 Approximated System for TLP Roll Motion

## 8.6.2 Results

The plot for heave motion for platform is shown in Figure 8-20. It must be noted that the motion of platform is not only the heave but due to combination of lift, and drag forces, moment also generate in the platform and it undergoes roll motion as well. the roll motion plot is shown in Figure 8-21. The calculation of displacement of platform is important as the simulation is run with platform fixed in its place but under the influence of the forces computed by OpenFOAM, it will undergo heave and roll motion significantly. These motions result in the change in tension of tendons. The combined heave and roll motion of platform results in different vertical motions on the both sides of platform. The vertical motion of the side on which wave hits (front) and of opposite side (back) is shown in Figure 8-22. The tensions in the tendons on the front and back of platform are calculated by simply multiplying the stiffness with the displacement + pre-tension (Figure 8-23). It must be noted that the tension plot is not for the group of tendons on the front and back, instead it is for a single tendon in the front and in the back. The randomness appears in the plot is because of difference between the frequency of forcing wave and natural frequency of platform.

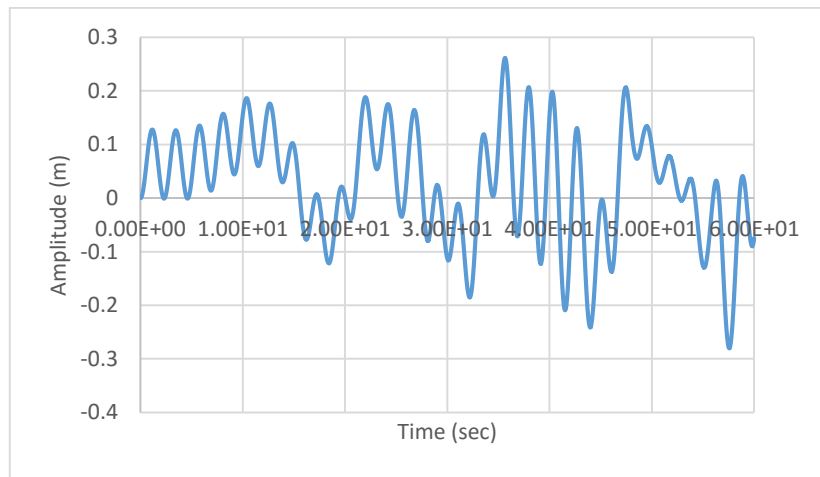


Figure 8-20 Heave Motion of Platform

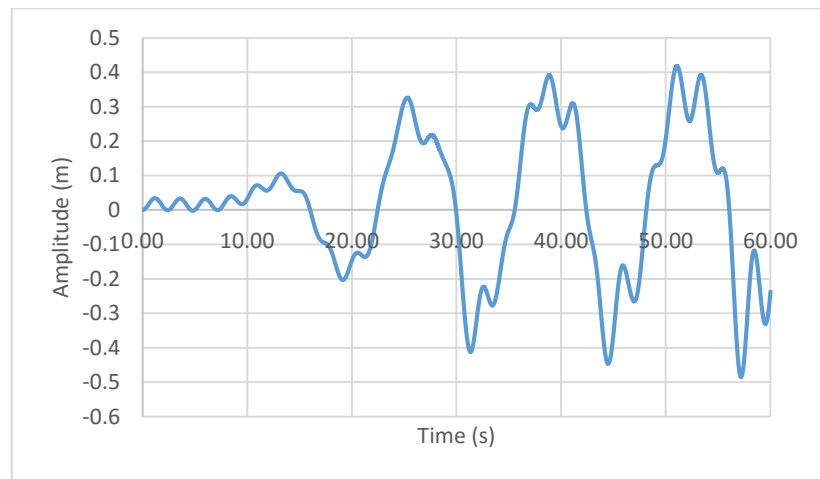


Figure 8-21 Roll Motion of Platform

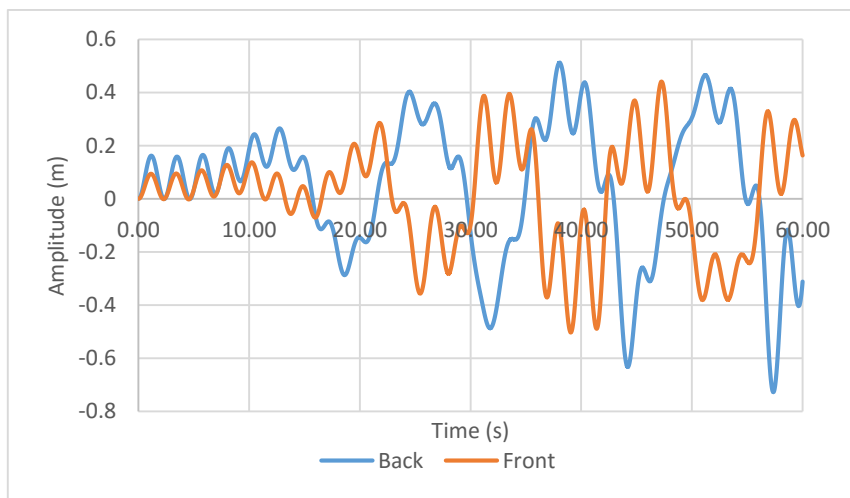


Figure 8-22 Vertical Displacements of Front and Back Sides

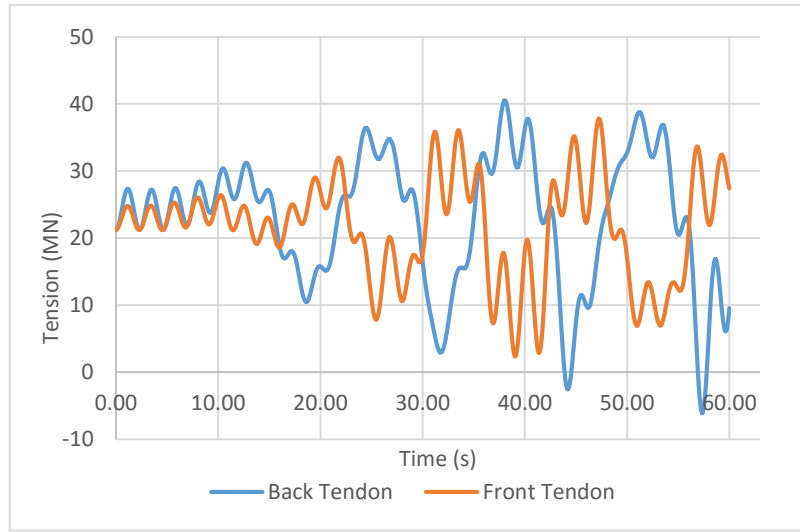


Figure 8-23 Tension in Front and Back Tendons (Stokes Fifth Wave Case)

From the plots of tensions in front and back tethers, the general perception develops that the tension in the back tethers is more as compared to in the front tethers. It is realistic as the drag force has major influence along positive x-axis, hence the moment created by drag rotates the platform Counter clockwise. It results in more vertical displacement at the back side of platform. More displacement means more tension created in the tendons.

Another phenomenon to observe in the plot of tension is that tension increasing with the passage of time. After every wavelength, the peaks of plot are getting higher and broader, means as more and more waves pass across the platform, the energy transfer rate between waves and platform increases. If simulation is run for considerably long time, the energy transfer will be larger for the waves hitting the platform in the later times. This is a drawback as the extreme event occurs rarely in the lifetime of the platform and it is almost impossible that an extreme event wave is followed by another extreme event wave. Hence design loads calculation through simulation of Stokes fifth waves hitting the platform consecutively, with the characteristic parameters of extreme event wave, have considerable amount of conservations.

## 9 NEW WAVE THEORY

Waves2Foam does not have the option of generating a superposed wave at desired focal point and time, but it provides an option to the user to develop their own wave theory and compile it with Waves2Foam. Waves2Foam then treats the theory as the other built in theories and generate the waves according to the formulations defined.

Several wave superposition theories have been developed so far by different researchers. Dean and Sharma (1981) method for second order directional seas and associated wave forces is considered the pioneer in the superposed wave generation technique (Sharma & Dean, 1981). It uses a hybrid model incorporating a combination of linear and non-linear wave elements. As discussed before, most of the conventional approaches of wave load computations incorporate either nonlinearity or linear superposition of random waves. For example, (Johannessen, Haver, Bunnik, & Buchner, 2006) used stokes fifth waves for ULS design loads calculations for Snorre A TLP. (Sharma & Dean, 1981) provides a better realization of the characteristics of waves faced by offshore structures by their hybrid model by combining the best features of the conventional models thus generating a better realization of sea waves incorporating randomness, nonlinearity, and directionality. The focusing wave is a common practice and has been applied by many researchers as a close idealization to the real extreme event. Examples are (Wu, Chen, Bahuguni, Lu, & Kumar, 2015), (Fernández, Sriram, Schimmels, & Oumeraci, 2014), (Pelinovsky, Kharif, Talipova, & Slunyaev, 2002), (Ning, Teng, Taylor, & Zang, 2008) (Borthwick, Hunt, Feng, Taylor, & Stansby, 2006) and (Brandini & Grilli, 2001).

As OpenFOAM and waves2Foam are developed on the basic code of python and C++ hence generation of new wave theory does not only require the knowledge of theoretical formulation of desired wave but also a firm command over python and C++. Due to limited time and resources, the new wave theory is not generated in the current study instead the previously developed focusing wave theories i.e. focNewwave Theory (for superposition of 2D waves) and foc3DNewwave theory (for superposition of 3D waves) are used (courtesy of Dr. Knut Erik, University of Stavanger and Anand Bahuguni, Lloyd's Register Group Limited, London). These wave theories are based upon the formulation defined by (Sharma & Dean, 1981).

(Sharma & Dean, 1981) used perturbation method for modeling of reasonably accurate real wave field and incorporates nonlinearities. The kinematics of every water particle in the wave field at a point ( $x, y, z$ ) can be calculated by 2<sup>nd</sup> order potential solution. If the kinematics is used in the computation of analytical wave force, it will result in a cumbersome solution. Simulation of random directional 2<sup>nd</sup> order sea surface, adopted in current study and as done by (Sharma & Dean, 1981) is performed through following steps,

1. The linear Gaussian approximation of random sea surface is formulated by following discrete form:

$$\eta(\vec{x}, y) = \sum_{m=1}^M \sum_{n=1}^N \sqrt{S(\sigma_m, \theta_n) \Delta \sigma_m \theta_n} \cos(\vec{k}_{m,n} \cdot \vec{x} - \sigma_m t + \epsilon_{m,n}) \quad (9-1)$$

2. Using above equation, if we select M different frequencies and N directions, the resulting linear approximation of the wave field will yield MN components. (Pierson, 1955) proved that when M and N tend to infinity, the finite sum obtained by above equation will yield a 3D stationary Gaussian process.
3. In the next step, 2<sup>nd</sup> order corrections are calculated using the equations derived in Section 4.1.2. For the above approximation, there will be MN<sup>2</sup> second order correction components. The

phases of non-linear components are related to those of linear components. As a result, the process of summing up of non-linear and linear components is not Gaussian any more.

4. In order to obtain time history of the water elevation  $\eta$ , 1<sup>st</sup> and 2<sup>nd</sup> order spectra of  $\eta$  is calculated by adding the amplitude of same frequencies and performing an inverse Fast Fourier Transform (FFT).
5. Velocity and acceleration at any point is calculated through following steps.
  - a. For each component, the spectra of velocity and acceleration are resolved along x and y axes
  - b. Fourier coefficients of  $a_n$  and  $b_n$  are calculated by adding contribution from each of the above components.
  - c. Time domain realizations of velocity and acceleration are calculated using inverse FFT.
6. Wave forces exerted per unit length of pile are computed using Morison formula and the velocities and accelerations obtained in the previous step.
7. The total force exerted on the structure is computed by the integration of per unit length forces up-to the free water surface that was calculated in step 3.

For the current study, due to short available time and lack of computational resources, only unidirectional focused extreme wave is generated for extreme load calculation over the Snorre A TLP and comparison with the loads of Stokes fifth wave.

## 9.1 Test cases

This section covers a 2D test case to understand the behavior of new wave theories. Same boundary conditions are used for wave generation using superposition method as was adopted for the Stokes fifth wave.

### 9.1.1 2D test case

The computational domain and input parameters for 2D test case are shown in Figure 9-1 and Table 9-1.

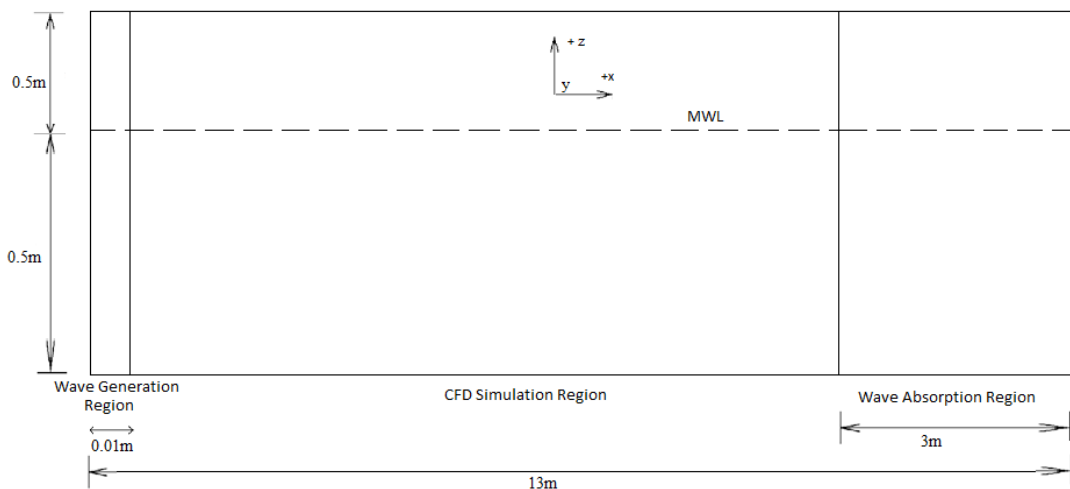


Figure 9-1 Computational Domain (2D Test Case)

Table 9-1 Input Parameters for 2D Test Case

Property	value
Type of flow (Laminar or turbulent)	Laminar
Water depth	0.5 m
Wave height	0.178 m
Wave direction	Along positive x-axis
<i>freqMin</i>	0.3 sec <sup>-1</sup>
<i>freqMax</i>	1.8 sec <sup>-1</sup>
<i>nWaveComp</i>	100
<i>Xf</i>	(3.27 0 0)
<i>Tf</i>	1.58 sec
<i>Fp</i>	0.811 sec <sup>-1</sup>
<i>deltaT</i>	0.001 sec
<i>endTime</i>	100 sec
<i>writeControl</i>	runTime

The description of the input parameters that are different from the those used for Stokes fifth wave is as follows:

**Wave height:** The required wave height at the defined focus point. Superposed waves are not like the regular waves in texture. They have either very large crest, if crests of individual waves are superposed, or very deep trough, if troughs of individual waves are superposed. Moreover, the troughs around the superposed crest are not of same shape and depression. Hence it is very difficult to generate a superposed wave of defined wave height (crest + trough) at the defined point. The wave theory used for this purpose only generates the crest at the defined point with height equals to atleast half of the defined wave height.

***freqMin:*** as the focused phase wave is generated for a specific spectrum, freqMin is the minimum frequency of the selected spectrum.

***freqMax:*** The maximum frequency of the selected spectrum.

***nWaveComp:*** The number of wave components chosen for the generation of superposed wave. Larger the number of waves, more precise will be they will fit in the selected spectrum. On the other hand, increasing the number of waves increase the simulation time and required simulation power. The number of wave components are selected based on the available time and resources.

***xf:*** The location in the computational domain where the superposition in needed to be achieved.

***tf:*** The time instant at which the superposition in needed.

***fp:*** The required frequency of the superposed wave. The significant wave period of Stokes fifth wave cannot be used directly for the focused wave generation through *focNewwave* theory. (Wu, Chen, Bahuguni, Lu, & Kumar, 2015) used the factor of 0.93 by examining the work of (Boccotti, 1983). The same factor is used for the current study. *fp* is related to the significant wave period, *Ts* by Equation xyz.

$$fp = \frac{1}{T_p} = \frac{0.93}{T_s}$$

The same boundary conditions, as for the 2D test case for Stokes fifth wave are used as shown in Figure 6-2 and Table 6-3.

### 9.1.1.1 Post-processing

The generated wave can be viewed in Figure 9-2 at time instants 0.16, 0.6, 1 and 1.4 seconds. The focused time is 0.158 secs, just before the instant 0.16 shown in the Figure 9-2. The wave can clearly be seen with a high crest height at time instants 0.16 seconds with gradual decrease in crest height with the progression of time. The effect is more evident in the Figure 9-3-a where surface elevation plots for the time instants 0.158 seconds is shown. The horizontal axis indicates the number of 80 gauges that are installed along the length of computational domain from 0.5m-10m, with the gauge number at the focusing point is 25. The surface elevation plot at the time instant 0.158 seconds is shown in Figure 9-3-b. The only prominent wave height is at time instant 0.158 (focusing time instant).

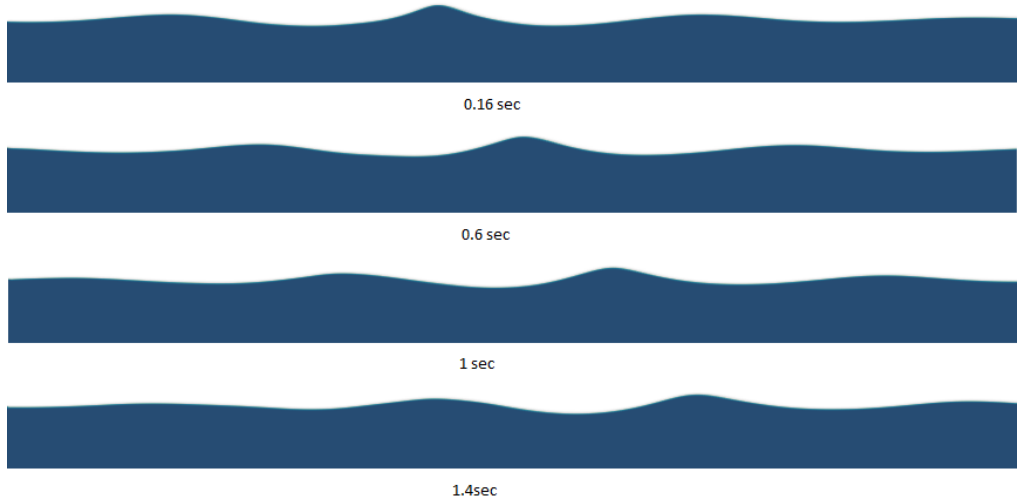


Figure 9-2 Visualization of Free Surface (from Time Instant 0.15-1.4)

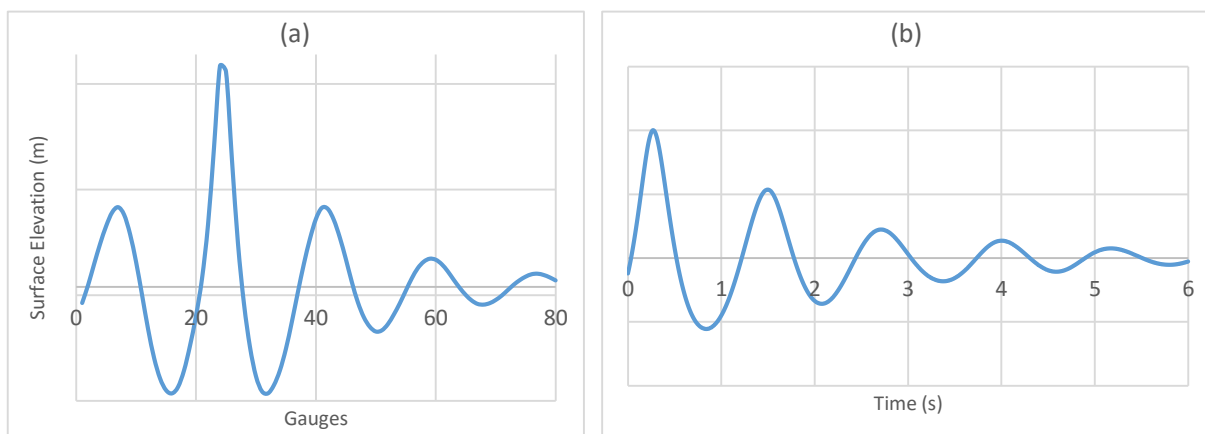


Figure 9-3 Surface Elevation Plots, a) at Time Instant 0.158 seconds. b) at Distance 3.27 Meters from Inlet

## **10 EXTREME WAVE EVENT GENERATION USING SUPERPOSITION OF WAVES**

From section 9-1, it can be concluded that the focused wave has high degree of non-linearity. Unlike the Stokes fifth wave, the regular crests and troughs do not exactly follow each other instead the heights of consecutive crests and depressions of consecutive troughs are different and difference is totally random. Moreover, the focused crest is higher and thinner for the surrounding troughs which are with less depression and way wider. The number of wave components along with the location and time instant of focused wave is defined but the resultant wave is not necessarily to have the same wave height or crest elevation as per of the regular Stokes wave of the same input parameters. Hence to match the focused wave with the Stokes fifth wave and to compute the wave loads, two different matching standards are adopted by (Wu, Chen, Bahuguni, Lu, & Kumar, 2015).

1. Crest elevation of the Stokes wave is achieved for the focused wave at the specified point and wave loads are calculated.
2. Wave height is achieved for focused wave, equal to the wave height of Stokes fifth wave.

### **10.1 Matching standard 1**

The input parameters for the foc3DNewwave relative to the input parameters used in section 8-2 are given in Table 10-1. The conversions of parameters, values of factors used in the conversions and frequency range laying under Jonswap spectrum is taken from (Wu, Chen, Bahuguni, Lu, & Kumar, 2015).

*Table 10-1 Wave Input Parameters of foc3DNewwave*

<b>Input parameters</b>	<b>Stokes fifth</b>	<b>Foc3DNewwave</b>
<b>Water depth</b>	308m	308m
<b>Crest elevation</b>	16.7 m (Figure 8-4)	16.74
<b>Wave height</b>	29.7m	29.7m
<b>Wave period</b>	13 sec (T)	T/0.93 = 13.9785 sec (T <sub>p</sub> )
<b>Peak frequency (fp)</b>	-	0.071538 sec <sup>-1</sup>
<b>Frequency band in Jonswap spectrum</b>	-	0.0237-0.1924
<b>Number of wave components</b>	1	40
<b>Wave length</b>	288m (L)	326.6m (L <sub>p</sub> )

The location of focal point and focal time instant is also chosen according to the recommendation provided in (Wu, Chen, Bahuguni, Lu, & Kumar, 2015). As only unidirectional wave is being considered in the current study, the waves will have same wave height along z-axis. Hence, only the focal point along x-axis is required.

$$\text{focal point along } x - \text{axis} = 1.5 * L = 1.5 * 288 = 432m = \text{used } 420\text{ m}$$

$$\text{focal tme} = 10.5 * T_p = 1.5 * 13.9785 = 20.96775 \text{ sec} = \text{used } 20 \text{ seconds}$$

The waves are not necessarily focus on the desired location and time. Instead they focus on the location closer to the specified location and at time closer to the specified time. The exact location varies with

mesh density. As mesh convergence study has already been carried out in the Section 8-5, the same fine mesh of case 3 is used for focused wave generation. The mesh attributes are given in Table 8-6.

Computational domain is shown in the Figure 10-1. The dimensions of computational domain are set based upon the input parameters discussed in the previous section.

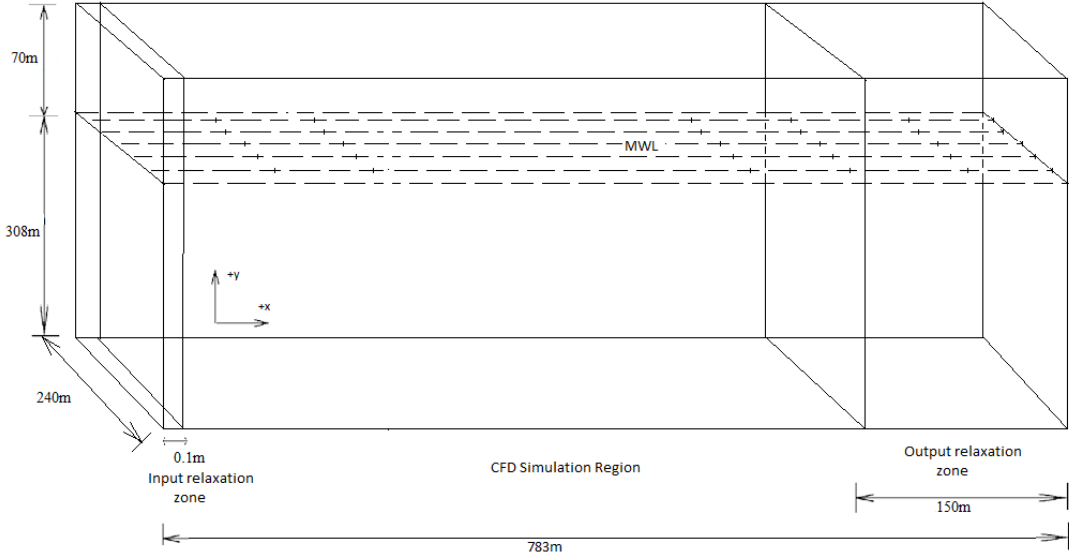


Figure 10-1 Computational Domain for *foc3DNewwave*

As the focal point and time is mesh dependent, the mesh for the computational domain displayed in Figure 10-1 must be according to the final mesh with the platform, with not only the same cell sizes but also with the same features of mesh progression and different mesh densities at different locations. A new mesh is developed for this purpose with the same mesh features as per used in the simulation discussed in Section 8.3. A 2D overview of the mesh is shown in Figure 10-2. The mesh is identical to the one used in Section 8.3 (Figure 8-7) but without platform.

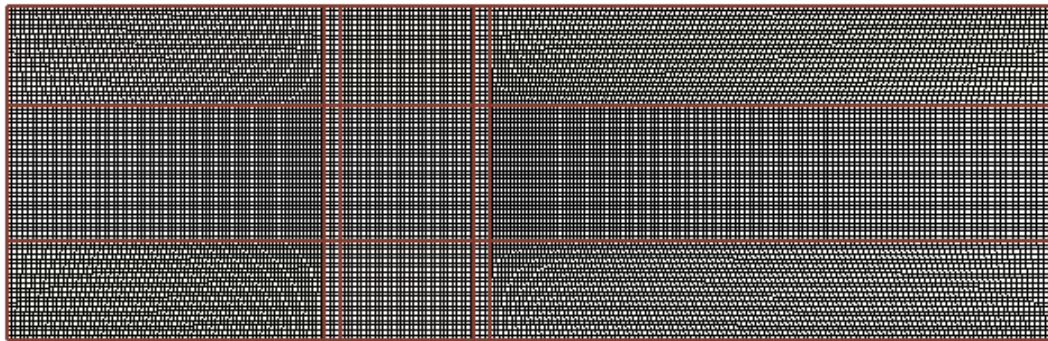


Figure 10-2 2D Section of Mesh without Platform

As mentioned before, the actual focal point and time doesn't necessarily coincide with the specified point and time. The actual focal time and point shifts somewhat from the specified time and point and this shifting is based upon the mesh attributes. Moreover, the focusing phenomenon develops the focused crest of specified dimensions not the trough, hence the resulting wave is with the desired crest elevation of Stokes fifth wave but trough depression is not necessarily to match with the trough depression. The plots of surface elevation ranging from 19-26 seconds with difference of 0.5 seconds among the consecutive values is shown in Figure 10-3. It can be seen that the maximum elevation is achieved around 22.5 seconds.

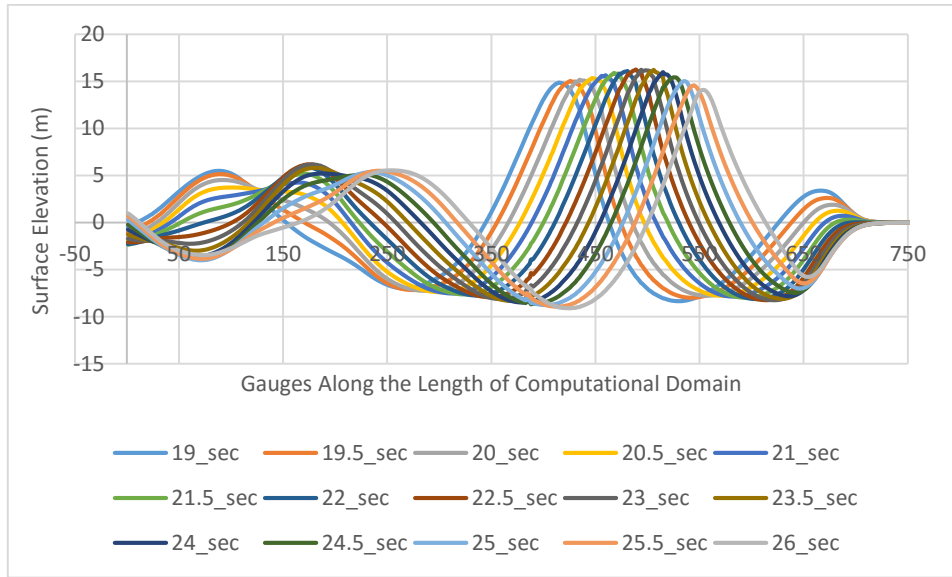


Figure 10-3 Surface Elevation Ranging from 19-26 seconds

After analysis of surface elevation data, the actual location and time of superposed wave is tabulated in the Table 10-2.

Table 10-2 Attributes of Focal Point

Parameter	Specified Value	Actual Value
<b>Focal Point</b>	( 420 0 50.5 ) m	( 494 0 50.5 ) m
<b>Focal Time Instant</b>	20 seconds	22.85 seconds

The comparison of elevation of superposed wave with the free surface elevation of Stokes fifth wave shown in Figure 8-4 is presented in Figure 10-5. The time series of Stokes fifth wave from Figure 8-4 is shifted to match with the superposed wave. The crest elevations match closely with only a minor phase change, hence first standard matching is fulfilled. It must be noted that the time period of both waves also matches hence the factor used for conversion of  $T_s$  to  $T_p$  (taken from (Wu, Chen, Bahuguni, Lu, & Kumar, 2015)) is right.

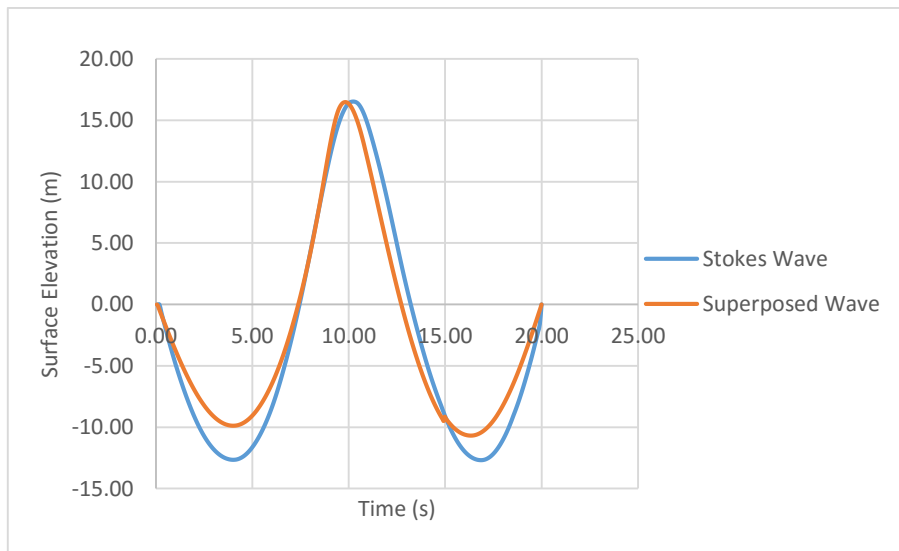


Figure 10-4 Comparison of Surface Elevation of Stokes Fifth and Superposed Wave

### **10.1.1 Simulation of wave fulfilling matching standard 1 with platform**

The computational domain developed for the wave fulfilling the matching standard 1 and hitting the platform, is presented in Figure 10-5. The dimensions of the regions and location of platform is set according to the results of previous section. Platform is placed at the point where the highest elevation of crest was achieved in the previous section i.e. ( 494 0 50.5 ) meters in global coordinates.

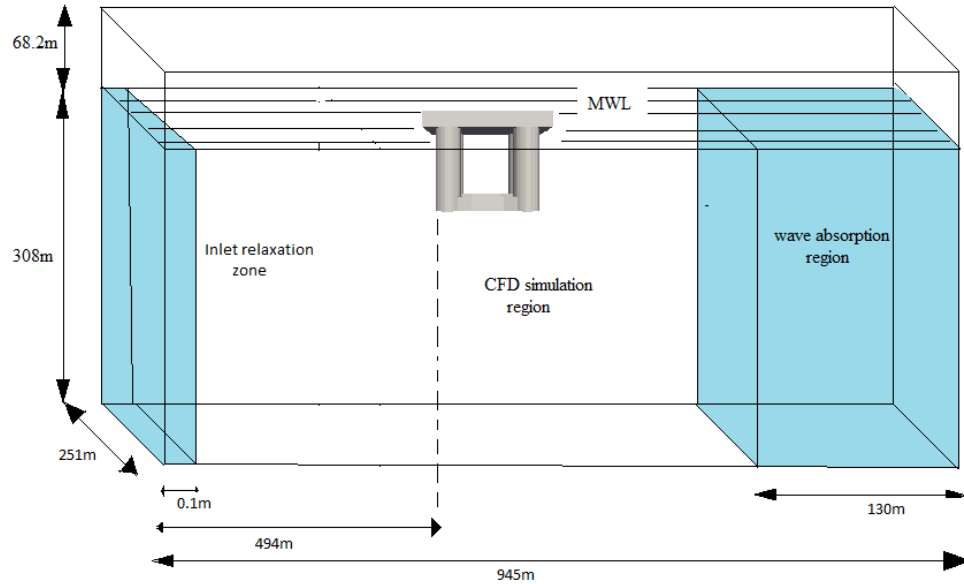


Figure 10-5 Computational Domain (Matching Standard 1 Case)

#### **10.1.1.1 Results**

The free surface 3D contour showing the flow across the platform in Figure 10-6. The xy planar view of computational domain is shown in Figure 10-7 at instant 22.5 seconds, followed by surface elevation plot at focal point (Figure 10-8). in Figure 10-7, the wave is just hitting the platform at its maximum height.

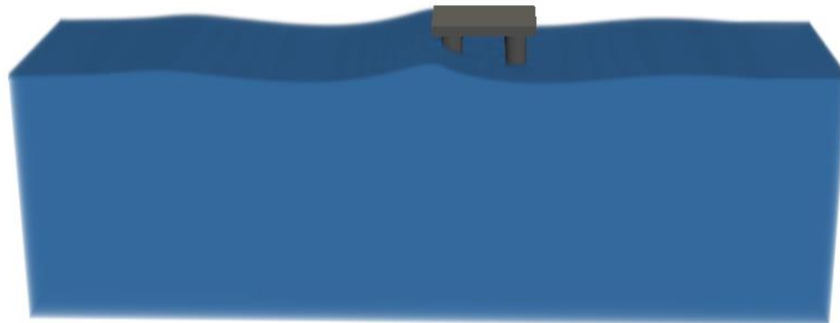


Figure 10-6 3D Visualization of Free Surface (Superposed Wave)

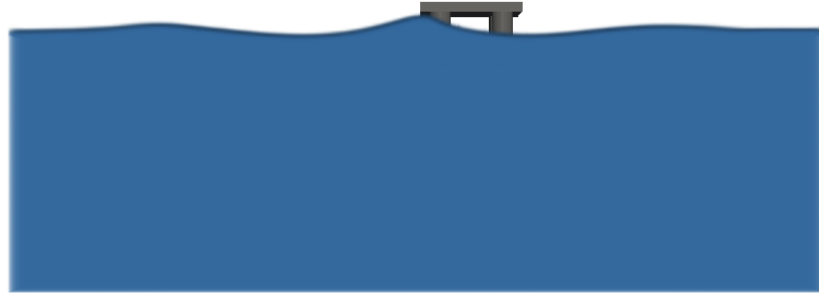


Figure 10-7 2D View of Superposed Wave

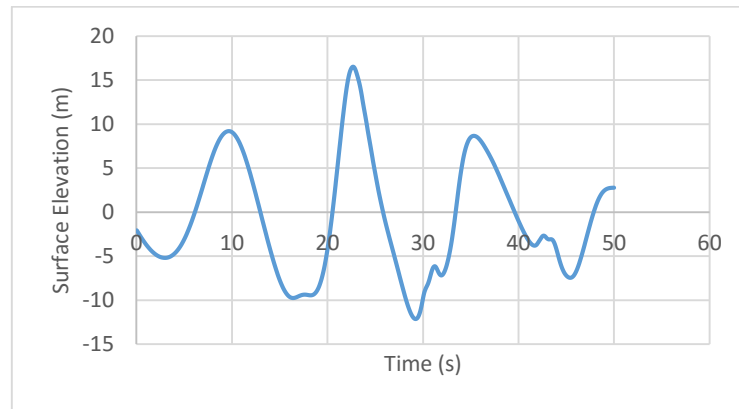


Figure 10-8 Surface Elevation Plot at Focal Point

The plots of tension in tendons at front and back of platform are displayed in Figure 10-9. The plots for lift and drag forces, moment and vertical displacement at front and back of platform are shown in Appendix (a).

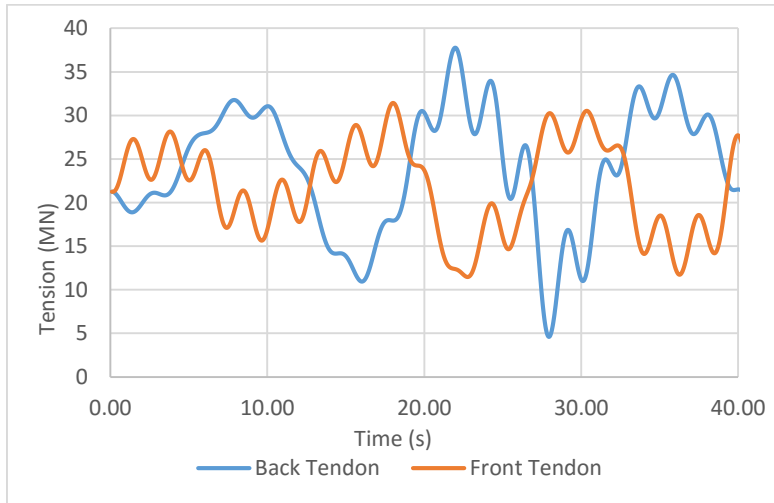


Figure 10-9 Tension in Tendons at Front and Back side of Platform (Matching Standard 1 Case)

## 10.2 Matching standard 2

Same input parameters as per mentioned in Table 10-1 are used except instead of only crest elevation, trough depression is also matched with the trough depression of Stokes fifth wave used in Section 8. From the Figure 8-4, the trough depression of generated Stokes fifth wave is -12.64 meters.

Generation of wave according to matching standard 2 is a tricky process. Following shortcomings are observed in new wave theory (foc3DNewwave) from the previous experience.

- The superposition of wave does not occur at the specified focal point and time, instead the superposed wave appears somewhere closer to the specified location.
- For the highest elevated crest, the elevation is not necessarily match the specified crest elevation. It usually exceeds the specified value.
- The trough depression at the focal point do not necessarily match the specified depression. The trough shows random behavior with different depressions at different locations.
- The selection of focal time does not have much effect on the crest elevation or trough depression at the focal point. Choosing focal time according to the recommendation of (Wu, Chen, Bahuguni, Lu, & Kumar, 2015) results in smaller difference in the chosen focal point and actual focal time, but it also requires more computational time as focal time is of order 20 seconds.
- The selection of focal time also does not have much effect on the crest elevation or trough depression at the focal point. Less focal time and less distance between focal point location and inlet is chosen to decrease the computational time of hit and trial process followed further in this section.

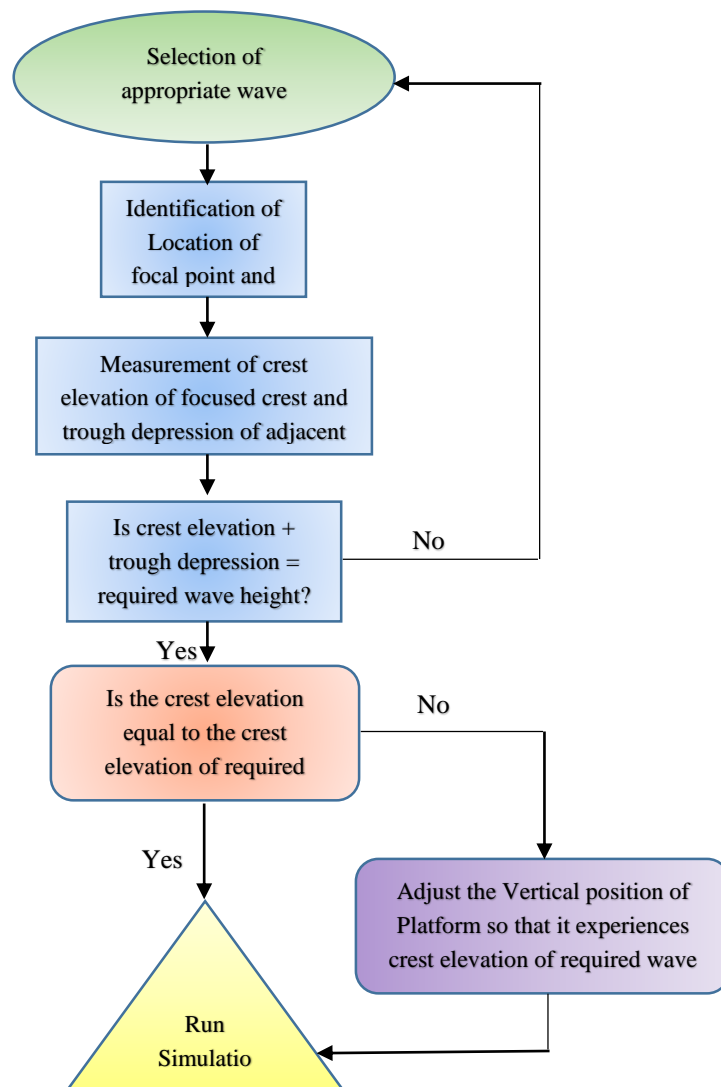


Figure 10-10 Methodology of Wave Simulation, Fulfilling Matching Standard 2

For matching standard 2, the final goal is to achieve a wave height with the elevation and depression equal to the Stokes fifth wave elevation and depression. Moreover, the wave must also be the highest elevated wave of the whole computational domain and computational time. This is achieved through hit and trial method by changing the input wave height and observing the highest elevated wave in the computational domain. The target wave height is 29.7 meters (from Table 10-1). The methodology for generation of wave for matching standard 2 is shown in flow chart of Figure 10-10.

After following the steps defined in flow chart of Figure 10-10, a wave with the characteristics mentioned in Table 10-3 is found fulfilling the matching standard 2. The surface elevation at the actual focal point is shown in Figure 10-11. The crest elevation of superposed wave is higher than the crest elevation of Stokes fifth wave of Section 8. On the other hand, the trough depression of superposed wave is lower than the Stokes Fifth wave. The difference in elevation is 1.13 meters while difference in depression is 1.3 meters. The wave height of both the waves closely matches but to keep the crest elevation hitting the platform equal in both cases, the platform is raised in the currently evaluated case, by 1.16 meters, relative to its position in Section 8-2.

*Table 10-3 Computed Actual Location of Focal Point and Focal Time*

Parameter	Specified Value	Actual Value
<b>Focal Point</b>	( 200 0 50.5 ) m	( 273 0 50.5 ) m
<b>Focal Time Instant</b>	6 seconds	12.35 seconds
<b>Crest elevation</b>	16.74 m	17.9 m
<b>Trough depression</b>	12.65 m (downwards)	11.35 m (downwards)

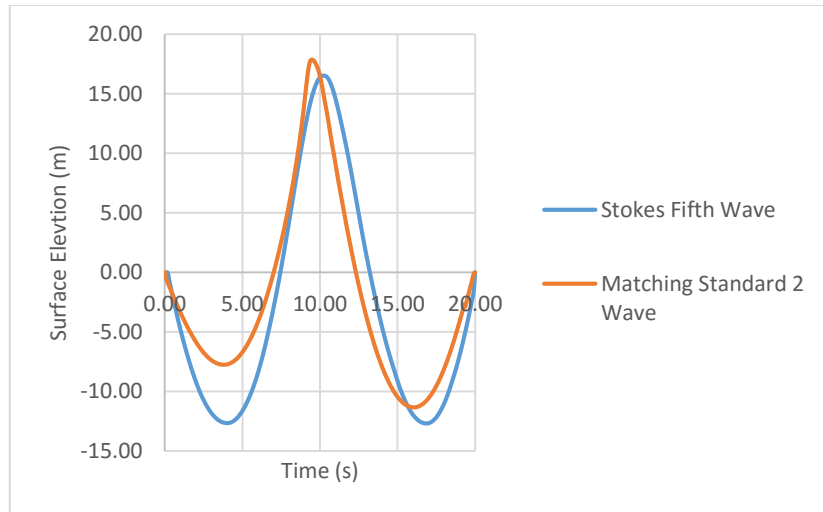


*Figure 10-11 Comparison between Matching Standard 2 Wave and Stokes Fifth Wave*

### **10.2.1 Simulation of wave fulfilling matching standard 2 with platform**

The computational for matching standard 2 case, is presented in Figure 10-12. The dimensions of the regions and location of platform is set according to the results of previous section. platform is placed at the point where the highest elevation of crest was achieved i.e. ( 273 0 50.5 ) meters in global coordinates.

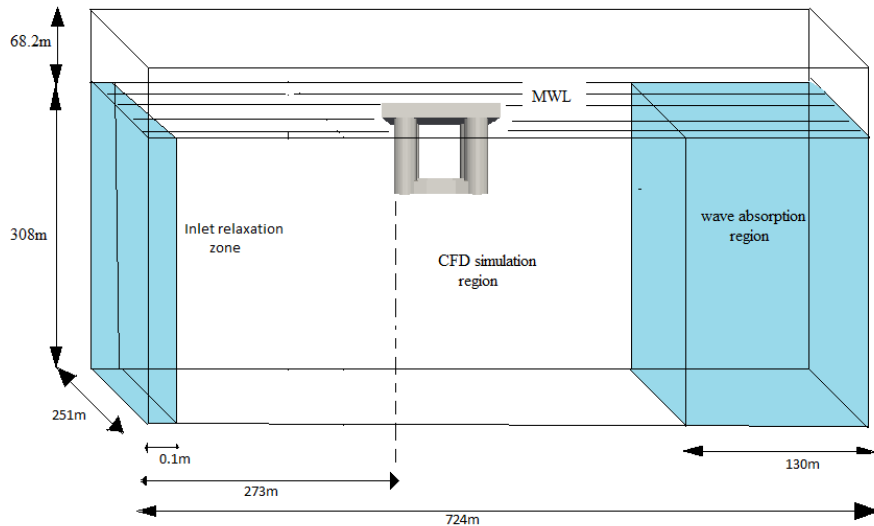


Figure 10-12 Computational Domain (Matching Standard 2 Case)

### 10.2.1.1 Results

The plots of tension in tendons at front and back of platform are displayed in Figure 10-13. The plots for lift and drag forces, moment and vertical displacement at front and back of platform are shown in Appendix (b).

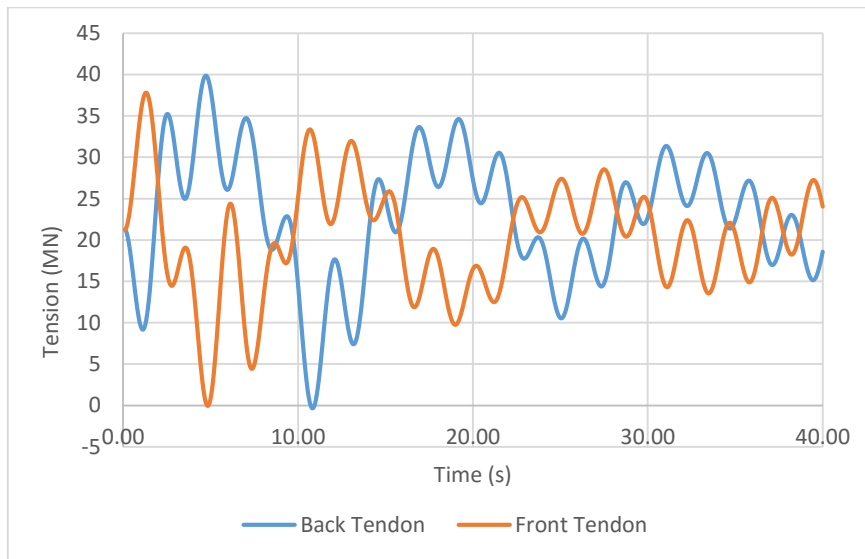
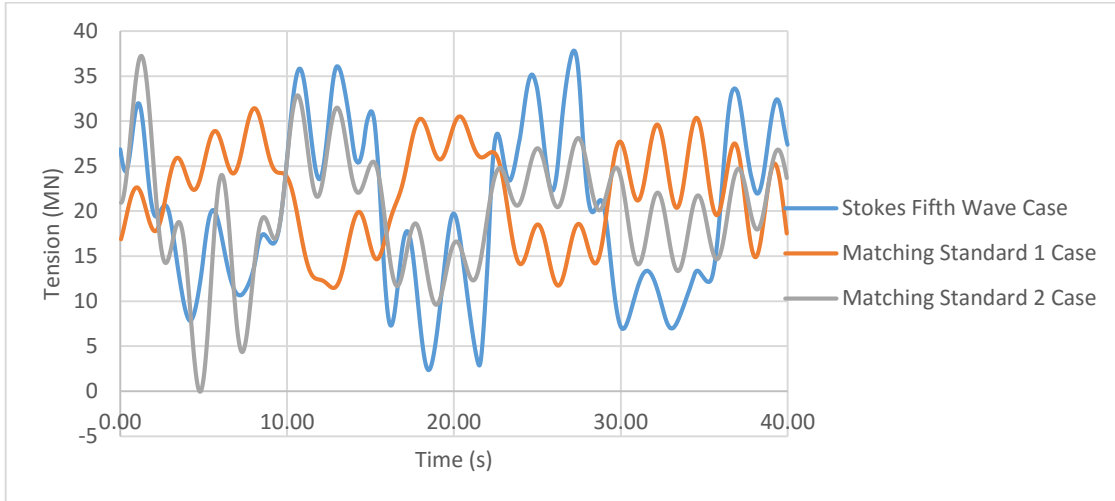


Figure 10-13 Tension in Tendons at Front and Back side of Platform (Matching Standard 2 Case)

## 11 COMPARISON OF RESULTS

The tensions in the front and back tethers for all three evaluated cases, plotted on the same paper, are shown in Figures 11.1 and 11.2 respectively. The entries along x-axis are time instants. For the matching standard 1 and 2 cases, that time interval is chosen during which the superposed wave hits the platform, hence the maximum tension appears in tethers during this time interval. The time instants of Stokes fifth wave case and matching standard 1 case are adjusted accordingly to fix them on the same paper with matching standard 2 case.



*Figure 11-1 Comparison of Tensions in Front Tethers between Matching Standard 1 Case, Stokes Fifth Wave Case and Matching Standard 2 Case*

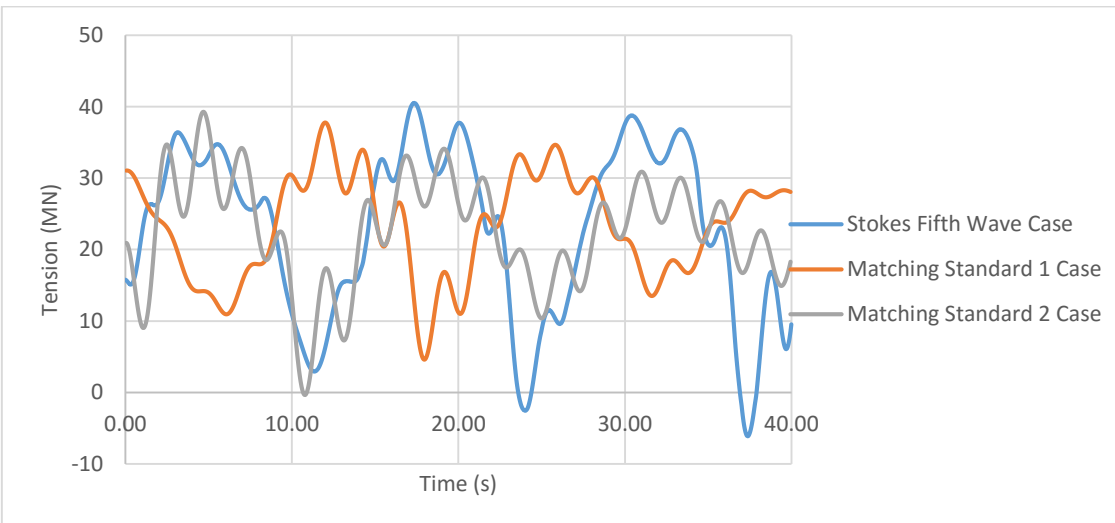


*Figure 11-2 Comparison of Tensions in Back Tethers between Matching Standard 1 Case, Stokes Fifth Wave Case and Matching Standard 2 Case*

As a general overview, the matching standard 1 case tensions for both front and back tethers stay lower, as compared to other two cases, throughout the time interval. It is logical because for the matching standard 1 case, only the crest elevation was matched with the crest elevation of Stokes fifth wave case. The trough depression was lower than the trough depression of Stokes fifth wave. The matching standard 2 case shows higher peaks which are comparable to the peaks of Stokes fifth wave case. For better

visualization and comparison, the tensions in front and back tethers, for Stokes fifth wave case and matching standard 2 case, are shown separately in Figures 11-3 and 11-4.

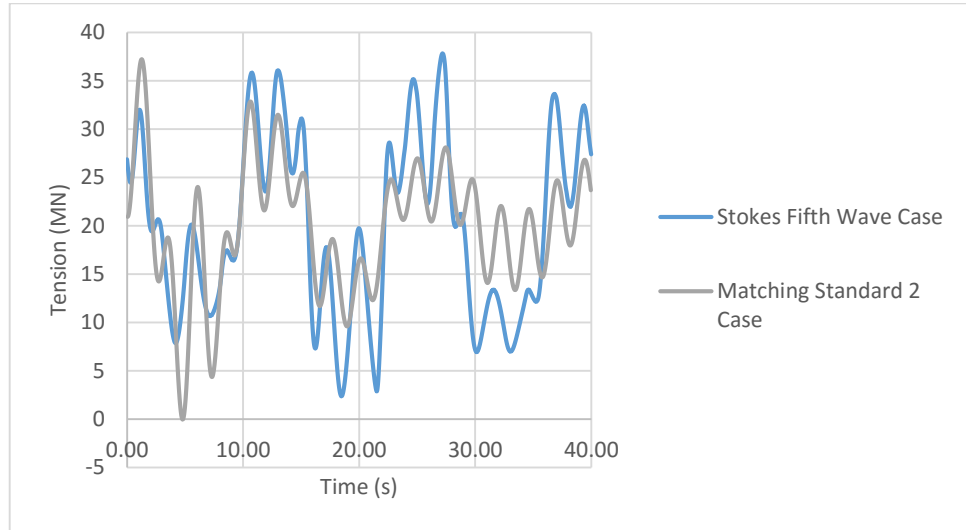


*Figure 11-3 Comparison of Tensions in Front Tethers between Stokes Fifth Wave Case and Matching Standard 2 Case*

Generally, the peaks of Stokes fifth wave case for, front tethers' tension, are higher than the matching standard 2 case. In the higher and prominent peaks of Figures 11-3, most of the peaks are of Stokes fifth wave case. A higher peak at the very start of curve (around 2 seconds) appears for matching standard 2 case. Except for this particular peak, all the peaks of matching standard 2 case are lower than the peaks of Stokes fifth wave case. The highest value of tension in front tethers, for matching standard 2 case reaches up to 37.02 MN, which is not the highest value of all the three cases as around 27 seconds, a peak of same height appears for Stokes fifth wave and tension reaches up to 37.82 MN.

Same dominant peaks for Stokes fifth wave case can be observed in the plots of tension of back tethers. The highest peak is also for the Stokes fifth case i.e. 40.46 MN. It must be noted here that the tension in back tethers is more as compared to tension in front tethers, because of imbalance in forces and roll motion. The peak tension of the system computed by the three cases are shown in Table 11-1. The highest tension in the system of all three evaluated cases is for the Stokes fifth order case.

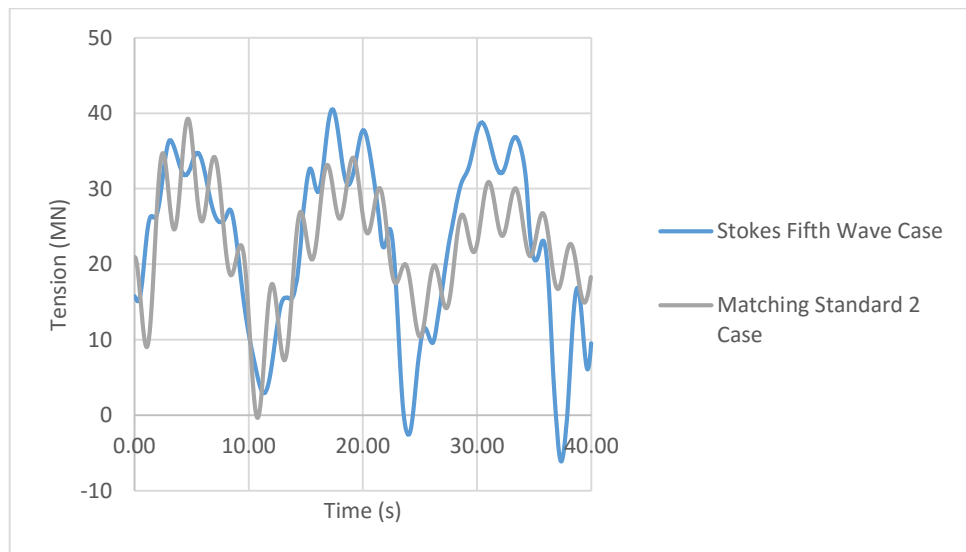


*Figure 11-4 Comparison of Tensions in Back Tethers between Stokes Fifth Wave Case and Matching Standard 2 Case*

Table 11-1 Maximum system Stress for the Three Evaluated Cases

Cases	Highest tension (MN)
<b>Stokes fifth wave case</b>	40.46
<b>Matching standard 1 case</b>	37.3
<b>Matching standard 2 case</b>	39.24

While analyzing a TLP for design loads, the highest tension alone is not used as a design input. The amount of energy transferred by waves, to the platform is also an important input parameter of design. The transfer of energy is not dependent upon the highest tension alone, instead it depends upon the consistency in the higher peaks. A better understanding of amount of energy transmitted by waves to platform can be attained by analyzing the RMS values of tension in tethers in each case. Table 11-2 presents the RMS values of tension in tethers.

Table 11-2 RMS values of Front and Back Tether Tension for 3 Evaluated Cases

Cases	RMS (front tethers' tension)	RMS (back tethers' tension)
<b>Stokes fifth wave case</b>	22.5873764	25.88045129
<b>Matching standard 1 case</b>	22.63767991	24.30490937
<b>Matching standard 2 case</b>	21.03010453	23.71243628

The matching standard 2 case has RMS values lowest of the three. It is interesting because despite of having higher peaks, the energy transfer in the matching standard 2 case is still less. The Stokes fifth wave case has RMS values greater than others in the back tether tension, and closer to the highest value in front tether tension. It means, for the Stokes fifth wave case, not only the tension peaks are higher, the energy transfer between the waves and platform is also higher.

As both maximum tension and energy transfer contributes towards the design loads, they can be presented together in non-dimensionalized form. The non-dimensional values of maximum tension and RMS for the three cases are given in the Table 11-3. The parameters are non-dimensionalized by dividing them with the maximum of the three values from the three cases. As RMS values for tension in back tethers are more than for tension in front tethers, hence only the RMS values of only back tethers are non-dimensionalized.

Table 11-3 Non-dimensionalizing of Parameters

Parameter	Stokes fifth wave case	Matching standard 1 case	Matching standard 2 case
<b>Maximum tension</b>	1	0.922	0.9698
<b>RMS</b>	1	0.9391	0.916
<b>Combined factor</b>	1+1 = 2	0.922+0.9391 = 1.8611	0.9698+0.916 = 1.886

The combined factor indicated that the Stokes fifth waves impose more loads on the platform as compared to the waves of other two evaluated cases. Comparatively, Stokes fifth wave case imposes  $2/1.8611 = 1.072$  times more loads on platform as compared to matching standard 1 case and  $2/1.886 = 1.06$  times more loads on platform as compared to the matching standard 2 case. These numbers are quite close to results of published work of (Sharma & Dean, 1981). According to (Sharma & Dean, 1981), the Stokes fifth order wave induces 1.05 times more loads on a structure as compared to the unidirectional superposed wave. They also concluded that the more real idealization of extreme event, as compared to the unidirectional superposed wave, is the directional superposed wave. According to them, Stokes fifth wave imposes 1.65 times more loads as compared to the directional superposed wave, but the directional superposing of waves is not been considered in the current study because of lack of time and computational resources.

## **12 CONCLUSION**

In the current study, the extreme event wave using three different techniques has been generated and its impact load on Snorre A TLP has been analyzed. The followed techniques are Stokes fifth order wave, superposed wave matching the crest elevation and superposed wave matching the wave height of Stokes fifth order wave generated in the first case. The individual components of superposed waves are assumed to be unidirectional. Following conclusions are drawn at the end of current study:

- Using Stokes fifth order wave for calculating design loads of Snorre A TLP adds conservations to the design loads.
- The loads imposed by Stokes fifth waves increase progressively with the passage of time and with every new crest and trough. This phenomenon is quite unreal as it is impossible for an extreme event wave to generate right after another extreme event. Moreover, differences in the calculations appear for the simulations with same input parameters but different run time.
- The differences between the loads calculated for Stokes fifth wave case and superposed wave cases are not very high i.e. 8 and 6 percent for cases 2 and 3 respectively, but the differences are in accordance with the study of (Sharma & Dean, 1981). It means the results are reasonably accurate and can be used as ground for further research.
- For the real sea, the wave troughs are broad and less deep and crests are narrow and higher. The trough of superposed wave for the matching standard 1 case is found to be very broad and very less deep as compared to the trough of matching standard 2 case superposed wave, that has the same shape and depression as Stokes fifth wave. The trough of matching standard 1 case superposed wave is also less deep as compared to the trough of real extreme event wave. Moreover, the troughs of both Stokes fifth wave and matching standard 2 case superposed wave are also not the real idealization of ocean extreme event wave as trough depressions are very high. The differences in the results of Stokes fifth case and matching standard 2 case are due to superposition phenomenon. The real idealization of extreme event wave is somewhat in between the matching standard 1 case and matching standard 2 case waves.

## **13 FUTURE RECOMMENDATIONS**

The results obtained from current study are realistic and the work can be used for the further research. Only the unidirectional superposed waves are used in the current study as a closer realization to the real extreme event wave as compared to Stokes fifth order wave, however, the research has shown that the directional superposed wave i.e. the superposed wave with the individual components moving in different directions, is even closer realization to the extreme event wave as compared to the unidirectional superposed wave. Moreover, due to lack of time and computational power, the mesh used was not as much dense as found in the previous related work. Hence accuracy of current study and more optimized design of tendons of Snorre A TLP can be achieved by:

- Using directional superposition phenomenon
- And by using denser mesh with smaller cell size as per recommended by the previous work.

## 14 REFERENCES

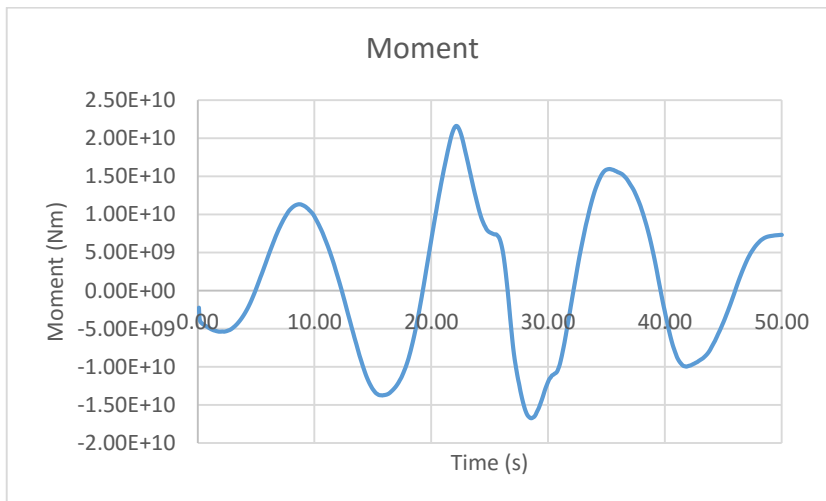
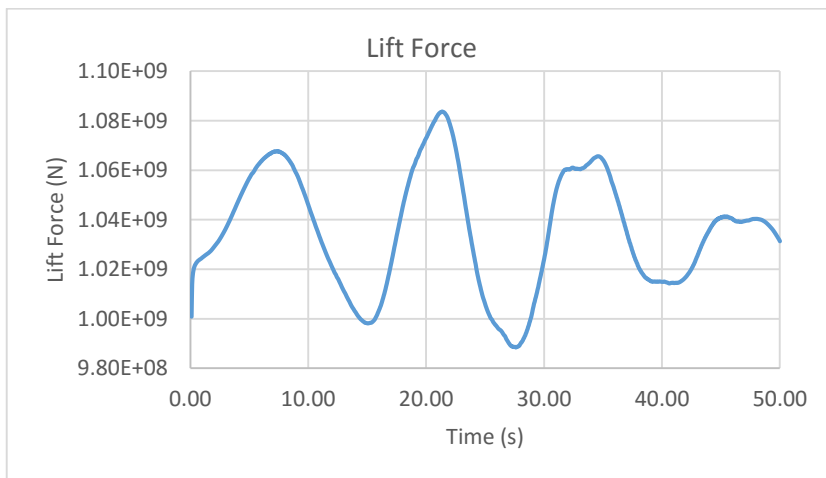
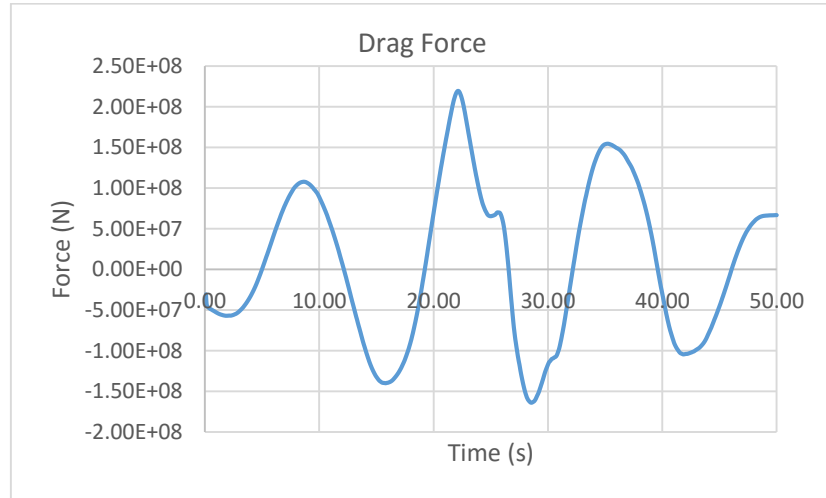
- Afshar, A. M. (2010). *Master's Thesis. Numerical Wave Generation In OpenFOAM®*. Denmark: Chalmers University of Technology.
- AUTODESK. (2016, 06 17). *How to Perform a Mesh Convergence Study*. Retrieved from AUTODESK KNOWLEDGE NETWORK: <https://knowledge.autodesk.com/support/simulation-mechanical/troubleshooting/caas/sfdarticles/sfdarticles/How-to-Perform-a-Mesh-Convergence-Study.html>
- Boccotti, P. (1983). Some new results on statistical properties of wind waves. *Applied Ocean Research* 5 (3), 134–140.
- Borthwick, A. G., Hunt, A. C., Feng, T., Taylor, P. H., & Stansby, P. K. (2006). Flow kinematics of focused wave groups on a plane beach in the UK Coastal Research Facility. *Coastal engineering*, 1033-1044.
- Brandini, C., & Grilli, S. (2001). Modeling of freak wave generation in a 3D-NWT. *Eleventh International Offshore and Polar Engineering Conference*. International Society of Offshore and Polar Engineers.
- Cengel, Y. A., & Cimbala, J. M. (n.d.). *Fluid Mechanics, Fundamentals and Applications* (3rd ed.). McGraw-Hill College.
- CFD Direct. (2016, 06 02). *About OpenFOAM*. Retrieved from CFD Direct, The Architects of OpenFOAM: <http://cfd.direct/openfoam/about/>
- Christopher, J. G. (2015). *OpenFOAM, The OpenSource CFD Toolbox, User Guide*. OpenFOAM Foundation Ltd.
- Fernández, H., Sriram, V., Schimmels, S., & Oumeraci, H. (2014). Extreme wave generation using self correcting method—Revisited. *Coastal Engineering*, 15-31.
- Gie, T. S., & Boom, W. d. (1981). The Wave Induced Motion of a Tension Leg Platform in Deep Waters. *OTC 4074* (pp. 94-96). Houston, Texas, USA: Offshore Technology Conference.
- Grue, J., Clamond, D., Huseby, M., & Jensen, A. (2003). Kinematics of extreme waves in deep water. *Applied Ocean Research*, 355–366.
- Harding, S., & Banon, H. (1989). Reliability of TLP Tethers Under Maximum and Minimum. *OTC 5935*. Houston: Offshore Technology Conference.
- Heilskov, N. F. (2015). *Structural Design of Wave Energy Converters, State-of-the-Art and Implementation of Design Tools for Floating Wave Energy Converters, Part 2: Implementation and Results*. Hørsholm, Denmark: DHI Business Management System.
- Hirt, C. W., & Nichols, B. D. (1981). Volume of Fluid (VOF) Method for the Dynamics of Free Boundaries. *Jouranl of computationoal physics*, 201-225.
- IHRDC. (2016, 04 17). *Floating Production Units*. Retrieved from IHRDC, A worldwide Leader in Oil and Gas Training: [https://www.ihrdc.com/els/ipims-demo/t36797/offline\\_IPIMS\\_s36804/resources/data/PE10.htm](https://www.ihrdc.com/els/ipims-demo/t36797/offline_IPIMS_s36804/resources/data/PE10.htm)
- Jacobsen, N. G., Fuhrman, D. R., & Fredsøe, J. (2012). A wave generation toolbox for the open-source CFD library: OpenFOAM. *International journal for numerical methods in fluids*, 1073-1088.

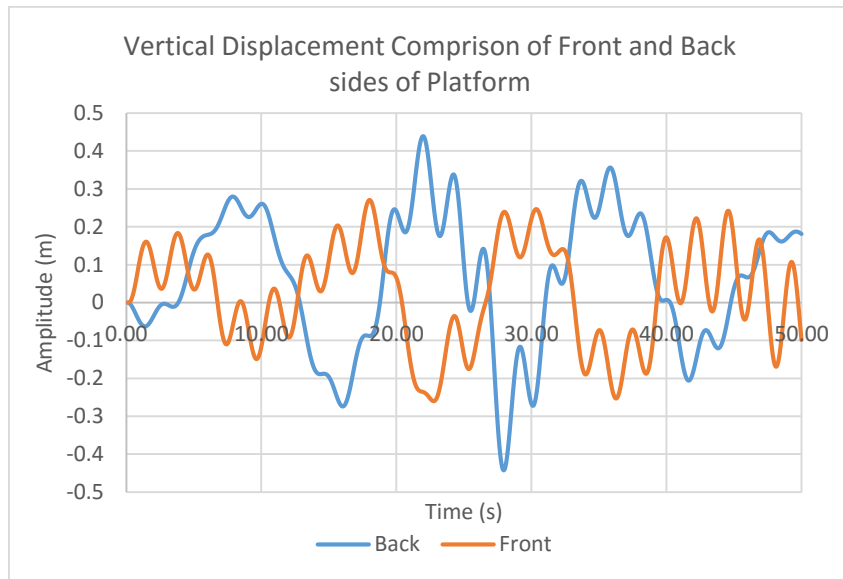
- Jensen, B., Christensen, E. D., & Jacobsen, N. G. (2014). Simulation of Extreme Events of Oblique wave Interaction with Porous Breakwater Structures. *Coastal Engineering*, 1-13.
- Johannessen, T., Haver, S., Bunnik, T., & Buchner, B. (2006). *Extreme Wave Effects on Deep Water TLPs, Lessons Learned From Snorre A Model Tests*. Aker Kværner Engineering & Technology, Statoil, MARIN.
- Kibbee, S. E., Chianis, J., Davies, K., & Sarwono, B. (1994). The Seastar Tension-. Houston: Offshore Technology Conference. OTC.
- MIT OpenCourseWare. (2016, 06 02). *Surface gravity waves*. Retrieved from Wave Motion in the Ocean and the Atmosphere: [http://ocw.mit.edu/courses/earth-atmospheric-and-planetary-sciences/12-802-wave-motion-in-the-ocean-and-the-atmosphere-spring-2008/lecture-notes/MIT12\\_802S08\\_lec03.pdf](http://ocw.mit.edu/courses/earth-atmospheric-and-planetary-sciences/12-802-wave-motion-in-the-ocean-and-the-atmosphere-spring-2008/lecture-notes/MIT12_802S08_lec03.pdf)
- MODEC-Inc. (2016, April 15). *About Offshore Oil & Gas Industry*. Retrieved from MODEC: [http://www.modec.com/about/industry/oil\\_gas.html](http://www.modec.com/about/industry/oil_gas.html)
- Moe, G. (n.d.). LINEAR WAVE THEORY. In G. Moe. Trondheim: NTNU.
- National Commission on the BP Deepwater Horizon Oil. (2010). *A Brief History of Offshore Oil Drilling, Staff Working Paper No. 1*.
- Ning, D. Z., Teng, B., Taylor, R. E., & Zang, J. (2008). Numerical simulation of non-linear regular and focused waves in an infinite water-depth. *Ocean Engineering*, 887-899.
- NORSOK. (1999). *NORSOK Standard N-003 "Action and Action Effects"*. Norway: NORSOK.
- Obhrai, C. (2015). Lecture notes, Marine Technology-Linear waves. Stavanger: University of Stavanger.
- Offshore technology.com. (2016, 05 16). *Glider, Gulf of Mexico, United States of America*. Retrieved from Offshore technology.com: <http://www.offshore-technology.com/projects/glider/glider1.html>
- Offshore technology.com. (2016, 04 17). *Marco Polo Field, United States of America*. Retrieved from Offshore technology.com: <http://www.offshore-technology.com/projects/marcopololo/marcopololo5.html>
- Paixao, P. (2016, 04 17). *Types of Offshore Platforms Part 3*. Retrieved from Petróleo e Construção Naval: <http://petrogasenaval.blogspot.no/2015/07/tipos-de-plataformas-offshore-parte-1.html>
- Palomares, G. D.-L. (2015). *MasterThesis: CFD Simulation on a Partially Submerged Cylinder Under Regular Waves Using OpenFOAM*. Stavanger: University of Stavanger.
- Pauling, J. R., & Horton, E. (1970). Analysis of the Tension Leg Stable Platform. *OTC NO. 1263*. Offshore Technology Conference.
- Pelinovsky, E., Kharif, C., Talipova, T., & Slunyaev, A. (2002). Nonlinear wave focusing as a mechanism of the freak wave generation in the ocean. *ACTES DE COLLOQUES-IFREMER*, 193-204.
- Pierson, W. J. (1955). Wind generated gravity waves. *Advances in geophysics*, 93-178.
- PSA, SFT and NSHD. (2001). *Regulations Relating to Design and Outfitting of Facilities etc: In The Petroleum Activities (The Facilities Regulations)*. Norway: Petroleum Safety Authority Norway (PSA), Norwegian Pollution Control Authority (SFT), Norwegian Social and Health Directorate (NSHD).

- Sharma, J. N., & Dean, R. G. (1981). Second-Order Directional Seas and Associated Wave Forces. *Society of Petroleum Engineers Journal*, 129-140.
- Task Group on Complaint Offshore Platforms. (1989). *Tension Leg Platform*. (Z. Demirbilek, Ed.) New York: American Society of Civil Engineers.
- TurboSquid. (2016, 04 17). *Tension Leg Platform*. Retrieved from TurboSquid: <http://www.turbosquid.com/3d-models/tension-leg-platform-3d-model/312110>
- Vannucci, D., & RINA. (2011, 04 16). ORECCA, Platform Technologies for Offshore Renewable Energy Conversion. (p. 18). Brussels: EWEA. Retrieved from EWEA: [http://www.ewea.org/annual2011/fileadmin/ewec2011\\_files/documents/Workshops/ORECCA/ORECCA\\_EWEA\\_2011\\_Diego\\_Vannucci.pdf](http://www.ewea.org/annual2011/fileadmin/ewec2011_files/documents/Workshops/ORECCA/ORECCA_EWEA_2011_Diego_Vannucci.pdf)
- Waseda, T., Rheem, C. K., Sawamura, J., Yuhara, T., & Kinoshita, T. (2005). Extreme Wave Generation in Laboratory Wave Tank. *Proceedings of the Fifteenth International Offshore and Polar Engineering Conference* (pp. 1-2). Seoul, Korea: International Society of Offshore and Polar Engineering.
- Wells, B. (2016, April 15). *Offshore Petroleum History*. Retrieved from American Oil & gas Historical Society: <http://aoghs.org/offshore-history/offshore-oil-history/>
- Wikipeida. (2016, 04 15). *Oil platform*. Retrieved from Wikipedia: [https://en.wikipedia.org/wiki/Oil\\_platform](https://en.wikipedia.org/wiki/Oil_platform)
- World Ocean Review. (2016, 04 16). *Oil and Gas*. Retrieved from World Ocean Review: <http://worldoceanreview.com/en/wor-3-overview/oil-and-gas/where-and-how-extraction-proceeds/3/>
- Wu, Y., Chen, Y., Bahuguni, A., Lu, X., & Kumar, P. (2015). *Study of Wave in deck loading on offshore structures during extreme events*. Singapore: Lloyd's Register, Institute if High Performance Computing.
- XU, N. (2009). *Static Stability of Tension Leg Platforms*. Texas: Texas A&M University.

## 15 APPENDIX

### a) Matching Standard 1 case





**b) Matching standard 2 case**

